Therapeutic iron: Evaluation of methods to assess intravenous iron safety profiles and the development of a novel formulation for oral iron delivery

Kimberley Span

The studies described in this thesis were financially supported by Vifor (International) Ltd. The views expressed in this manuscript are the personal views of the authors. Vifor Pharma participated in meetings and supported the research financially.

The printing of this thesis was financially supported by:

Vifor (International) Ltd. Switzerland
HypoCenter Berlin
FASP N.V. Aruba
AVIS Rent-A-Car Aruba
Best International Group N.V. Aruba
Domiberia Benelux B.V.

Span K
Therapeutic iron:
Evaluation of methods to assess intravenous iron safety profiles and the development of a novel formulation for oral iron delivery

Thesis with a summary in Dutch
Department of Pharmaceutics, Utrecht Institute for Pharmaceutical Sciences (UIPS), Utrecht University, the Netherlands.

ISBN: 978-94-92679-35-2
Cover and bookmark photography: © KimberleySpan
Lay-out and printing by: proefschriftenprinten.nl

Therapeutic iron: Evaluation of methods to assess intravenous iron safety profiles and the development of a novel formulation for oral iron delivery

Therapeutisch ijzer: een evaluatie van methoden om veiligheidsprofielen van intraveneus ijzer te beoordelen en de ontwikkeling van een nieuwe formulering voor orale ijzertoediening
(met een samenvatting in het Nederlands)

Proefschrift

ter verkrijging van de graad van doctor aan de Universiteit Utrecht
op gezag van de rector magnificus, prof. dr. G.J. van der Zwaan,
ingevolge het besluit van het college voor promoties in het
openbaar te verdedigen op maandag
12 maart 2018 des ochtends te 10.30 uur

door

Kimberley Span
geboren op 25 augustus 1982
te Guayaquil, Ecuador

Promotoren: Prof.dr.ir. W.E. Hennink
Prof.dr. H. Schellekens

Copromotor: Dr. V. Brinks

"Success is not final, failure is not fatal: it is the courage to continue that counts."
- attributed to W. Churchill

Pa mi famia stimá
(For my beloved family)

Table of contents

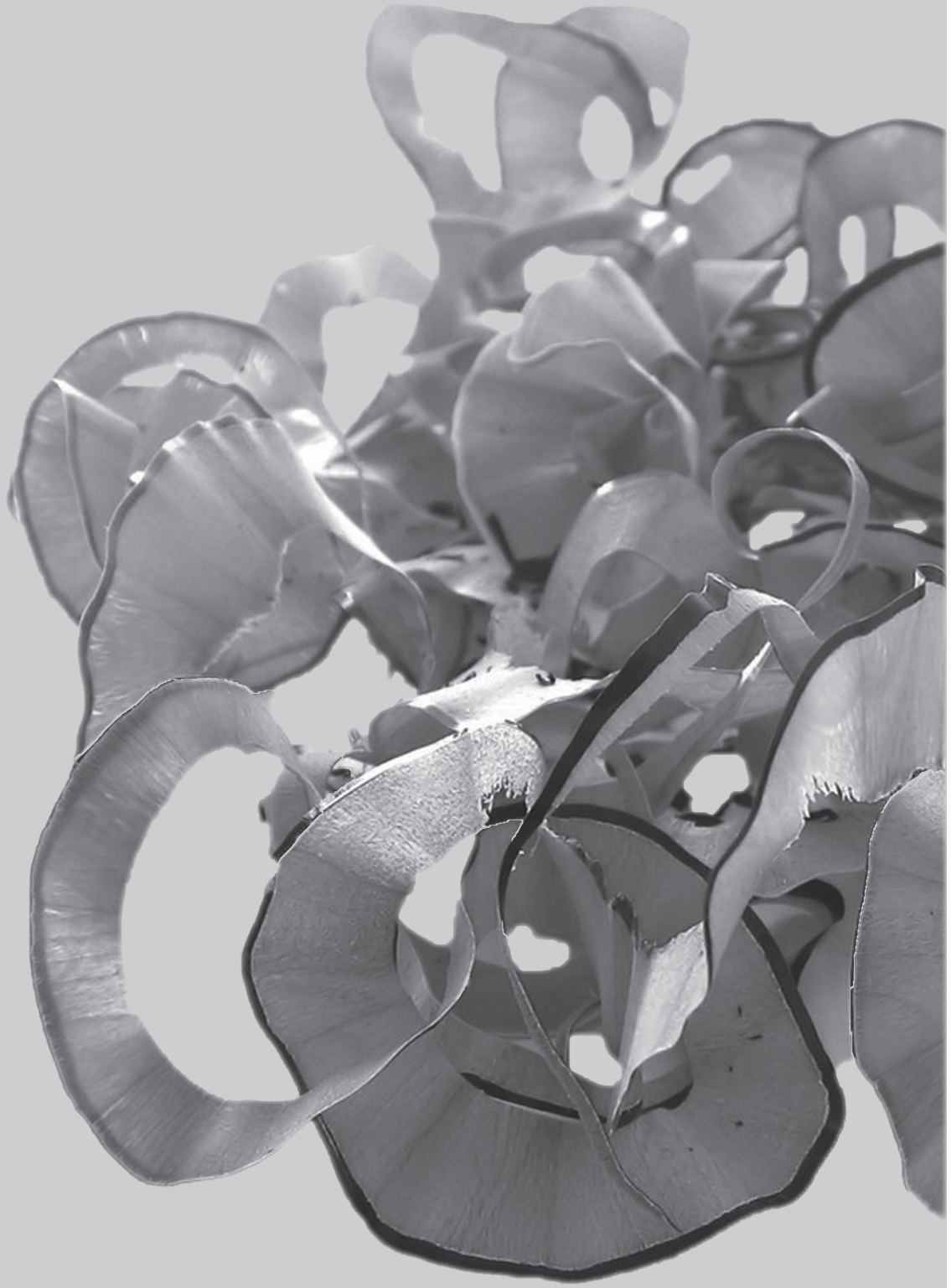

CHAPTER 1

General introduction

1. INTRODUCTION

Iron is an important nutrient for all forms of life. It can be incorporated into heme but also into iron sulpher clusters and plays a vital role in many metabolic processes such as DNA replication and repair, as a catalyst in biosynthesis, for respiratory electron transfer purposes and oxidative production of cellular energy (1-4). Iron present in heme is essential for life of higher organisms, as heme is a prominent component of the oxygen-transporting protein hemoglobin and iron in this heme complex serves as a carrier for oxygen (1-7). Therefore, an imbalance in iron metabolism may result in several pathological disorders. For instance, severe iron loss caused by for example bleeding, insufficient iron utilization due to chronic diseases or a disturbance in iron uptake from the gut can lead to iron deficiency and even to iron deficiency anemia (8, 9).
Iron deficiency is the most prevalent nutritional deficiency and the number one cause of anemia. The World Health Organization reported in 2008 that there were more than 1 billion people iron deficient and around 700 million people suffering from iron related anemia (10). Iron anemia can result in several symptoms such as impaired physical performance, overall weakness including fatigue and mental illnesses (11, 12). Even though iron is an imperative nutrient, excess iron could result in cell damage and ultimately in organ failure.

2. IRON METABOLISM

There is around 3 to 4 grams of iron present in the body of a healthy adult. More than 50% of the iron is incorporated in heme which in turn is a component of the proteins hemoglobin and myoglobin (13). Heme, which is present in meat, is therefore also one of the two dietary iron forms while the other being non-heme which can be found mainly in vegetables and grains (14). The prevalence of non-heme iron is much higher than that of heme iron, but the latter is absorbed up to 30% more efficiently (15). Dietary iron is mostly absorbed via the duodenum and upper jejunum to further be taken up by the epithelial cells or enterocytes of the intestine (16, 17). In order to replenish the iron lost because of period bleeding or during pregnancies, women absorb around 2 mg of iron per day while men absorb approximately 1 mg of iron per day (18). Non-heme iron is taken up by the enterocytes via the divalent metal-ion transporter 1 (DMT-1) (16, 19-21). As ferric iron is more common in food and has a lower aqueous solubility than ferrous iron, ferric iron is first reduced to its ferrous state before being absorbed. In contrary to non-heme iron, the exact absorption mechanism of heme iron is not completely understood, but it is assumed that heme binds to the brush border membrane of the duodenum enterocytes and is subsequently transported through the cell membrane via another transporter. It has been reported that the hemoglobin scavenging receptor CD163 (22), the lipoprotein

receptor-related proteins (LRP1) (23), the heme-responsive gene1 (HRG1) (24-26) and feline leukemia virus subgroup C receptor protein (FLVCR2) (27) might all play a role in the uptake of heme. The further iron internalization into cells have been studied in detail (28, 29). In short, once the iron is taken up by the enterocytes of the duodenum, it is either stored in ferritin or it can be transported into the blood circulation to bind to the protein transferrin, which is responsible for the distribution of the iron over the body. Iron is then absorbed by other cells via the transferrin receptor (TfR), which binds to transferrin in which iron is loaded. This binding occurs within clathrin-coated pits that subsequently fuse with the membranes of endosomes and release their content into these vesicles. The pH of the endosome is approximately 5 and after some shape changing of the iron-transferrin complex, because of the environmental conditions, the iron is then released as ferric iron. Next, the ferric iron is reduced to ferrous iron by the enzyme ferrireductase and transported via the metal transporter DMT1 into the cytoplasm. There, the ferrous iron enters the labile iron pool where it can be stored either as ferritin or incorporated into heme (28). The protein ferroportin then serves to transfer the iron from in- to outside the cell. Iron metabolism is mainly regulated by the hormone hepcidin which is produced in the hepatocytes of the liver (30). Hepcidin orchestrates the iron absorption and efflux by adjusting the levels of ferroportin. Circulating hepcidin, binds to ferroportin on the cell surface and degrades this protein. As a consequence, high levels of hepcidin results in a decrease of ferroportin and thus in less iron levels in the blood circulation (31).

3. IRON TREATMENTS

There are two common ways to treat iron deficiency, namely via oral iron delivery or via intravenous administration.
Oral supplementation is the most patient-friendly and cost-effective method for the treatment of iron deficiency. In general, oral iron is used in children, teenagers and in environments where there is a lack of resources (11). It is administered in case there is no adequate dietary iron supply or when there is no severe iron deficit. There are several oral iron products on the market available. Most of these products consist of iron salts such as ferrous sulfate, ferrous fumarate, ferrous succinate, ferrous gluconate and ferrous ascorbate with the first mentioned ferrous sulfate being the most commonly used (11, 32). Even though oral iron treatment can be a cost effective and readily available treatment for iron deficiency, it is not always feasible to use. The absorption of oral iron might be limited in patients suffering from malabsorption illnesses. Further, orally administered iron might cause side effects due to gastro intestinal intolerances and it is also not feasible in the case of severe blood loss (11, 33).
Intravenous iron products circumvent problems associated with the intestinal iron uptake and allow the delivery of large amounts of iron directly into the circulation.

Therefore, intravenous iron medications can be the treatment modality of choice in particularly in case of attained or hereditary decrease of intestinal iron uptake, in case of severe bleeding and high iron demand, in case of iron deficiency anemia due to the use of erythropoietin stimulant agents that is necessary during some chronic diseases and when oral iron medication is not tolerated (34).

Similar to oral iron delivery products, there are several parenteral iron replacement products on the market. These intravenous iron formulations are colloidal dispersions made up of polynuclear ferric-oxyhydroxide cores that are stabilized by several types of carbohydrate ligands such as mono, di, oligo and polysaccharides (35, 36). The current available intravenous iron preparations on the market are iron sucrose, iron gluconate, ferumoxytol, iron isomaltoside 1000, ferric carboxy-maltose, iron coated with low- and high molecular dextran, of which the latter is no longer used in many countries due to possibilities of severe allergic reactions (34,35). The pharmacokinetics and the subsequent processing of the iron products by the mono-nuclear phagocyte system are highly dependent on the carbohydrate surrounding the iron core as this coating is one of the determinants for the stability of the colloidal iron particles and thus the release of iron from the complex (7, 37-39). One of the reasons behind the safety concerns is that unstable iron complexes can result in secondary hemochromatosis (iron overload). Unlike primary hemochromatosis which is hereditary, secondary iron overload is caused by multiple blood transfusions, but also due to excess exogenous iron administration and uptake (40, 41). Iron plays an essential role in oxygen radical biochemistry (42). Five to 10% of the oxygen inhaled by humans is reduced to yield reactive oxygen species (ROS) such as superoxide-, hydrogen peroxide- and hydroxyl radicals (42). Relatively large concentrations of non-complex bound iron can result in an increase of non-transferrin bound iron (NTBI), which in turn can act as a strong redox catalyst for the Fenton reaction (38, 43). In the Fenton reaction, iron reacts with hydrogen peroxide to form a hydroxide ion and a hydroxyl free radical (28). This hydroxyl free radical in turn can further oxidize and cause severe damage to tissues and lead to several clinical complications (44). Therefore the formation of non-complex bound iron after administration of iron-based products should be avoided. It has been reported that the manufacturing process is of utmost importance for the stability and safety of iron-based medicinal products (45). A defined and validated manufacturing process is of great importance in order to minimize the possibility of obtaining unstable products and batch-to-batch variations. Mühlebach and Flühmann (2015) reported in detail the sensitive parameters and key steps that should be taken into consideration for the manufacturing of intravenous iron carbohydrate formulations (35). In short, the starting iron source material should be extensively controlled for chemical contaminations, the preparation conditions such as pH, temperature and reaction time as well as purification steps should be regulated and the final manufacturing steps like the container quality and sterilization should also be considered. Because of the above mentioned, Mühlebach and Flühmann further

elaborate on the fact that the manufacturing process therefore also can have an impact when developing iron-based generics, the so-called similars (35). For instance, studies comparing iron sucrose similars to the original iron sucrose product, non-clinical and clinical, have demonstrated significant variations between the iron sucrose products (46-49).

The European Medicine Agency (EMA) recognized that there were issues regarding the similarity between iron products and published in 2015 a final reflection paper indicating the requirements for assessing non-colloidal intravenous iron preparations in reference to an iron originator product (50). The EMA stated that the commonly used laboratory evaluations such as comparing plasma concentrations in animals or humans after administration of the product, as well as physicochemical evaluations such as iron complex particle size, structure, charge and surface characteristics, are not sufficient when evaluating iron formulations. This is supported by the fact that the results obtained from physicochemical parameters, do not elucidate on the *in-vivo* performance and fate of the iron formulations. As a result, besides the physicochemical characterization, elaborated non-clinical (including biodistribution) studies followed by clinical pharmacokinetics and efficacy/safety assessment should also be done (50).

The *in-vivo* non-clinical evaluations are necessary to get insight into iron metabolism and disposition, with the aim to assess possible safety differences of the various iron preparations, before clinical trials are set up and performed. Therefore, a suitable animal model (strain) should be defined and sensitive biomarkers should be determined.

4. AIM OF THE THESIS

Nano-colloidal iron based medicinal products have demonstrated to be complex formulations to be produced. It has been shown that these products exhibit differences in physicochemical properties as well as in their overall drug profile, when submitted to small manufacturing process variations (48, 51, 52). It is therefore of utmost importance to develop and define sensitive evaluation methods when original iron formulations with generics are compared from a pharmaceutical point of view. Several non-clinical animal studies have been previously published with the aim to compare the original iron sucrose product (Venofer®) to new iron sucrose similars. The objective of this thesis is to evaluate non-clinical *in-vivo* models that aim to assess safety profiles of intravenous iron products as these methods are not easy to standardize and the outcomes of the various studies are not in agreement regarding the superiority of the original iron sucrose product. Furthermore, it is interesting to investigate other possible methods such as magnetic resonance imaging (MRI) to obtain further insight into the iron biodistribution after intravenous iron administration. In addition a novel formulation for oral iron delivery, based on heme iron loaded into polymeric micelles, was developed

and characterized. This, with the aim to develop an oral iron replacement formulation with improved bioavailability and less side effects.

The research described in this dissertation was financially supported by Vifor (International) Ltd.

5. THESIS OUTLINE

As oral iron medicines can be an easy and more available iron therapeutic treatment compared to parenteral iron treatment, it is of interest to develop novel oral formulations that are more efficient while causing less side effects. In chapter 2, we developed an iron-complex formulation based on hemin-loaded polymeric micelles composed of the biodegradable and thermosensitive polymer, methoxy-poly(ethylene glycol)-b-poly[*N*-(2-hydroxypropyl) methacrylamide-dilactate]. In the subsequent chapters, we focused on intravenous iron treatments. Chapter 3 aims to compare previously published results from non-clinical studies of iron sucrose intravenous therapy. To this end, two experiments in which Venofer® was compared with two iron sucrose similars were performed in a similar experimental set-up as previously reported in literature. The outcome of this chapter was that the results obtained were difficult to standardize and thus to compare. Therefore in chapter 4, the rat strain (Sprague Dawley) that was used in our studies as well as in the previously published ones, was in depth analyzed, with the aim, to assess whether this model is suitable to conduct comparative studies of iron based nano-particle products. To this end, a dose effect of Venofer® (iron sucrose) and of Ferrlecit® (sodium ferric gluconate) was studied in male Sprague Dawley rats. The latter iron product was included as positive control since Ferrlecit® has been reported to be less stable than Venofer® and thus can result in higher iron related toxicity. In chapter 5, we investigated the potential of magnetic resonance imaging to evaluate the biodistribution of exogenous iron within 24 hours after one single injection of Venofer® (iron sucrose). Finally, chapter 6 discusses the various iron treatments, pre-clinical iron therapy evaluation methods and makes recommendations for future research on iron formulations.

6. REFERENCES

1. Rouault TA. Iron-sulfur proteins hiding in plain sight. Nature Chemical Biology. 2015;11:442-5.
2. Lill R. Function and biogenesis of iron–sulphur proteins. Nature. 2009;460:831-8.
3. Sheftel A, Stehling O, Lill R. Iron–sulfur proteins in health and disease. Trends in Endocrinology & Metabolism. 2010;21(5):302-14.
4. Gozzelino R, Jeney V, Soares MP. Mechanisms of cell protection by heme oxygenase-1. Annual Review of Pharmacology and Toxicology. 2010;50:323-54.
5. Macdougall IC, Geisser P. Use of intravenous iron supplementation in chronic kidney disease: an update. Iranian Journal of Kidney Diseases. 2013;7(1):9-22.
6. Schiesser D, Binet I, Tsinalis D, Dickenmann M, Keusch G, Schmidli M, Ambühl PM, Lüthi L, Wüthrich RP. Weekly low-dose treatment with intravenous iron sucrose maintains iron status and decreases epoetin requirement in iron-replete haemodialysis patients. Nephrology Dialysis Transplantation. 2006;21(10):2841-5.
7. Elford P, Bouchard J, Jaillet L, Pearson N, Rogue A, Sabadie C, Forster R. Biodistribution and predictive hepatic gene expression of intravenous iron sucrose. Journal of Pharmacological and Toxicological Methods. 2013;68(3):374-83.
8. Camaschella C. Iron-Deficiency Anemia. New England Journal of Medicine. 2015;372(19):1832-43.
9. Mircescu G, Critchon RR, Geisser P. Iron therapy in renal anaemia. International Medical Publishers. Uni-Med, London. 2013; 1st Edition.
10. Benoist de B, McLean E, Egli Ines, Cogswell M. Worldwide prevalence of anaemia 1993-2005: WHO global database on anaemia. 2008.
11. Schrier SL, Auerbach M, Mentzer WC, Tirnauer JS. http://www.uptodate.com/contents/treatment-of-iron-deficiency-anemia-in-adults. 2016; Accessed Nov 2017.
12. Muñoz M, Gomez-Ramirez S, Liumbruno GM, Grazzini G. Intravenous iron and safety: is the end of the debate on the horizon? Blood Transfusion. 2014;12:287-9.
13. Ganz, T. Systemic iron homeostasis. Physiological Reviews. 2013;93:1721-41.
14. Sharp PA. Intestinal iron absorption: regulation by dietary and systemic factors. International Journal for Vitamin and Nutrition Research. 2010;80:231–42.
15. Villarroel P, Flores S, Pizarro F, de Romaña D, Arredondo M. Effect of dietary protein on heme iron uptake by Caco-2 cells. European Journal of Nutrition. 2011;50(8):637-43.
16. Collins JF, Anderson GJ. Intestinal iron absorption. In: Johnson LR, Ghishan FK, Kaunitz J, Merchant JL, Said HM, Wood JD. Physiology of the gastrointestinal tract. Elsevier, New York. 2012; 5th Edition: 1921-47.
17. Frazer DM, Anderson GJ. Iron Imports. I. Intestinal iron absorption and its regulation. American Journal of Physiology - Gastrointestinal and Liver Physiology. 2005;289(4):G631-G5.
18. Leong W-I, Lonnerdal B. Iron nutrition. In: Anderson GJ, McLaren GD. Iron physiology and pathophysiology in humans. Springer, New York. 2012;81–99.

19. Courville P, Chaloupka R, Cellier MF. Recent progress in structure–function analyses of Nramp proton-dependent metal ion transporters. Biochemistry and Cell Biology. 2006;84(6):960-78.
20. Atanasova BD, Li AC, Bjarnason I, Tzatchev KN, Simpson RJ. Duodenal ascorbate and ferric reductase in human iron deficiency. The American Journal of Clinical Nutrition. 2005;81(1):130-3.
21. Latunde-Dada GO, Simpson RJ, McKie AT. Duodenal Cytochrome B Expression Stimulates Iron Uptake by Human Intestinal Epithelial Cells. The Journal of Nutrition. 2008;138(6):991-5.
22. Kristiansen M, Graversen JH, Jacobsen C, Sonne O, Hoffman H-J, Law SKA, Moestrup SK. Identification of the haemoglobin scavenger receptor. Nature. 2001;409:198-201.
23. Hvidberg V, Maniecki MB, Jacobsen C, Højrup P, Møller HJ, Moestrup SK. Identification of the receptor scavenging hemopexin-heme complexes. Blood. 2005;106(7):2572-9.
24. Rajagopal A, Rao AU, Amigo J, Tian M, Upadhyay SK, Hall C, Uhm S, Mathew MK, Fleming MD, Paw BH, Krause M, Hamza I. Haem homeostasis is regulated by the conserved and concerted functions of HRG-1 proteins. Nature. 2008;453:1127.
25. Latunde-Dada GO, Takeuchi K, Simpson RJ, McKie AT. Haem carrier protein 1 (HCP1): Expression and functional studies in cultured cells. FEBS Letters. 2006;580(30):6865-70.
26. Shayeghi M, Latunde-Dada GO, Oakhill JS, Laftah AH, Takeuchi K, Halliday N, Khan Y, Warley A, McCann FE, Hider RC, Frazer DM, Anderson GJ, Vulpe CD, Simpson RJ, McKie AT. Identification of an Intestinal Heme Transporter. Cell. 2005;122(5):789-801.
27. Duffy SP, Shing J, Saraon P, Berger LC, Eiden MV, Wilde A, Tailor CS. The Fowler Syndrome-Associated Protein FLVCR2 Is an Importer of Heme. Molecular and Cellular Biology. 2010;30(22):5318-24.
28. Crichton RR, Danielson BG, Geisser P. Iron therapy: With special emphasis on intravenous administration. Uni-Med, Bremen. 2008; 4th Edition: 81-2.
29. Evstatiev R, Gasche C. Iron sensing and signalling. Gut. 2012;61(6):933-52.
30. Park CH, Valore EV, Waring AJ, Ganz T. Hepcidin, a Urinary Antimicrobial Peptide Synthesized in the Liver. Journal of Biological Chemistry. 2001;276(11):7806-10.
31. Nemeth E, Tuttle MS, Powelson J, Vaughn MB, Donovan A, Ward DM, Ganz T, Kaplan J. Hepcidin Regulates Cellular Iron Efflux by Binding to Ferroportin and Inducing Its Internalization. Science. 2004;306(5704):2090-3.
32. Comparison of oral iron supplements. Pharmacist's Letter/Prescriber's Letter 2008;24(8):240811.
33. Huch R.; Schaefer R. Iron Deficiency and Iron Deficiency Anaemia. Thieme Medical Publishers, New York; 2006.
34. Bugnara C, Beris P. ESH Handbook on Disorders of Iron Metabolism; 2009 Edition: 513-529.
35. Mühlebach S, Flühmann B. Iron Carbohydrate Complexes: Characteristics and Regulatory Challenges. In: Crommelin D, de Vlieger J. Non-Biological Complex Drugs. AAPS Advances in the Pharmaceutical Sciences Series. Springer. 2015:(20);149-170.
36. Auerbach M, Ballard H. Clinical Use of Intravenous Iron: Administration, efficacy and safety.

ASH Education Program Book. 2010;338-347.
37. Neiser S, Rentsch D, Dippon U, Kappler A, Weidler, PG, Gottlicher J, Steininger R, Wilhelm M, Braitsch M, Funk F, Philipp E, Burckhardt S. Physico-chemical properties of the new generation IV iron preparations ferumoxytol, iron isomaltoside 1000 and ferric carboxymaltose. Biometals, 2015;28(4):615-35.
38. Koskenkorva-Frank TS, Weiss G, Koppenol WH, Burckhardt S. The complex interplay of iron metabolism, reactive oxygen species, and reactive nitrogen species: insights into the potential of various iron therapies to induce oxidative and nitrosative stress. Free Radical Biology & Medicine. 2013;65:1174-94.
39. Bailie GR, Schuler, C, Leggett RE, Li H, Li H-D, Patadia H, Levin R. Oxidative effect of several intravenous iron complexes in the rat. BioMetals. 2013;26(3):473-478.
40. Bacon BR, Adams PC, Kowdley KV, Powell LW, Tavill AS. Diagnosis and management of hemochromatosis: Practice Guideline by the AASLD. Hepatology. 2011;54(1):328-43.
41. Fleming RE, Ponka P. Iron Overload in Human Disease. New England Journal of Medicine. 2012;366(4):348-59.
42. Geisser P. Iron Therapy: with Special Emphasis on Oxidaitive Stress. Georg Thieme Verlag, Stuttgart. 1996.
43. Gutteridge JMC, Rowley DA, Halliwell B. Superoxide-dependent formation of hydroxyl radicals and lipid peroxidation in the presence of iron salts: detection of 'catalytic' iron and anti-oxidant activity in extracellular fluids. Biochemical Journal. 1982;206:605-9.
44. Crielaard BJ, Lammers T, Rivella S. Targeting iron metabolism in drug discovery and delivery. Nature Reviews Drug Discovery. 2017;16:400-423.
45. Schellekens H, Klinger E, Muhlebach S, Brin JF, Storm G, Crommelin DJ. The therapeutic equivalence of complex drugs. Regulatory Toxicology and Pharmacology. 2011;59:176-183.
46. Toblli, JE, Cao, G, Oliveri, L, Angerosa, M. Differences between original intravenous iron sucrose and iron sucrose similar preparations. Arzneimittelforschung. 2009;59:176-190.
47. Toblli JE, Cao G, Oliveri L, Angerosa M. Differences between the original iron sucrose complex Venofer® and the iron sucrose similar Generis®, and potential implications. Portuguese Journal of Nephrology and Hypertension. 2009;23:53-63.
48. Toblli JE, Cao G, Oliveri L, Angerosa M. Comparison of oxidative stress and inflammationinduced by different intravenous iron sucrose similar preparations in a rat model. Inflamm Allergy. Drug Targets. 2012;11(1):66-78.
49. Rottembourg J, Kadri A, Leonard E, Dansaert A, Lafuma A. Do two intravenous iron sucrose preparations have the same efficacy?. Nephrology Dialysis Transplantation. 2011;26(10):3262-67.
50. EMA, 2015. Reflection Paper on the Data Requirements for Intravenous Iron-based Nano-colloidal Products Developed with Reference to an Innovator Medicinal Product. 2015; EMA/CHMP/SWP/620008/2012. http://www.ema.europa.eu/docs/en_GB/document_library/Scientific_guideline/2015/03/WC500184922.pdf
51. Lee ES, Park BR, Kim JS, Choi GY, Lee JJ, Lee IS. Comparison of adverse event profile of

intravenous iron sucrose and iron sucrose similar in postpartum and gynecologic operative patients. Current Medical Research and Opinion. 2013;29(2):141-7.
52. Stein J, Dignass A, Chow KU. Clinical case reports raise doubts about the therapeutic equivalence of an iron sucrose similar preparation compared with iron sucrose originator. Current Medical Research and Opinion. 2012;28(2):241-3.

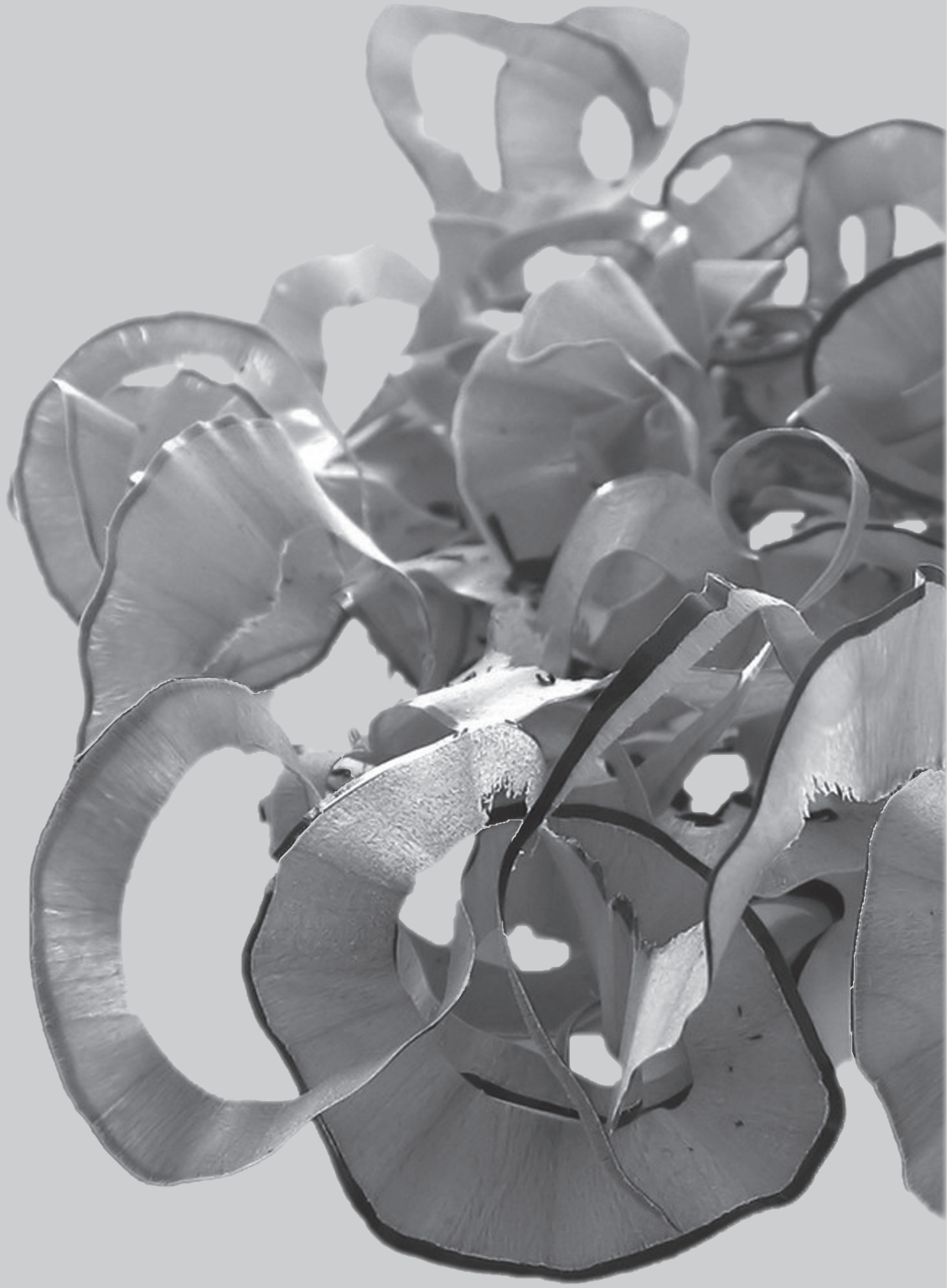

CHAPTER 2

A Novel Oral Iron- Complex Formulation: Encapsulation of Hemin in Polymeric Micelles and its *in-vitro* Absorption

Kimberley Span*, Johan J.F. Verhoef*, Hedi Hunt, Cornelus F. van Nostrum, Vera Brinks, Huub Schellekens, Wim E. Hennink
*equal contribution

Published in European Journal of Pharmaceutics and Biopharmaceutics. 2016;108:226-34

Abstract

Anemia resulting from iron deficiency is one of the most prevalent diseases in the world. As iron has important roles in several biological processes such as oxygen transport, DNA synthesis and cell growth, there is a high need for iron therapies that result in high iron bioavailability with minimal toxic effects to treat patients suffering from anemia. This study aims to develop a novel oral iron-complex formulation based on hemin-loaded polymeric micelles composed of the biodegradable and thermosensitive polymer methoxy-poly(ethylene glycol)-b-poly(*N*-(2-hydroxypropyl) methacrylamide-dilactate), abbreviated as mPEG-*b*-p(HPMAm-Lac_2). Hemin-loaded micelles were prepared by addition of hemin dissolved in DMSO:DMF (1:9, one volume) to an aqueous polymer solution (nine volumes) of mPEG-*b*-p(HPMAm-Lac_2) followed by rapidly heating the mixture at 50°C to form hemin-loaded micelles that remain intact at room and physiological temperature. The highest loading capacity for hemin in mPEG-*b*-p(HPMAm-Lac_2) micelles was 3.9%. The average particle diameter of the hemin-micelles ranged from 75 to 140 nm, depending on the concentration of hemin solution that was used to prepare the micelles. The hemin-loaded micelles were stable at pH 2 for at least 3 hours which covers the residence time of the formulation in the stomach after oral administration and up to 17 hours at pH 7.4 which is sufficient time for uptake of the micelles by the enterocytes. Importantly, incubation of Caco-2 cells with hemin-micelles for 24 hours at 37°C resulted in ferritin levels of 2500 ng/mg protein which is about 10 fold higher than levels observed in cells incubated with iron sulfate under the same conditions. The hemin formulation also demonstrated superior cell viability compared to iron sulfate with and without ascorbic acid. The study presented here demonstrates the development of a promising novel iron complex for oral delivery.

1. INTRODUCTION

Anemia is one of the most common health problems at present. According to the World Health Organization the prevalence of anemia is dependent on ethnic groups and geographic location, but it is assumed that 50% of these cases is because of iron deficiency (1). This occurrence is similar for both developing and developed nations and can arise due to various reasons such as pregnancy, growth in children and diseases that cause low iron bioavailability from the diet (2-4).

A healthy iron metabolism is important as iron is the main mineral involved in oxygen transport, DNA synthesis, cell growth and survival (5, 6). The iron homeostasis is primarily regulated by intestinal absorption as the uptake of iron takes place predominately in the duodenum and upper jejunum by enterocytes. This absorption is regulated by the hormone hepcidin that is produced in hepatocytes of the liver and binds to the iron transporter protein ferroportin that carries iron from the duodenal enterocytes into the circulation (7). It is known that hepcidin binding to the iron transporter leads to its degradation, therefore augmented hepcidin production results in less ferroportin and thus less iron transportation (export). As a consequence a decrease of iron absorption and efflux from the enterocytes occurs. This incidence results in a disturbed iron homeostasis and ultimately could cause less iron in the circulation (8-10). Due to the importance of a balanced iron metabolism, it is of interest to develop therapies that can remediate iron deficiency. There are two forms of dietary iron, namely non-heme iron that is present in vegetables and grains, and there is heme iron that is predominately found in red meat in the form of hemoglobin and myoglobin (11). It is known that even though the prevalence of non-heme iron is higher than the heme form, the latter is being absorbed up to 30% more effectively (12). Nevertheless, because non-heme iron supplements are relatively cheap and easy to produce, the pharmaceutical industry has developed several oral formulations based on iron salts such as iron sulfate. However, these formulations are associated with various side effects such as gastrointestinal disturbances which are probably caused by the redundant amount of iron in the preparations that remain unabsorbed in the colon (13). There is consequently an urgent need for more advanced oral preparations with higher bioavailability and less side effects. Many studies have explored the possibilities of novel therapies based on non-heme iron, but even though there are some heme-iron based oral iron medications on the market such as Proferrin (heme iron polypeptide), far less research has been done exploiting heme-iron for oral supplementation (6, 14). Unlike non-heme iron which is taken up by enterocytes via the divalent metal transporter 1 (DMT1), the exact uptake mechanism for heme remains elusive. It is, however, generally accepted that heme binds to the brush border membrane of the duodenum enterocytes and is subsequently transported by a different transporter as non-heme iron through the cell membrane to the cytoplasm (15-17). The assumption that heme is recognized by a heme-transporter opens possibilities to investigate other

sources for iron supplementation containing structures similar to heme such as ferric protoporphyrin IX chloride (hemin). Hemin in contrast to heme contains a chloro ligand attached to the iron center (structure is shown in figure 1). This compound is essentially insoluble in water of neutral pH and soluble in solutions of sodium hydroxide due to the substitution of the chloro ligand by a hydroxyl group resulting in the formation of hematin (18). The prominent factors for the development of a novel oral therapy would be improving the stability, bioavailability and solubility of the iron supplement (19). Thus, in order to exploit hemin for oral iron therapy, the first challenge to tackle is to solubilize it in aqueous medium of physiological pH. Moreover a suitable formulation has to resist the harsh environment of the gastrointestinal tract.

Especially nano-sized drug delivery systems have shown to be able to encapsulate several hydrophobic substances while increasing the uptake of the loaded drug and protecting it from degradation while passing through the gastrointestinal tract (20-22). There is a wide range of nanoparticles based on liposomes and on natural as well as synthetic polymers that have been investigated for the encapsulation of hydrophobic drugs (23-25). Within our department a novel class of thermosensitive biodegradable block copolymers based on methoxy-poly(ethylene glycol)-b-poly(*N*-(2-hydroxypropyl) methacrylamide-dilactate) (mPEG-*b*-p(HPMAm-Lac_2) has been developed , which under certain conditions form micelles consisting of a hydrophobic core, in which hydrophobic drugs can be solubilized and a hydrophilic corona, making these particles water dispersible (26, 27; 30, 31). mPEG-b-(HPMAm-Lac2) consists of the hydrophilic polymer mPEG and poly(HPMAm-Lac2). The latter polymer is thermosensitive and, when dissolved in water, exhibits a lower critical solution temperature (LCST) (27), as has also been described for polymers such as poly(*N*-isopropylacrylamide) and elastin-like peptides (28, 29). Below the LCST poly(HPMAm-Lac2) 13 °C, water molecules are bound to the polymer chains and prevents intra- and inter polymer interactions resulting in a water-soluble polymer. When the polymer solution is heated above its LCST, water is expelled and the polymer chains become hydrophobic resulting in precipitation (27). Therefore, in the present study we investigated whether these micelles can also encapsulate the hydrophobic hemin and thus be used as a potential oral iron formulation. To this end, hemin was encapsulated in mPEG-*b*-p(HPMAm-Lac_2) micelles via a rapid heating method. The formed micelles were characterized for encapsulation efficiency, loading capacity and particle size. Furthermore, the stability of the loaded micelles at different pH and also the physical state of hemin within the micelles was investigated. Finally, Caco-2 cells were incubated with the micelles to assess iron uptake in comparison to the commonly used iron supplement, iron sulfate.

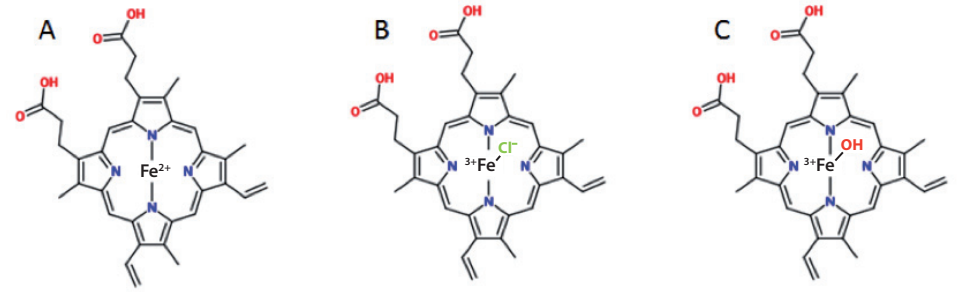

Figure 1. Molecular structure of (A) heme; (B) hemin and (C) hematin

2. MATERIALS AND METHODS

2.1 Materials

Hemin (molecular weight = 651.9 g/mol), ammonium acetate, iron (II) sulfate heptahydrate; $FeSO_4.7H_2O$, sodium hydroxide, sodium bicarbonate, ascorbic acid, saponin and tetrazolium salt XTT (sodium 2,3-bis(2-methoxy-4-nitro-5-sulfophenyl)-2H-tetrazolium-5-carboxanilide) were all purchased from Sigma Aldrich (Zwijndrecht, The Netherlands). Dimethylsulfoxide (DMSO) and dimethylformamide (DMF) were obtained from Biosolve Ltd. (Valkenswaard, The Netherlands). Phosphate buffered saline (PBS) pH 7.4 containing per liter 8.2 g NaCl, 3.1 g $Na_2HPO_4{\cdot}12H_2O$ and 0.3 g $NaH_2PO_4{\cdot}2H_2O$ was from Braun Melsungen AG (Melsungen, Germany).

Methoxy-poly(ethylene glycol)-*b*-poly(*N*-(2-hydroxypropyl) methacrylamide-dilactate) (abbreviated as mPEG-*b*-p(HPMAm-Lac2); Molecular weight of mPEG = 5000 g/mol) was synthesized as described by Soga et al. (26). Regenerated cellulose syringe filters (0.45 µm) were purchased from Grace Davision Discovery Science. Vivaspin centrifugal concentrator tubes with 50,000 MWCO filter were obtained from Sartorius AG (Goettingen, Germany). The Caco-2 cell line was generously provided by M.A.M Oosterveer-van der Doelen (Faculty of Veterinary Medicine, Utrecht University). Dulbecco's Modified Eagle's Medium, Minimum Essential Medium, antibiotic antimycotic cell culture solution consisting of amphotericin B and penicillin, non-essential amino acids and RIPA buffer were obtained from Invitrogen (Breda, The Netherlands). Micro BCA_{TM} protein assay and Ferritin Human ELISA kit (ab 108837) were purchased from Pierce (Rockford, USA) and Abcam (Cambridge, United Kingdom). Rabbit polyclonal Anti-LAMP1 IgG - Lysosome Marker (ab24170) and Goat polyclonal Anti-Rabbit IgG H&L (Alexa Fluor® 488) (ab150077) were purchased from Abcam (Cambridge, United Kingdom). Methacryloxyethyl thiocarnamoyl rhodamine B was purchased from Polysciences Europe. Leica Confocal microscopy with Leica application suite advanced fluorescence (LAS AF) light software was used to visualize cellular uptake of labelled micelles.

2.2 Preparation of hemin-loaded micelles

Hemin-loaded mPEG-*b*-p(HPMAm-Lac$_2$) micelles were prepared via the "rapid heating method" essentially as described by Neradovic et al. (32) and by Rijcken et al. (27) with some modifications. In short, the polymer was dissolved at a concentration of 2 mg/ml in 120 mM ammonium acetate pH 5 in a glass vial and stirred on ice for 1 hour. 120 mM ammonium acetate pH 5 was prepared by dissolving 0.925 grams of ammonium acetate in 100 ml purified water. The pH of this solution was subsequently adjusted with 0.1 N HCl to pH 5. This solvent was used as at this pH the hydrolysis of the lactate groups is limited, resulting in a high stability of the micelles (36). Next the mixture was stored overnight at 4 °C and subsequently stirred for 15 minutes on ice and kept on ice until the micelles were made. This procedure was followed to ensure that the polymer solution remained below the critical micelle temperature (CMT) of 4 °C. Solutions of 0.4 - 2 mg/ml hemin in a mixture of DMSO:DMF (1:9 v/v) were freshly made and also kept on ice. Subsequently, 0.1 ml of hemin solution was added to 0.9 ml of polymer solution, vortexed for 4 seconds and the hemin/polymer mixture was then transferred into a water bath of 50 °C and hemin loaded micelles were formed under vigorous shaking for 1 minute. Finally, after cooling to room temperature, the hemin-loaded micelles were filtered through a 0.45 µm filter to remove precipitated, non-encapsulated, hemin.

2.3 Determination of hemin loading capacity and encapsulation efficiency of the micelles

The concentration of hemin encapsulated in the micelles was measured via UV-spectrophotometric analysis (Spectrostar BMG Labtech). A sample of the micellar dispersion was diluted 10x in DMSO to disintegrate the micelles and solubilize the encapsulated hemin. A calibration curve of hemin standards was made in a concentration range of 0-50 µg/ml in DMSO. The samples and the standards were measured at a wavelength of 388 nm and the concentration of encapsulated hemin was determined using the calibration curve. The encapsulation efficiency (EE%) and the loading capacity (LC%) were calculated as follows:

$$EE = \frac{\text{concentration hemin measured}}{\text{concentration of the hemin added}} \times 100\%$$

$$LC = \frac{\text{concentration hemin measured}}{\text{concentration (hemin measured + polymer added)}} \times 100\%$$

2.4 Dynamic light scattering

The size and polydispersity index of the micelles were measured using dynamic light scattering (DLS) using a ALV / CGS-3 (ALV gmbh, Langen Germany) with a JDS Uniphase laser functioning at a wavelength of 632.8 nm, an optical fiber-based detector, a digital ALV/LSE 5003 correlator and a temperature controller set at 25 °C. The refractive index and viscosity used for the data treatment were respectively 1.333 and 0.89 cp. All measurements were performed at a 90 ° angle. The Z-average mean particle size (Z_{ave}) and the polydispersity were calculated using the ALV-60 0 V.3.X software. The samples were made by diluting 10 to 20 µl micelle dispersion in 1 ml of 120 mM ammonium acetate pH 5.

2.5 Physical state of hemin in the micelles

Hemin-loaded micelles with the highest loading capacity and encapsulation efficiency were made as described in section 2.2. In detail, 0.1 ml of 120 µg/ml hemin in DMSO:DMF (1:9) was added to 0.9 ml of 1.8 mg/ml mPEG-*b*-p(HPMAm-Lac$_2$) in 120 mM ammonium acetate pH 5. Hemin was also dissolved in DMSO to obtain the same hemin concentration as the diluted micelle sample. UV-VIS spectra (λ 200 – 700 nm) of the solutions were recorded.

2.6 Stability of hemin-loaded micelles

The stability of hemin-loaded micelles at pH 2 and pH 7.4 at 37 °C was determined by measuring the particle size (Z_{ave}) and polydispersity for 17 hours. For the stability at pH 2, the hemin-loaded micelles were formed in 120 mM ammonium acetate pH 5 as described in section 2.2 followed by lowering to pH 2 by addition of 4 M HCl. To determine the stability of the hemin-loaded micelles at pH 7.4, the polymer was dissolved in PBS pH 7.4 containing 8.2 g NaCl, 3.1 g $Na_2HPO_4 \cdot 12H_2O$ and 0.3g NaH_2PO_4 $2H_2O$ per liter.

2.7 Synthesis of mPEG-*b*-p((HPMAm-Lac$_2$)-co-RhodMA

Rhodamine labeled mPEG-*b*-p(HPMAm-Lac$_2$) was synthesized according to a previously reported polymerization procedure (33, 34). In short, methacryloxyethyl thiocarnamoyl rhodamine B and HMPA-Lac$_2$ (molar ratio 1:99) together with $(mPEG)_2$ –ABCPA macroinitiator in a molar ratio of initiator to monomer of 1:150 were dissolved in 3 ml acetronitril (ACN) at a scale of 700 mg monomer. The mixture was flushed for 15 minutes with nitrogen at room temperature and subsequently stirred overnight at 70 °C. Next, the formed polymer was precipitated in diethyl ether and then dissolved in water. Dialysis was done for two days against ACN: H_2O (1:1), three days against THF:H_2O

(1:1) and 4 days against H_2O in order to purify the polymer and remove low molecular weight impurities. The dialysis medium was refreshed 3 times a day. After dialysis, the rhodamine labeled polymer was recovered by lyophilization and characterized via ^1H NMR and GPC as described by Soga et al. (26) and Rijcken et al. (27).

2.8 *In-vitro* cell studies

2.8.1 Caco-2 cell culture

The Caco-2 cells were cultured in Dulbecco´s Modified Eagle´s Medium (DMEM) containing 3.7 g/L sodium bicarbonate, 4.5 g/L glucose completed with 10 % fetal bovine serum (FBS), 1 % antibiotics/antimycotics (100 IU penicillin G sodium/ml, 100 µg/ml streptomycin sulfate and 0.25 µg/ml amphotericin B) and 1 % non-essential amino acids. The cells were seeded at a density of 100,000 cells per cm^2 on polystyrene well plates at 37 °C in a humidified atmosphere containing 5 % CO_2 and were allowed to differentiate for 14 days prior the experiments. Medium was replaced every 2-3 days.

2.8.2 Sample preparation for cellular uptake studies

Hemin-loaded micelles with the highest loading capacity and encapsulation efficiency were made as described in section 2.2 and 2.3. Multiple dispersions of 1 ml were pooled and concentrated using viva spin centrifugal concentrator tubes (cut-off 50.000 kDa, Santorius Stedim, Germany) for 40 minutes at 4,000 x *g*, resulting in micellar dispersions concentrated around 70 times.

The concentration of hemin in the micellar concentrate was determined by diluting the micellar dispersion 40x in PBS and then further diluting 10x in DMSO. Next, UV-spectroscopy at 388 nm was used to determine the hemin concentration. This hemin-loaded micellar dispersion was used to perform dose response and time dependent cellular uptake as well as cytotoxicity studies. The volume of the micellar dispersion needed for the dose response and time dependent uptake studies was adjusted to 150 µl with PBS and mixed with 1350 µL cell culture medium to obtain 1.5 ml sample mixtures with concentrations of 10 – 200 µM hemin. The hemin micellar formulations were added to the Caco-2 cells and incubated for 24 hours, unless otherwise stated, at 37 °C humidified atmosphere containing 5 % CO_2. For the iron sulfate samples or iron sulfate combined with ascorbic acid in a molar ratio of (1:5), the necessary amount was dissolved in 150 µl PBS and mixed with 1350 µL cell culture medium to obtain iron sulfate solutions with concentration ranging from 10 to 200 µM.

2.8.3 Cellular uptake studies

After incubation of the Caco-2 cells with hemin-loaded micelles and iron sulfate

formulations for 24 hours, the medium was removed and the cells were washed with PBS. The cells were then lysed with 350 µl RIPA buffer supplemented with a 1 % proteinase inhibitor cocktail. The lysed cells were stored at -20 °C until analyzed. Prior to analysis, the cells were thawed and spun down at 20.000 rpm for 15 minutes. Next, the protein concentration of the samples was measured using a Micro BCA protein assay kit (Pierce, Rockford USA). A dilution range of 1-200 µg/ml bovine serum albumin was used for calibration. In order to assess the iron uptake, the total ferritin content of the cell lysates was measured using a double sandwiched ELISA against human ferritin kit (ab 108837 Abcam, Cambridge United Kingdom). Both the protein and ferritin assays were performed according to the manufacturer's protocol.

2.8.4 Cell viability

The viability of the Caco-2 cells after incubation with the different formulations was assessed using a yellow tetrazolium salt XTT colorimetric assay that measures the metabolic activity of cells as first described by Scudiero et al. (35). In short, Caco-2 cells were seeded at a density of 20,000 cells/well in a 96 well plate and incubated at 37 °C. After 24 hours, the cell culture medium was removed and replaced by an iron sample mixture of 150 µl, consisting of 100 µl medium and 50 µl made up of a volume of the different iron sample needed to obtain different concentrations adjusted with PBS. The cells were incubated for 24 hours and then washed with PBS. Next, 50 µl of fresh medium and 50 µl of XTT solution were added to the cells, which were subsequently incubated for 1 hour at 37 °C. Finally, the plates were measured using UV-spectroscopy at a wavelength of 490 nm and the relative cell survival after 24 hours treatment was compared to non-treated Caco-2 cells.

2.8.5 Intracellular localization of hemin-loaded micelles

A rhodamine labeled polymer was synthesized as described in section 2.7 and the hemin loaded (mPEG-*b*-p((HPMAm-Lac_2)-*co*-RhodMA) micelles were prepared as described in section 2.2 except that the rhodamine labeled polymer was dissolved in PBS pH 7.4 instead of 120 mM ammonium acetate. The Caco-2 cells were seeded at a density of 50,000 cells/well in a 16-well glass chamber slide system (Lab-Tek; chamber slide™ system 178599) and grown for 5 days in an incubator at 37 °C to reach 80% confluency. The rhodamine micelles dispersion was then diluted 4x with phenol red free DMEM culture medium. Next, the cells were incubated with the diluted dispersion for 3 hours and subsequently the medium was replaced and the cells were washed twice with PBS. The Caco-2 cells were subsequently fixed with 4 % paraformaldehyde for 30 minutes, the fixative was then discarded and the cells were washed again twice with PBS. Binding buffer was made by preparing a stock solution of 50 mg Saponin from Sigma Aldrich

and 100 mg BSA in 50 ml PBS. After the Caco-2 cells were fixed they were quenched for 10 minutes with 50 nM NH_4Cl dissolved in water and washed twice with PBS. The binding buffer was then added to the cells and incubated for 30 minutes at room temperature. Next the primary antibody LAMP-1 to stain lysosomes, was dissolved in binding buffer (1 µg/ml). This antibody solution was then pipetted onto the cells and incubated for 60 minutes at room temperature. Subsequently, the secondary antibody Alexa-488 was used to detect the binding of the primary antibody and was dissolved in binding buffer (10 µg/ml). After 60 minutes of incubation with the primary antibody at room temperature, the Caco-2 cells were washed 4 x with PBS and the secondary antibody conjugated to Alexa-488 was added and incubated for 60 minutes. Finally, the cells were washed 3 times with PBS and once with Milli-Q ultrapure water and then mounted on the glass chamber slide system using FluorSave from Calbiochem, San Diego. Confocal microscopy was used to visualize the uptake of the rhodamine labeled micelles by measuring the red color within the cells and also to visualize lysosomes as the LAMP-1 antibody staining produced a green color.

3. RESULTS and DISCUSSION

3.1 Characterization of mPEG-*b*-p(HPMAm-Lac_2) block copolymer

Synthesis and characterization of mPEG(5000)-*b*-p(HPMAm-Lac2) block copolymer was performed and characterized as described by Soga et al. (26, 36). The polymer was obtained in a yield of 73 % and the number average molecular weight as determined by NMR analysis was 17400 g/mol. GPC analysis of the polymer (using PEG calibration) gave a number average molecular weight of 18500 g/mol, the weight average molecular weight was 37200 g/mol and the dispersity (*Đ*) was 2.0 which is close to earlier reported data (36).

3.2 Preparation and characterization of hemin loaded micelles

Hemin-loaded micelles with different loadings of hemin were prepared as described in section 2.2 by addition of a small volume of hemin in DMSO to a cold aqueous polymer solution (1.8 mg/ml, which is far above the critical micelle concentration (CMC) of 0.015 mg/ml as reported for this polymer (36)), followed by rapidly heating the solution to 50 °C. After filtration to remove non-encapsulated hemin, the obtained particles were characterized for hemin loading, size and size distribution. When no polymer was present, the addition of the DMSO/hemin solution to water resulted in the formation of large aggregates as shown in figure 2C. In contrast, when adding the hemin solution to the polymer solution the encapsulation capacity of the micelles was obvious since a brownish micellar dispersion free of aggregates was obtained (figure 2D).

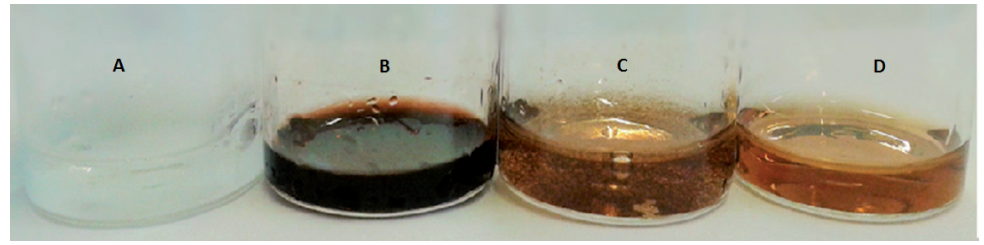

Figure 2. (A) mPEG-p(HPMAm-Lac_2) dissolved in 120 mM ammonium acetate (2 mg/ml); (B) Hemin dissolved in DMSO : DMF 1:9 (1.2 mg/ml); (C) Hemin in DMSO : DMF 1:9 (1.2mg/ml) of which 0.1 ml was added to 0.9 ml of 120 mM ammonium acetate; (D) Hemin- loaded micelles prepared by addition of 0.1 ml of 120 µg/ml of hemin in DMSO:DMF 1:9 to 0.9 ml of 1.8 mg/ml mPEG-b-p(HPMAm-Lac_2).

Figure 3 shows the loading of hemin in mPEG-*b*-p(HPMAm-Lac_2) micelles for three independently prepared micellar dispersions per hemin concentration with corresponding standard deviations in order to obtain insight in the batch-to-batch variability. Figure 3A demonstrates that the highest encapsulation was achieved by adding 120 µg/ml of hemin in DMSO to 1.8 mg/ml polymer solution in water. The loading capacity (LC) and encapsulation efficiency (EE) for this formulation were 3.9% and 61.4%, respectively. Figure 3A also shows that a higher concentration of hemin resulted in a decreasing EE. This is probably due to the fact that there is not enough polymer present to encapsulate the hemin, therefore resulting in saturation of the micelles with hemin and the formation of hemin aggregates with the excess hemin subsequently being filtered away (37, 38).

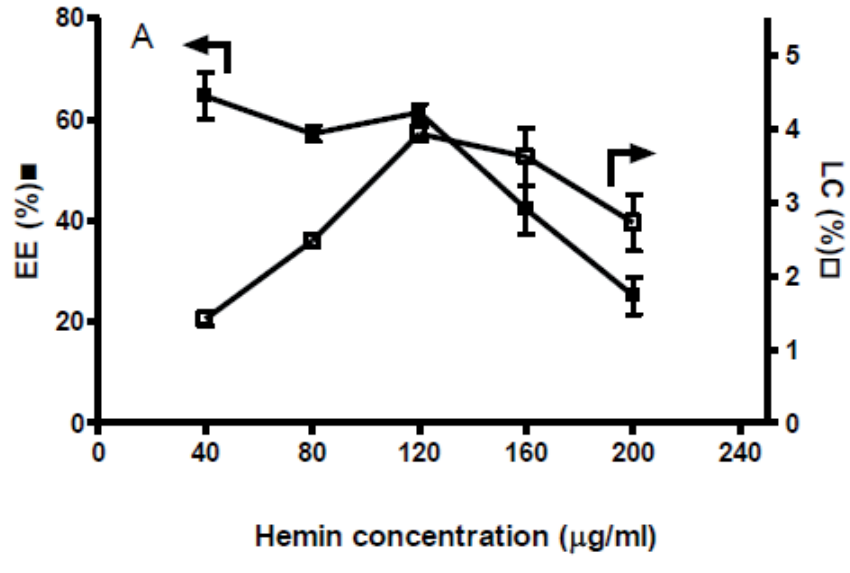

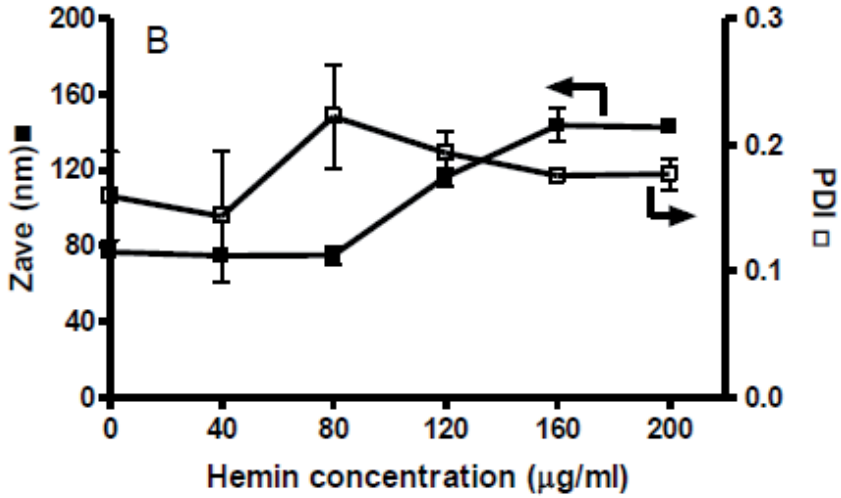

Figure 3. Loading of hemin in mPEG-*b*-p(HPMAm-Lac$_2$) micelles; (A) encapsulation efficiency on the left axis and loading capacity on the right axis and (B) Z-average diameter and polydispersity of hemin loaded micelles. Results represent mean ± standard deviation of three independently prepared samples.

Figure 3A further shows that the loading capacity increased from 2.5% at a hemin concentration of 40 µg/ml to 3.9% at a hemin concentration of 120 µg/ml and then leveled off, which is probably due to saturation of the micelles with hemin. Figure 3B demonstrates that when increasing the hemin concentration, the average size of the micelles also increased from 75 nm to 140 nm. The particle size at the highest hemin encapsulation was 116 nm and the polydispersity index was 0.19.

3.3 Physical state of hemin in micelles

Hemin loaded-micelles were prepared as described in section 2.2 and subsequently diluted ten times with ammonium acetate pH 5 to obtain a dispersion with a hemin concentration of 11.4 µM and a polymer concentration of 0.18 mg/ml. The polymer concentration was above the CMC of 0.015 mg/ml (36), in order to ensure that the micelles remain intact during measurement. As control, hemin was dissolved in DMSO to obtain molecularly dissolved hemin at the same concentration as the diluted micelle sample.

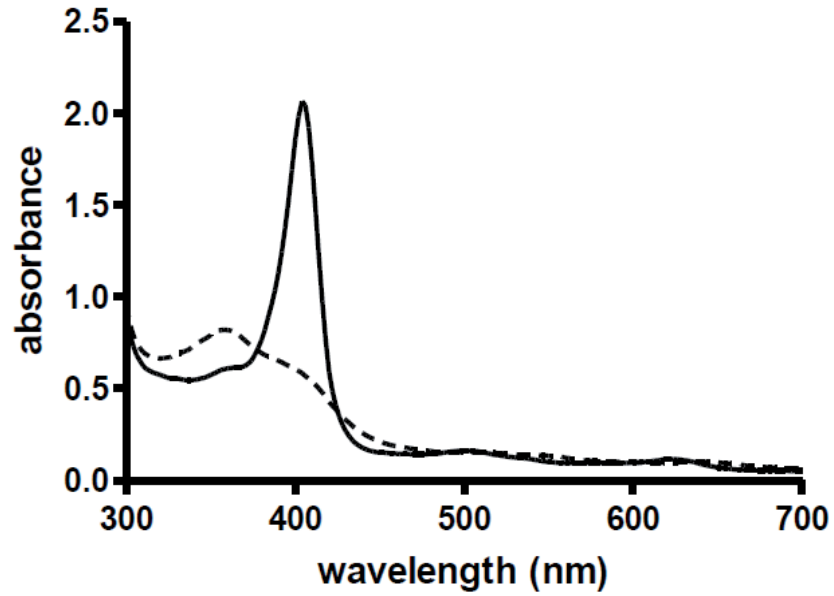

Figure 4. UV-Vis spectra of hemin ; (—) hemin (11.4 µM) in DMSO, (- -) hemin loaded micelles (11.4 µM of hemin) in 120 mM ammonium acetate pH 5.

Figure 4 shows for hemin dissolved in DMSO a so called Soret- or B band at a maximum of 404 nm, which is common for metalloporphyrins (39, 40). Figure 4 further shows that the absorption for hemin loaded micelles is significantly broadened as compared to the absorption of hemin solubilized in DMSO. This can be ascribed to the aggregation of hemin in the micelles as previously reported for a silicon phthalocyanine photosensitizer loaded in mPEG-*b*-p(HPMAm-Lac$_2$) micelles (34). Furthermore, the soret band for the hemin loaded-micelles shifted to lower wavelengths of respectively 385 nm compared to hemin dissolved in DMSO (404 nm). This shift is also known as a hypsochromic shift and is indicative for H-aggregation. Metalloporphyrins that form H-aggregates which are caused by strong metal to porphyrin orbital interaction are also called hypsoporphyrins. This interaction results in an enhanced porphyrin π-π^* energy separation which subsequently leads to the hypsochromic shift as observed in figure 4 (41, 42). The results presented in figure 4 imply that hemin is most likely present in an aggregate state within the micelles which can be beneficial as premature release of hemin when transiting through the digestive system is retarded.

3.4 Stability of hemin-loaded mPEG-*b*-p(HPMAm-Lac$_2$) micelles

In order for the hemin micelles to be effective for therapy, they should not disintegrate in the upper part of the digestive system and therefore the stability of the particles

was examined at both pH 2 (stomach) and pH 7.4 (duodenum). Hemin loaded mPEG-*b*-p(HPMAm-Lac$_2$) micelles with the highest encapsulation and loading capacity (figure 3A) were used for these studies.

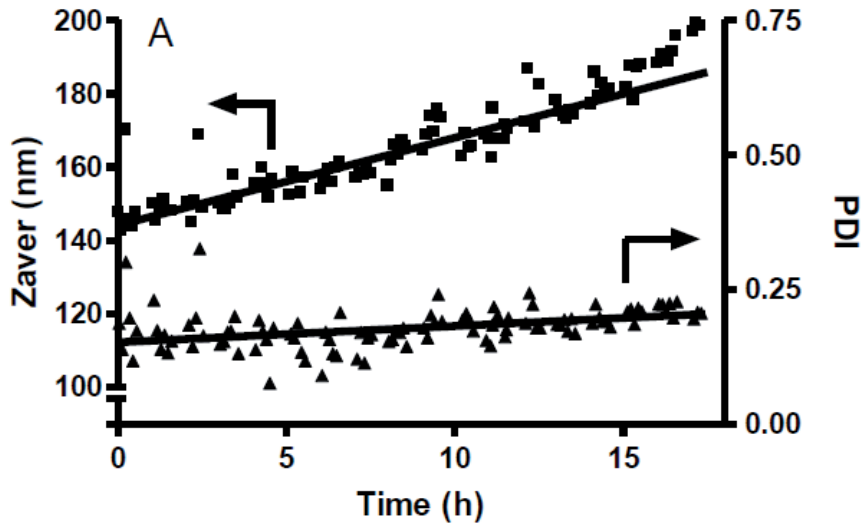

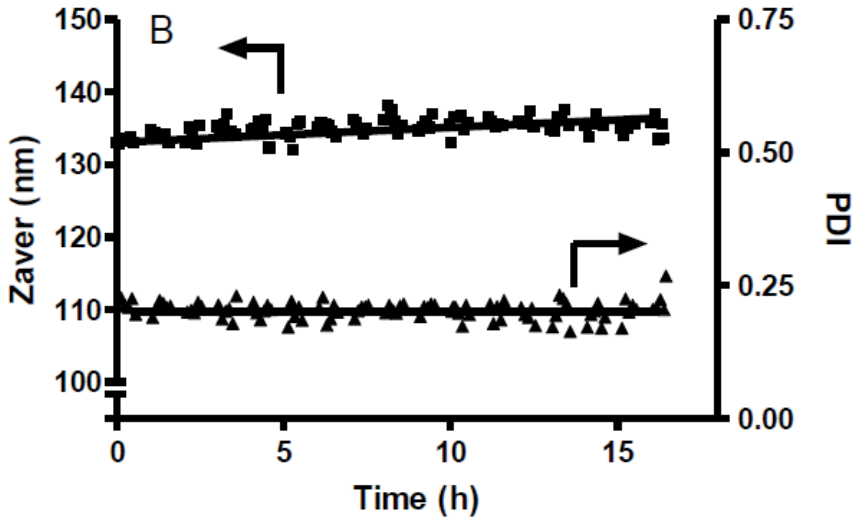

Figure 5. Z-average size (Z_{ave}) and polydispersity (PDI) of hemin micelles at 37 °C as a function of time at pH 2 (figure 5A) and at pH 7.4 (figure 5B); Figure 5A: micelles were prepared at pH 5 as described in section 2.2 and then adjusted to pH 2 with 4 M HCl; Figure 5B: micelles were prepared using a polymer solution in PBS pH 7.4 as described in section 2.6

Figure 5A illustrates that at pH 2 the size of the micelles slightly increases from 143 to 199 nm upon incubation for 17 hours at 37 °C, whereas at pH 7.4 (figure 5B) the size remained constant in time. The polydispersity remained constant in time at both pH's, at an average of 0.18 at pH 2 and 0.21 at pH 7.4. The scattered intensity data provided as supporting information (figure S2) demonstrates that at pH 2 the scattered intensity slowly decreases in time indicating slow degradation of the micelles, while at pH 7.4 the scattered intensity of the micelles remains constant throughout the measurement. However, during the first three hours which covers the common transit time in the stomach (43, 44), the average size and scattered intensity remained almost constant at pH 2. At pH 7.4 the micelles were stable up to 17 hours which could be beneficial for the uptake by the enterocytes after their oral administration.

3.5 Cellular *in-vitro* uptake of hemin-loaded mPEG-*b*-p(HPMAm-Lac$_2$) micelles.

To study the feasibility of hemin-loaded micelles as formulation for oral iron delivery, several experiments were performed on Caco-2 cell cultures. The Caco-2 cell line has been extensively used to study nutrient and drug transport, as these cells upon differentiation express a comparable microvilli brush border with functionality similar to the enterocytes present in the small intestines (45, 46). Ferritin is also a well-known marker for cellular iron uptake as it is the protein that stores iron when not needed elsewhere in the organism (47). Once the Hemin loaded micelles are internalized by cells and the hemin is released, it is degraded by the enzyme heme oxygenase which is present on the endoplasmic reticulum resulting in the formation of Fe^{2+}, biliverdin and carbon monoxide (48). Subsequently the iron in the cytoplasm enters the common iron pool and is then transported to the bloodstream via the protein ferroportin. The excess iron which is not required to enter in the circulatory system is stored in the cytosolic protein ferritin (8, 49). The regulation of ferritin synthesis occurs via the translation of ferritin H and L mRNA's in presence of accessible iron in the labile iron pool which can be defined as a cell chelatable pool consisting of mainly Fe^{2+} associated with various ligands with an affinity for iron (50-52). This results in an increase or decrease of ferritin synthesis and thus ferritin expression when iron levels are high or down regulated when iron levels are low (8, 53). In the present study, Caco-2 cells were incubated with dispersions of hemin-loaded micelles with different concentrations, as well as with iron sulfate or iron sulfate in combination with ascorbic acid. Also, a cytotoxicity assay was done to assess the cytocompatibility of the formulations.

3.5.1 Uptake of hemin-loaded mPEG-b-p(HPMAm-Lac$_2$) micelles by Caco-2 cells

In order to study uptake of hemin-loaded micelles, mPEG-*b*-p((HPMAm-Lac$_2$)-*co*-RhodMA) was synthesized as described is section 2.7. GPC analysis (figure 6) equipped with both a

RI- and UV-detector was performed to determine the number average molecular weight and the amount of free rhodamine in the sample. The number average molecular weight (M_n) using PEG standards for calibration was 23500 g/mol; M_w/M_n = 2.0. Furthermore GPC analysis showed that the amount of free label was less than 3 %.

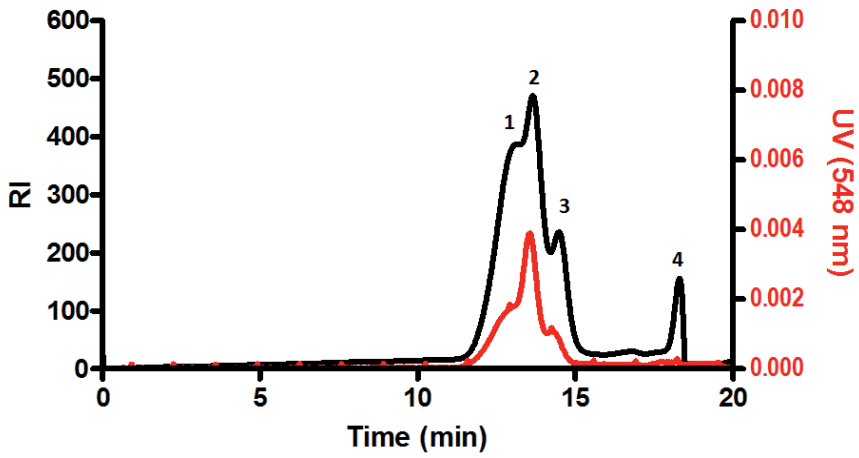

Figure 6. GPC profile (1) mPEG-*b*-p((HPMAm-Lac_2)-*co*-RhodMA; (2) traces of the PEG-macroinitiator; (3) free PEG; (4) injection peak. The red line is the UV signal at 548 nm and black line is RI signal.

Rhodamine labeled mPEG-*b*-p(HPMAm-Lac_2) micelles were prepared as described in section 2.8.5 to perform cellular uptake studies.

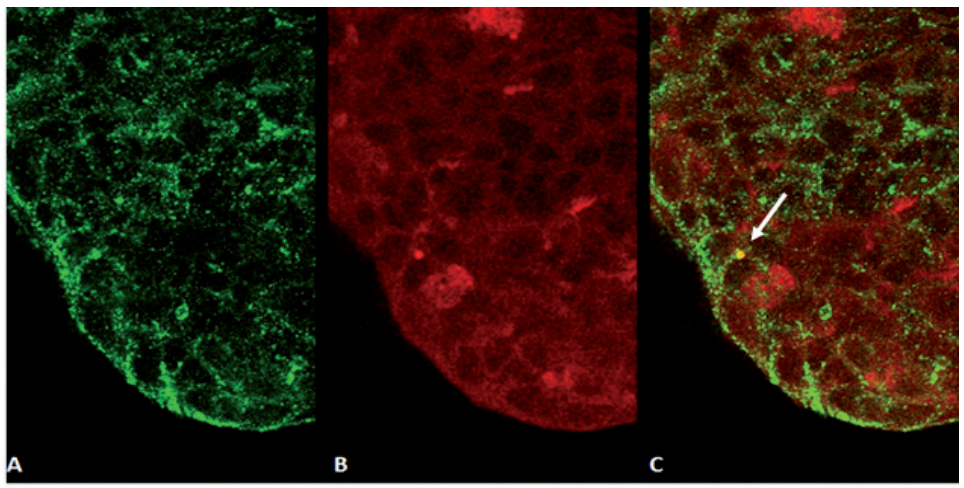

Figure 7. Confocal microscopy of Caco-2 cells incubated for 3 hours at 37 °C with rhodamine labeled hemin-micelles. Figure 7A: lysosome staining in green; figure 7B: rhodamine labelled micelles in red; figure 7C: overlap of lysosome staining and rhodamine

In order to observe whether hemin-loaded micelles were taken up by the Caco-2 cells, confocal microscopy was performed using rhodamine labelled hemin-micelles and the commonly used lysosome marker LAMP-1 (54). Figure 7B depicts that after an incubation time of 3 hours, the cells take up the labelled micelles, but Figure 7C shows that most of the green fluorescence of the lysosomes does not overlap with the red rhodamine fluorescence. This indicates that the rhodamine micelles were not present in lysosomal vesicles as would be expected if the uptake mechanism was via endocytosis (53). Similar results were also obtained by Rijcken et al. (34) who incubated murine melanoma B16F10 cells with (mPEG-*b*-p((HPMAm-Lac_2)-*co*-RhodMA) micelles to investigate the cellular uptake of these particles. Furthermore, the particles studied in this paper had an average size of 116 nm as shown in figure 3B, which is well above the optimal particle size of 25-30 nm for endocytosis according to a study performed by Zhang et al. (56). Nevertheless uptake of hemin into the cells in its free form is not expected because of its low aqueous solubility and therefore the high levels of ferritin that are formed after incubation of the hemin-micelles with the cells, as shown in section 3.5.2, are probably due to the internalized micelles. Talelli et al. (57), also demonstrated that similar rhodamine labeled micelles, both non-targeted as well as EGa1 nanobody targeted were indeed taken up by 14C cells. Sahay et al., (58) discussed the various pathways that nanoparticles composed of different materials use to enter cells, including nanomaterials that are able to bypass early endosomes and lysosomes. However some of these mechanisms are not fully understood, but up to date any of the endocytic pathways are considered the main cellular uptake mechanism for micelles (59).

3.5.2 Ferritin expression after in-vitro uptake of iron complex

Figure 8 presents the ferritin expression after incubating the Caco-2 cells for 24 hours with dispersions of hemin-loaded micelles or iron sulfate. After incubating the cells with medium containing iron sulfate in various concentrations, ferritin values reached a maximum of 250 ng/mg protein at a concentration of 150 µM. It can also be observed that at this iron sulfate concentration the expression of intracellular ferritin reached a plateau.

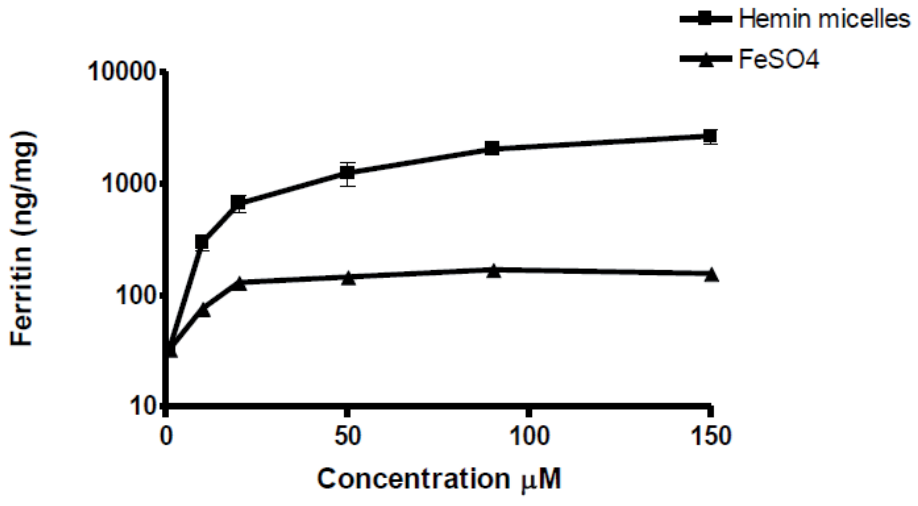

Figure 8. Formation of ferritin (in ng/mg cellular protein) by Caco-2 cells upon incubation with hemin or iron sulfate for 24 hours at 37 °C. Results represent mean ± standard deviation of three experiments.

Importantly, when the cells were incubated with medium containing hemin-loaded micelles, ferritin values of 2500 ng/mg protein were observed, which are more than 10 fold higher than obtained when incubating the cells with iron sulfate. This observation is in accordance with a previous study in which it has been reported that heme iron is probably being taken up more efficiently by Caco-2 cells than non-heme iron such as iron salts (11).

Additional experiments were performed to study the effect of combining ascorbic acid (vitamin C), a vitamin that beneficially enhances iron uptake (60).

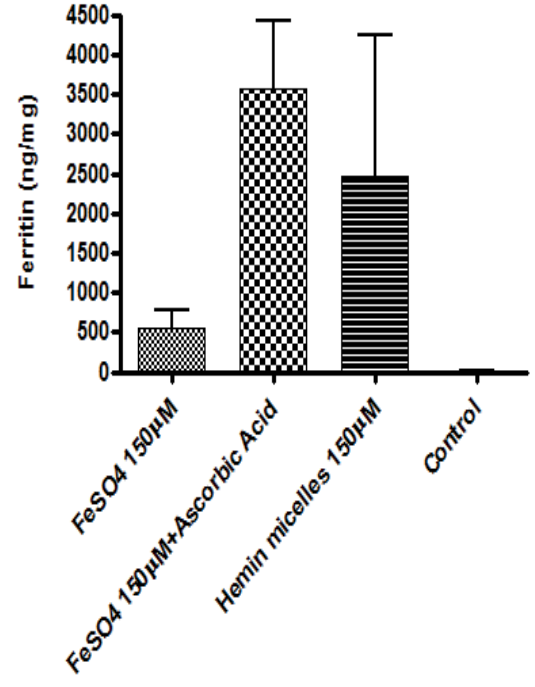

Figure 9. Formation of ferritin (in ng/mg cellular protein) by Caco-2 cells after 24 hours of incubation with 150 µM of hemin loaded mPEG-*b*-p(HPMAm-Lac$_2$) micelles, iron sulfate, iron sulfate plus ascorbic acid in a molar ratio of 1:5, and DMEM medium only. Results represent mean ± standard deviation of three experiments.

Figure 9 shows that when ascorbic acid was added to the medium, a substantial higher ferritin formation was observed, confirming literature claims (60). Furthermore, it can be observed that there were no significant differences between ferritin expressed by cells incubated with iron sulfate supplemented with ascorbic acid or hemin loaded micelles. However, ascorbic acid is a strong reductant which in excess could lead to the formation of undesired high Fe^{2+} amounts and result in possible pro-oxidative activity (61, 62). In addition, we investigated possible cytotoxic effects of the different iron formulations using the XTT assay. The results shown in figure 10 demonstrate that incubating Caco-2 cells with hemin– loaded micelles with a concentration up to 150 µM, has no effect on the cell viability whereas iron sulfate combined with ascorbic acid was clearly cytotoxic, with an IC_{50} value of 50 µM.

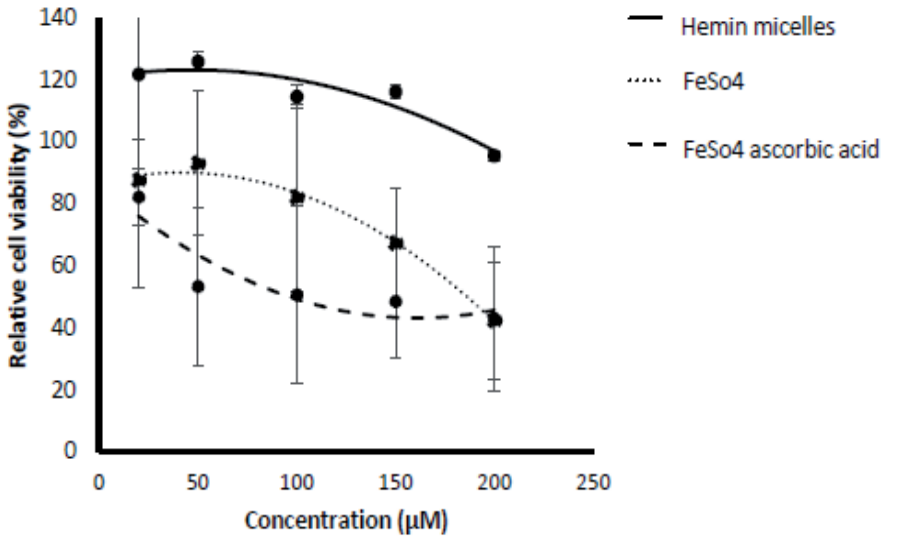

Figure 10. Viability of Caco-2 cells upon incubation of different concentrations of Hemin-loaded micelles; Iron sulfate; Iron sulfate : Ascorbic acid (1:5) and empty micelles. Results represent mean ± standard deviation of three experiments

3.5.3 Kinetics of ferritin formation in Caco-2 cells after incubation of iron samples

The kinetics of ferritin formation was investigated by incubating the Caco-2 cells with iron sulfate and hemin-loaded micelles with a concentration of 150 µM. The hemin-loaded micellar dispersion was made from 120 µg hemin/ml in 1.8 mg/ml polymer as described in section 2.8.2. Figure 11 illustrates that the amount of ferritin reached a maximum already after 3 hours upon incubation with both formulations at 37 °C. After this incubation time there is no significant difference in formation of ferritin.

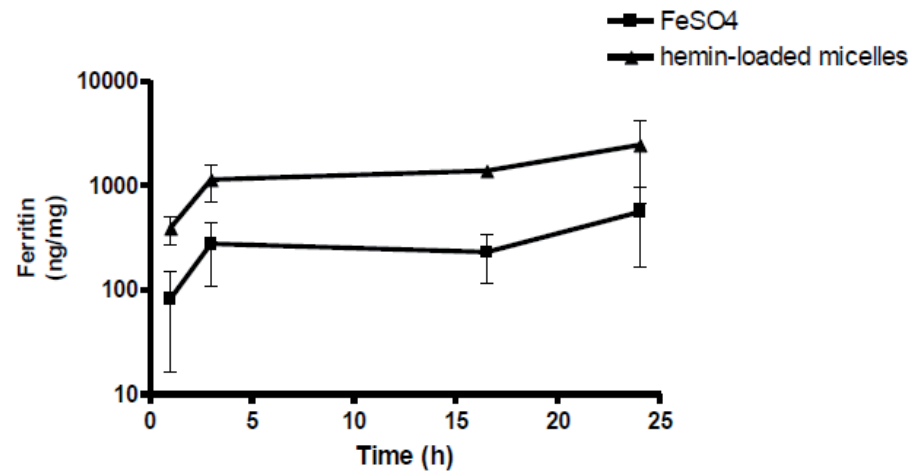

Figure 11. Formation of ferritin in ng/mg cellular protein as function of incubation time of Caco-2 cells with hemin-loaded micelles (150 µM) and iron sulfate (150 µM). Results represent mean ± standard deviation of three experiments.

In many previous studies using Caco-2 cells as a model cell line to investigate iron uptake, the cells were harvested after 24 hours upon incubation with iron supplements in order to allow ferritin formation (47, 63). However, here we demonstrate that 3 hours is sufficient to reach a maximum of ferritin formation upon incubation with both hemin-loaded micelles as well as iron sulfate.

4. CONCLUSIONS

The present study shows that hemin can successfully be loaded in mPEG-*b*-p(HPMAm-Lac_2) micelles forming water dispersible particles with an average size of around 100 nm. The hemin-loaded micelles demonstrated to remain stable up to 3 hours at pH 2 and 17 hours at pH 7.4. Importantly, upon incubation in Caco-2 cells the hemin-loaded micelles gave superior ferritin formation up to 10x times higher than when compared to the commonly used iron supplement iron sulfate. The new hemin formulation presented in this paper is therefore a promising formulation for iron oral delivery.

5. ACKNOWLEDGEMENTS

This research was financially supported by Vifor Pharma.

6. REFERENCES

1. Benoist de, Bruno., McLean, Erin., Egli, Ines., Cogswell., 2008. Worldwide prevalence of anaemia 1993-2005: WHO global database on anaemia, ISBN 978 92 4 159665 7
2. S. Yun, J.P. Habicht, D.D. Miller, R.P. Glahn, An In Vitro digestion/Caco-2 cell culture system accurately predicts the effects of ascorbic acid and polyphenolic compounds on iron bioavailability in humans, J. Nutr. 134 (2004) 2717–2721.
3. E.C. Theil, Iron homeostasis and nutritional iron deficiency, J. Nutr. 141 (2011) 724S–728S.
4. R.P. Glahn, M. Rassier, M.I. Goldman, O.A. Lee, J. Cha, A comparison of iron availability from commercial iron preparations using an in vitro digestion/Caco-2 cell culture model, J. Nutr. Biochem. 11 (2000) 62–68.
5. G.J. Anderson, D.M. Frazer, G.D. McLaren, Iron absorption and metabolism, Curr. Opin. Gastroenterol. 25 (2009) 129–135.
6. P. Santiago, Ferrous versus ferric oral iron formulations for the treatment of iron Deficiency: A clinical overview, Sci. World J. 2012 (2012) 5.
7. B.K. Fuqua, C.D. Vulpe, G.J. Anderson, Intestinal iron absorption, J. Trace Elem. Med. Biol. 26 (2012) 115–119.
8. R. Evstatiev, C. Gasche, Iron sensing and signalling, Gut 61 (2012) 933–952.
9. J. Wang, K. Pantopoulos, Regulation of cellular iron metabolism, Biochem. J. 434 (2011) 365–381.
10. A.A. Khan, J.G. Quigley, Control of intracellular heme levels: Heme transporters and heme oxygenases, Biochim. Biophys. Acta - Mol. Cell Res. 1813 (2011) 668–682.
11. S. Miret, S. Tascioglu, M. van der Burg, L. Frenken, W. Klaffke, In vitro bioavailability of iron from the heme analogue sodium iron chlorophyllin, J. Agric. Food Chem. 58 (2010) 1327–1332.
12. P. Villarroel, S. Flores, F. Pizarro, D. de Romaña, M. Arredondo, Effect of dietary protein on heme iron uptake by Caco-2 cells, Eur. J. Nutr. 50 (2011) 637–643.
13. D.S. Kalinowski, D.R. Richardson, The evolution of iron chelators for the treatment of iron overload disease and cancer, Pharmacol. Rev. 57 (2005) 547–583.
14. Comparison of oral iron supplements. Pharmacist's Letter/Prescriber's Letter 2008; 24 (8):240811.
15. M. Shayeghi, G.O. Latunde-Dada, J.S. Oakhill, A.H. Laftah, K. Takeuchi, N. Halliday, et al., Identification of an intestinal heme transporter, Cell 122 (n.d.) 789–801.
16. C. Cao, C. Thomas, K. Insogna, K. O'Brien, Duodenal expression of heme and non-heme iron transporters and tissue partitioning of dietary heme and non-heme iron in a rat mode of iron overload, FASEB J. 28 (2014), meeting abstract 246.8
17. T. Korolnek, I. Hamza, Like iron in the blood of the people: The requirement for eme trafficking in iron metabolism, Front. Pharmacol. 5 (2014) 126.
18. T.J. Egan, E. Hempelmann, W.W. Mavuso, Characterisation of synthetic β-haematin and effects of the antimalarial drugs quinidine, halofantrine, desbutylhalofantrine and mefloquine on its formation, J. Inorg. Biochem. 73 (1999) 101–107.
19. A.C. Hunter, J. Elsom, P.P. Wibroe, S.M. Moghimi, Polymeric particulate technologies for oral drug delivery and targeting: a pathophysiological perspective, Nanomedicine 8 (2012) S5–S20.
20. S. Mazzaferro, K. Bouchemal, G. Ponchel, Oral delivery of anticancer drugs III: formulation using drug delivery systems, Drug Discov. Today 18 (2013) 99–104.
21. G. Gaucher, P. Satturwar, M.-C. Jones, A. Furtos, J.-C. Leroux, Polymeric micelles for oral drug delivery, Eur. J. Pharm. Biopharm. 76 (2010) 147–158.
22. K. Thanki, R.P. Gangwal, A.T. Sangamwar, S. Jain, Oral delivery of anticancer drugs: Challenges and opportunities, J. Control. Release 170 (2013) 15–40.
23. L. Zhang, S. Wang, M. Zhang, J. Sun, Nanocarriers for oral drug delivery, J. Drug Target. 21 (2013) 515–527.
24. L. Mei, Z. Zhang, L. Zhao, L. Huang, X.-L. Yang, J. Tang, et al., Pharmaceutical nanotechnology for oral delivery of anticancer drugs, Adv. Drug Deliv. Rev. 65 (2013) 880–890.
25. C. Deng, Y. Jiang, R. Cheng, F. Meng, Z. Zhong, Biodegradable polymeric micelles for targeted and controlled anticancer drug delivery: Promises, progress and prospects, Nano Today 7 (2012) 467–480.
26. O. Soga, C.F. van Nostrum, W.E. Hennink, Poly(N-(2-hydroxypropyl) methacrylamide mono/di Lactate): A new class of biodegradable polymers with tuneable thermosensitivity, Biomacromolecules 5 (2004) 818–821.
27. C.J.F. Rijcken, T.F.J. Veldhuis, A. Ramzi, J.D. Meeldijk, C.F. van Nostrum, W.E. Hennink, Novel fast degradable thermosensitive polymeric micelles based on PEG-block-poly(N-(2-hydroxyethyl)methacrylamide-oligolactates), Biomacromolecules 6 (2005) 2343–2351.
28. D. Schmaljohann, Thermo- and pH-responsive polymers in drug delivery. Advanced Drug Delivery Reviews 58 (2006) 1655-1670.
29. S.R. MacEwanand A. Chilkoti, Applications of elastin-like polypeptides in drug delivery, Journal of Controlled Release 190 (2014) 314-330.
30. M. Talelli, C.J.F. Rijcken, T. Lammers, P.R. Seevinck, G. Storm, C.F. van Nostrum, et al., Superparamagnetic iron oxide nanoparticles encapsulated in biodegradable thermosensitive polymeric micelles: toward a targeted nanomedicine suitable for image-guided drug delivery, Langmuir 25 (2009) 2060–2067.
31. O. Naksuriya, Y. Shi, C.F. van Nostrum, S. Anuchapreeda, W.E. Hennink, S. Okonogi, HPMA-based polymeric micelles for curcumin solubilization and inhibition of cancer cell growth, Eur. J. Pharm. Biopharm. 94 (2015) 501–512.
32. D. Neradovic, O. Soga, C.F. Van Nostrum, W.E. Hennink, The effect of the processing and formulation parameters on the size of nanoparticles based on block copolymers of poly(ethylene glycol) and poly(N-isopropylacrylamide) with and without hydrolytically sensitive groups, Biomaterials 25 (2004) 2409–2418.
33. O. Soga, C.F. van Nostrum, M. Fens, C.J.F. Rijcken, R.M. Schiffelers, G. Storm, et al.,

Thermosensitive and biodegradable polymeric micelles for paclitaxel delivery, J. Control. Release 103 (2005) 341–353.
34. C.J.F. Rijcken, J.-W. Hofman, F. van Zeeland, W.E. Hennink, C.F. van Nostrum, Photosensitiser-loaded biodegradable polymeric micelles: Preparation, characterisation and in vitro PDT efficacy, J. Control. Release 124 (2007) 144–153.
35. D.A. Scudiero, R.H. Shoemaker, K.D. Paull, A. Monks, S. Tierney, T.H. Nofziger, et al., Evaluation of a soluble tetrazolium/formazan assay for cell growth and drug sensitivity in culture using human and other tumor cell lines, Cancer Res. 48 (1988) 4827–4833.
36. O. Soga, C.F. van Nostrum, A. Ramzi, T. Visser, F. Soulimani, P.M. Frederik, et al., Physicochemical characterization of degradable thermosensitive polymeric micelles, Langmuir 20 (2004) 9388–9395.
37. M.C. Jones, J.C. Leroux, Polymeric micelles – a new generation of colloidal drug carriers, Eur. J. Pharm. Biopharm. 48 (1999) 101–111.
38. M. Yokoyama, A. Satoh, Y. Sakurai, T. Okano, Y. Matsumura, T. Kakizoe, et al., Incorporation of water-insoluble anticancer drug into polymeric micelles and control of their particle size, J. Control. Release 55 (1998) 219–229.
39. V. Srinivas, Ch. Mohan Rao, Time profile of hemin aggregation: an analysis. Biochemistry International 21 (1990) 849-855
40. M.E. Lombardo, L.S. Araujo, A.B. Ciccarelli, A. Batlle, A spectrophotometric method for estimating hemin in biological systems, Anal. Biochem. 341 (2005) 199–203.
41. S. Hirohara, M. Obata, S. Ogata, K. Kajiwara, C. Ohtsuki, M. Tanihara, et al., Sugar-dependent aggregation of glycoconjugated chlorins and its effect on photocytotoxicity in HeLa cells, J. Photochem. Photobiol. B Biol. 84 (2006) 56–63.
42. M. Prushan, Absorption and Fluorescence spectroscopy of tetraphenyl porphyrin and metallo-tertraphenylporphyrin. (2005) 1–9. http://www.lasalle.edu/
43. M. Camilleri, L.J. Colemont, S.F. Phillips, M.L. Brown, G.M. Thomforde, N. Chapman, and A.R. Zinsmeister. Human gastric emptying and colonic filling of solids characterized by a new method. Am J Physiol. - Gastrointestinal and Liver Physiology 257 (1989) G284-G290.
44. L.P. Degen, S.F. Phillips, Variability of gastrointestinal transit in healthy women and men, Gut 39 (1996) 299–305.
45. M. Pinto, S. Robine-Leon, M. Appay, M. Kedinger, N. Triadou, E. Dussaulx, B. Lacroix, P. Simon-Assmann, K. Haffen, J. Fogh, A. Zweibaum, Biology of the Cell (1983) 47, 323-330.
46. B. Press, D. Di Grandi, Permeability for intestinal absorption: Caco-2 assay and related issues, Curr. Drug Metab. 9 (2008) 893–900.
47. R.P. Glahn, O.A. Lee, A. Yeung, M.I. Goldman, D.D. Miller, Caco-2 cell ferritin formation predicts nonradiolabeled food iron availability in an in vitro digestion/Caco-2 cell culture model, J. Nutr. 128 (1998) 1555–1561.
48. G. Kikuchi, T. Yoshida, M. Noguchi, Heme oxygenase and heme degradation, Biochem. Biophys. Res. Commun. 338 (2005) 558–567.
49. J. Hooda, A. Shah, L. Zhang, Heme, an essential nutrient from dietary proteins, critically

impacts diverse physiological and pathological processes, Nutrients 6 (2014) 1080–1102.
50. O. Kakhlon, Z.I. Cabantchik, The labile iron pool: characterization, measurement, and participation in cellular, Free Radic. Biol. Med. 33 (2002) 1037–1046.
51. M. Kruszewski, Labile iron pool: the main determinant of cellular response to oxidative stress, Mutat. Res. Mol. Mech. Mutagen. 531 (2003) 81–92.
52. R.C. Hider, X. Kong. Iron speciation in the cytosol: an overview. Dalton Transactions. 42 (2013) 3220-3229.
53. F.M. Torti and S.V. Torti. Regulation of ferritin genes and protein. Blood *99* (2002) 3505-3516.
54. T.G. Iversen, T. Skotland, K. Sandvig, Endocytosis and intracellular transport of nanoparticles: Present knowledge and need for future studies, Nano Today 6 (2011) 176–185.
55. I. Mellman, Endocytosis and molecular, Annu. Rev. Cell Dev. Biol. 12 (1996) 575–625.
56. S. Zhang, J. Li, G. Lykotrafitis, G. Bao, S. Suresh, Size-dependent endocytosis of nanoparticles, Adv. Mater. 21 (2009) 419–424.
57. M. Talelli, C.J.F. Rijcken, S. Oliveira, R. van der Meel, P.M.P. van Bergen en Henegouwen, T. Lammers, et al., Nanobody — Shell functionalized thermosensitive core-crosslinked polymeric micelles for active drug targeting, J. Control. Release 151 (2011) 183–192.
58. G. Sahay, D.Y. Alakhova, A. V Kabanov, Endocytosis of nanomedicines, J. Control. Release 145 (2010) 182–195.
59. I. Pepić, J. Lovrić, J. Filipović-Grčić, How do polymeric micelles cross epithelial barriers?, Eur. J. Pharm. Sci. 50 (2013) 42–55.
60. J.D. Cook, M.B. Reddy, Effect of ascorbic acid intake on nonheme-iron absorption from a complete diet, Am. J. Clin. Nutr. 73 (2001) 93–98.
61. B. Sturm, H. Laggner, N. Ternes, H. Goldenberg, B. Scheiber-Mojdehkar, Intravenous iron preparations and ascorbic acid: Effects on chelatable and bioavailable iron, Kidney Int. 67 (2005) 1161–1170.
62. I.D. Podmore, H. R. Griffiths, K. E. Herbert, N. Mistry, P. Mistry and J. Lunec, Nature 392 (1998), 559-559.
63. B.I. Mergler, E. Roth, S.F.A. Bruggraber, J.J Powell, D.I.A Pereira, Development of the Caco-2 Model for assessment of iron absorption and utilisation at supplemental levels. J. Pharm. Nutr. Sci. 2 (2012), 26-33.

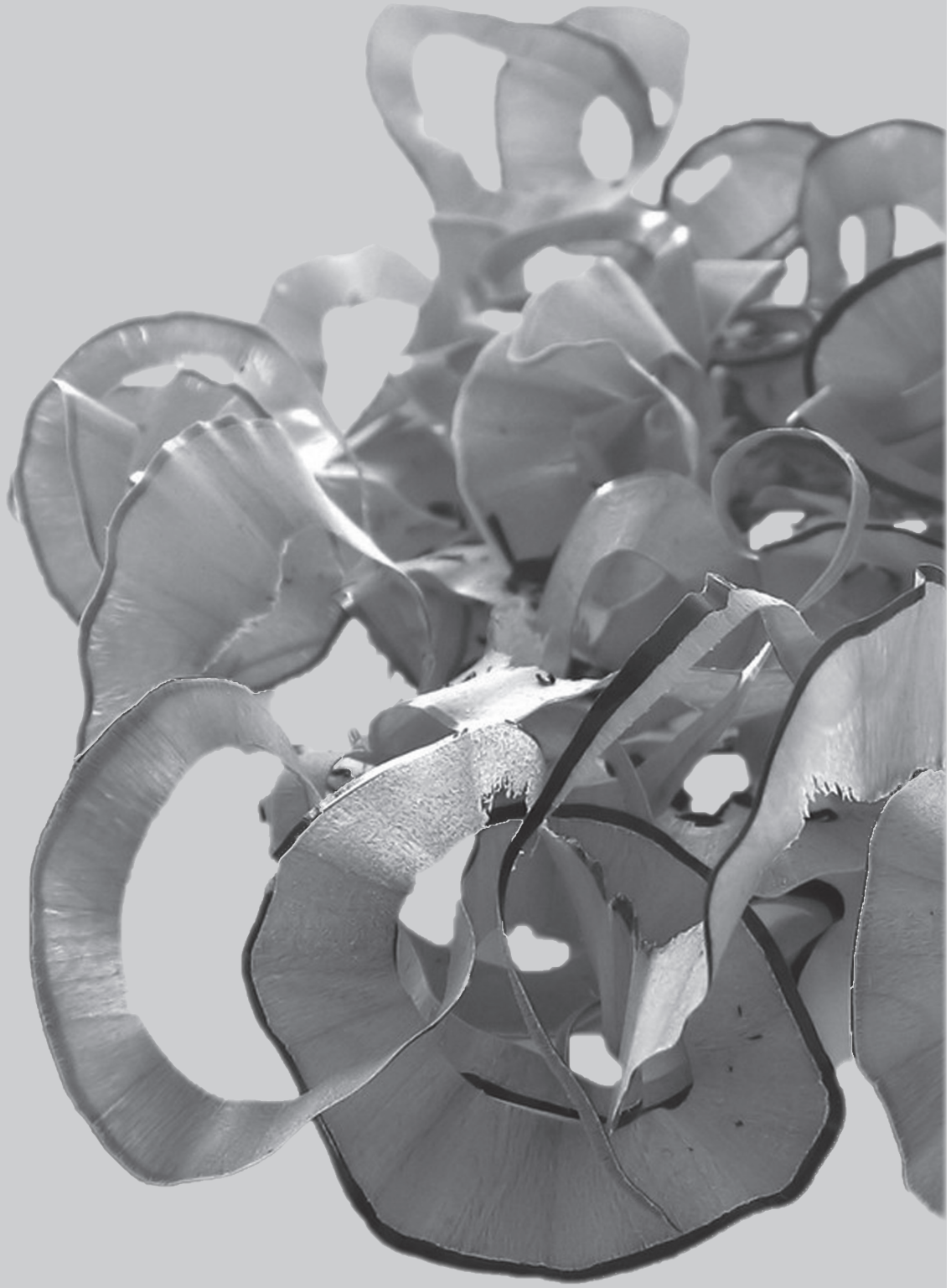

CHAPTER 3

Reproducibility of non-clinical studies of Venofer® versus iron sucrose similars (ISS) in a Sprague Dawley rat model

Kimberley Span, Ebel H.E. Pieters, Vera Brinks, Huub Schellekens and Wim E. Hennink

Abstract

Purpose The aim of this study was to assess the reproducibility of preclinical comparison studies of iron based products using the Sprague Dawley rat model.

Methods The original iron sucrose product Venofer® was compared with two iron sucrose similars (FerMylan® and FerMed®) by conducting a toxicological study with a comparable experimental design as previously published (1-4). To this end, iron related blood parameters, biochemical and oxidative stress analysis of liver and kidney as well as iron disposition in the liver were assessed. The non-anemic animals (both male and female) were injected intravenously once a week 40 mg Fe/kg body weight, receiving thus a total of five injections.

Results The measured iron related parameters, serum iron and transferrin saturation (TSAT), showed significantly increased values for the iron treated groups compared to the control group at day 29. However, none of the blood iron parameters showed statistically significant differences between Venofer® and the iron sucrose similars. In addition, the liver enzymes also did not demonstrate differences between the treatments. Proteinuria values for Venofer® at day 29 were elevated compared to FerMed®(ISS2) when measured in male rats, while FerMylan® (ISS1) iron disposition in the liver of female rats was significantly higher than in female rats that received Venofer®. In contrast to the previously published results (1), this study showed no major differences between the original iron sucrose product and the iron sucrose similars. However, there were significant differences in results between the female and male rats for serum iron, ALP liver enzyme and proteinuria levels. Mixed genders within a treatment group resulted in large standard deviations for serum iron and proteinuria, reflecting a large inter-variance within a treatment group.

Conclusion The results from various studies on iron medicinal products conducted with a similar experimental design are discordant regarding the safety and quality differences between the original iron sucrose and iron sucrose similars. One of the main factors to obtain reproducible results, is to use an appropriate animal model and experimental set-up. The Sprague Dawley strain in combination with the read-out parameters described in this study, does not appear to be suitable for this purpose. The results reported in this chapter sheds light onto difficulties to reproduce animal studies when conducting research on iron medicinal products.

1. INTRODUCTION

Anemia is predominately caused by iron deficiency (5). In most cases oral iron supplementation can be given because it is convenient for the patient and also affordable (6). However, in case of iron malabsorption or severe iron deficiency, e.g. in patients that require hemodialysis, oral supplementation does not result in the required effect. In these patients parenteral administration is favored (7). Current intravenous iron products consist of a polynuclear iron(III)-oxyhydroxide core surrounded by a carbohydrate shell, that stabilizes the core and delays the release of iron from the complex (8). Iron sucrose is a preferred formulation as compared to other iron products such as ferric gluconate and iron dextran complexes due to its superior safety profile (9-12). Iron sucrose is a water dispersable nano-sized complex with an average core size smaller than 10 nm, composed of a polynuclear iron(III) oxyhydroxide core stabilized with sucrose molecules (13-15). It was first developed and approved for use in Switzerland around 1950 (16, 17) and in 2000 a New Drug Application (NDA) was filed and approved in the United States for the use of Venofer® (iron sucrose originator) (18).

Venofer® has been well characterized in terms of safety and efficacy, however some concerns have risen regarding the safety of iron sucrose similars (ISS) that have been introduced in several markets in the recent years (19, 20). The pharmaceutical properties of the iron sucrose complexes as well as their in-vivo behavior are highly dependent on the manufacturing process and conditions because small differences in physicochemical properties might result in possible different toxicological effects (21). The European Medicines Agency (EMA) published a guideline outlining all necessary studies, in order to establish comparison between generics and originators of iron-based nanoparticle products (22). The guideline basically states that non-clinical studies are essential when performing comparison studies for market approval of generic iron products. Up to now, animal models are used in non-clinical studies as predictive models to prevent adverse drug effects (23). However, the use of animal models to predict adverse clinical events is under debate due to the ambiguity of these studies concerning sensitivity, predictability and reproducibility (23). Sprague Dawley rats are extensively used as a preclinical animal model (24, 25) and have been applied in safety and efficacy as well as comparative studies of iron products (1-4). These studies had different outcomes in terms of toxicological differences between the original iron sucrose product Venofer® and the various iron sucrose similars tested. It is therefore crucial, when aiming to establish similarities in quality between generics and the original iron product, to use accurate, sensitive and robust methods. Therefore it should be investigated whether the Sprague Dawley animal model is a suitable model for comparison studies between the originator and generics and that the outcome of the experiments is easily reproducible. In the present study we thus aimed to reproduce the results of previously published non-clinical toxicity studies using Sprague Dawley rats that received Venofer® and iron sucrose similars (ISS)

by intravenous injection. To this end, a blinded study with comparable experimental set-up as described by Toblli et al. (1, 2) was performed. During the execution of the experiment, there was no knowledge which iron product was administered to the rats and this remained unknown also during the processing and interpretation of the data. In the present study, Venofer® was compared to two different iron sucrose similars, which after the interpretation of the data were disclosed to be FerMylan® and FerMed®. The study consisted of one experiment including both male and female rats, and another experiment with only male rats. The different sexes were studied, as it has been previously reported that the pharmacokinetics and pharmacodynamics of drugs in clinical trials are different for females and males (26, 27).

2. MATERIALS AND METHODS

2.1 Animals

The study was performed according to Institutional Ethical Committee Regulations of Utrecht University, the Netherlands. Male and female Sprague Dawley rats (Harlan laboratories, the Netherlands) were fed standard rat chow (Special Diets Services, United Kingdom) and (acidified) water *ad libitum* unless stated otherwise and were housed in standard perspex cages. The rats were acclimatized for 4 weeks before starting the experiment and were subjected to a 12 hours light/dark cycle.

In experiment 1, 24 animals (12 female and 12 male Sprague Dawley rats) were used. Each treatment group consisted of 4 female and 4 male animals weighing ≈ 200 grams at the beginning of the experiment. The different treatment groups were: Venofer® (Veno), FerMylan® (ISS1) and saline solution (control group). Venofer® and FerMylan® had a concentration of 20 mg Fe/ml and were intravenously administered to the rats at a dose of 40 mg (iron Fe)/kg body weight. In order to administer the preparations to all animals with a similar dose of 40 mg (Fe)/kg, the volume of the iron products injected varied per rat (0.4 - 0.8 ml).

Nine male Sprague Dawley rats were used in experiment 2. Each treatment group consisted of 3 male animals per group weighing ≈ 300 grams at the beginning of the experiment. The different treatment groups were: Venofer® (Veno), FerMed® (ISS2) and saline solution (control group). Venofer® and FerMed® had a concentration of 20 mg Fe/ml and were intravenously injected into the rats at a dose of 40 mg (iron Fe)/kg body weight. Likewise the first experiment, the volume of the iron products injected varied per rat as this was dependent on the rat's weight. For both experiments, the animals received a weekly intravenous injection of the different formulations for four weeks (thus 5 injections total). Immediately after the injections at week 1 (day 1), 3 (day 15) and 5 (day 29) the animals were placed in metabolic cages in order to collect urine for 24 hours.

At the end of this time, the animals were deprived for 15 hours from food, but had access to (acidified) water *ad libitum*. After 24 hours, blood was collected via the tail vein and the urine was collected in measuring cylinders. Blood serum and urine was kept at -20°C until analysis. During experiment 2 an extra time point for blood and urine collection was included at 14 days prior the first injection. At the end of the experiment, the animals were sacrificed via an intraperitoneal injection with an overdose pentobarbital (1 - 2 ml), followed by a saline perfusion until complete blood depletion. The liver and kidneys were collected, frozen in liquid nitrogen and subsequently stored at -80°C until analysis. In order to perform the experiment as a blinded study, the different iron products administered to the rats were labelled as H1 and H2 for experiment 1 and H3 and H4 for experiment 2. As explained in the Introduction section of this Chapter, the different labels were disclosed after collection and interpretation of the data and are depicted in the manuscript correctly as being Venofer® (Veno), FerMylan® (ISS1) or FerMed® (ISS2).

2.2 Materials

Samples of Venofer® and the iron sucrose similars FerMylan® and FerMed® (20 mg iron/ml), were obtained from Vifor (International) Ltd, St. Gallen, Switzerland and saline solution (sodium chloride 0.9% w/v) was purchased from Braun Melsungen AG, Oss, The Netherlands. The iron related parameters, namely total serum iron (Fe) and total iron binding capacity (TIBC), were measured using an ADVIA 120 Siemens hematology analyzer and a Ferrentest (Diagnostic Chemicals Ltd, Charlottetown Canada). Isoflurane was purchased from Teva Pharmachemie B.V., Haarlem, The Netherlands, and sodium pentobarbital (60 mg/ml) was provided by the pharmacy of the Faculty of Veterinary Medicine of Utrecht University, The Netherlands. Protein quantification kit-rapid for protein quantification in urine and organs and the antibiotic antimycotic solution were purchased from Sigma-Aldrich Chemie B.V., Zwijndrecht, The Netherlands. Sarstedt S-monovettes tubes containing clotting activator silica beads or EDTA for blood collection were obtained from Sarstedt B.V, Etten Leur The Netherlands and heparin LEO, 5000 U.I./ml from Leo Pharma B.V, Amsterdam, The Netherlands. Alkaline Phosphatase Assay (ALP) kit was obtained from BioChain Inc. catalog no.:Z5030033, Hayward USA, Alanine Transaminase (ALT) was from Cayman Chemical Company catalog no.: 700260, Ann Harbor, USA, Aspartate Transaminase (AST) assay kit was obtained from BIOO SCIENTIFIC catalog no.: 3460-02, Austin, USA, Thiobarbituric Acid Reactive Substances (TBARS) measurement was performed using the OxiselectTM TBARS Assay kit MDA Quantification (Cell Biolabs Inc. San Diego, USA). Iron staining via the Prussian blue method was done with the Iron stain kit (product number HT20-1KT) from Sigma-Aldrich Chemie B.V., Zwijndrecht, The Netherlands. Phosphate buffered saline (PBS) pH 7.4 (containing per liter 8.2 g NaCl, 3.1 g $Na_2HPO_4 \cdot 12H_2O$ and 0.3 g $NaH_2PO_4 \cdot 2H_2O$) was from Braun Melsungen AG (Melsungen, Germany). All iron related parameters, the liver

enzymes ALP, ALT, AST, the TBARS assay and protein measurement in urine samples were performed as described by assay manuals unless stated otherwise.

2.3 Blood and urine collection from animals

Blood was collected as described in Section 2.1 via the tail vein at days 1, 15 and 29 of the experiment and at 24 hours after treatment. In experiment 2 an extra time point for blood collection was included 14 days before the first intravenous administration in order to confirm that the animals were not anemic before the start of the experiment (this was done by measuring hemoglobin in whole blood using the ADVIA 120 Siemens hematology analyzer). EDTA blood vials were used to collect whole blood for hemoglobin measurement and clotting activating silica vials were used for the collection of blood to obtain serum for serum iron, total iron binding capacity (TIBC) measurements as well as the various liver enzyme measurements (ALP, ALT and AST). As transferrin saturation (TSAT) is the ratio of serum iron and TIBC, these parameters were used to calculate the TSAT values (formula 1).

TSAT (%) = (Serum iron (µmol/L) / TIBC (µmol/L)) x 100% (1)

In order to obtain serum, the vials were centrifuged at 4°C for 10 minutes at 3,000 rpm. Afterwards, the serum was frozen and kept at -20°C until analyzed. During the 24 hours that the rats were placed in metabolic cages, urine was collected in measurement cylinders containing 1 ml of antibiotic antimycotic solution diluted 1:5 with deionized water. The urine was frozen and stored at -20°C until analysis. In addition, during experiment 2 the volumes of the urine collected for 24 hours of each rat were measured in order to be able to calculate the amount of proteinuria per day.

2.4 Prussian blue histology staining

After the organs were perfused, they were collected and immediately immersed into liquid nitrogen and stored at -80°C until analysis. The liver tissue was embedded in Optimum Cutting Temperature (OCT) compound for protection, before sections were made. Frozen 5 mm slices of the first liver lobe of each animal were cut longitudinally using a Leica CM3050 for cryo-sectioning and thaw mounted on a glass slide. Before the Prussian blue staining, the tissue sections on the glass slides were allowed to thaw at room temperature. Next, the sections were fixed 10 minutes in acetone and subsequently washed with demineralized water. The liver tissue was stained according to the protocol of the iron assay staining kit (procedure No.HT20, Sigma Aldrich). In short, the slides were incubated in working iron stain for 10 minutes and subsequently rinsed with deionized water. Next, the sections were incubated in working pararosaniline

solution for 3 minutes. Both working solutions were available in the iron staining assay kit and prepared according to the supplier manual. The hematoxyline dye solution was filtered using a 0.2 µm filter before use. Afterwards, the tissue sections were stained with the filtered hematoxylin solution for 30 seconds followed by 5 seconds staining with eosin-Y solution (1 gram in 1 liter 70% ethanol containing 5 ml glacial acid). The sections were then dehydrated by placing the slides in ethanol/water mixtures with increasing ethanol concentrations (from 50 to 100%) and finally in xylene. Finally, the liver tissues were dried overnight at room temperature. The histological analysis was done using Keyence microscope BZ-9000 series (Keyence Corporation of America, Itasca, IL, USA) at a magnification of 200x to examine the sections and using ImageJ software to count 5 tissue spots per tissue section per animal in order to calculate the average stained surface.

2.5 Statistical methods

All results for the iron parameters, liver enzymes, organ functionality and oxidative-stress as-well as histology, are expressed as mean ± standard deviation. Analysis was done using a Two-way ANOVA with Bonferroni as post-hoc analysis using GraphPad Prism version 4.02 for Windows, GraphPad Software, San Diego California USA.

3. RESULTS AND DISCUSSION

The animals used in both the experiments received a weekly injection of 40 mg iron per kg body weight of either Venofer®, an iron similar or they were injected with saline solution (equivalent volume) as control. The dose administered to the rats is much higher than the maximum clinical dose of 7 mg/kg (28). However, 40 mg/kg has been previously used in several iron related comparison studies (1-4) and thus the same dose was used in the present study in order to compare our results with the outcomes of the published studies.

3.1 Iron related blood assessment

The iron related blood parameters such as serum iron and Total Iron Binding Capacity (TIBC) were measured and transferrin saturation was derived from the aforesaid parameters as described in Section 2.3. Table 1 shows the serum iron and TIBC values of the rats (males and females combined) of experiment 1.

Experiment 1

Day of exp	Veno	ISS1	Control
Serum iron (µg/dL)			
day 1	146 ± 30	157 ± 21	122 ± 37
day 15	222 ± 93	201 ± 84	165 ± 96
day 29	345 ± 39***	294 ± 79*	189 ± 75
TIBC (µmol/L)			
day 1	74 ± 11	79 ± 4	75 ± 3
day 15	80 ± 7	80 ± 5	83 ± 7
day 29	80 ± 3	79 ± 8	87 ± 5
TSAT (%)			
day 1	36 ± 7	37 ± 6	29 ± 9
day 15	49 ± 17	45 ± 18	35 ± 19
day 29	78 ± 6***	66 ± 16**	39 ± 17

* Versus control group $p < 0.05$
** Versus control group $p < 0.01$
*** Versus control group $p < 0.001$

Table 1. Serum Fe in (µg/dL), total iron binding capacity (TIBC in µmol/L) and transferrin saturation (TSAT in %). Serum Fe and TIBC measured in serum derived from blood of rats collected at different time points upon administration of iron treatments or saline as control. Results represent mean ± standard deviation of 8 animals (male and female) per treatment group.

Table 1 shows that for all treatment groups the average serum iron increased in time. This was, even though not expected, also the case for the control group. Only at day 29 significant differences in serum iron values could be observed between the animals that received the iron formulations and the control animals (Venofer®; $p<0.001$ and ISS1; $P<0.05$), while TIBC values showed no differences between treatments. In addition, Table 1 also demonstrates that the TSAT values of the iron treated groups at day 29 were significantly different than the values found in the control group (Venofer®; $p<0.001$ and ISS1; $p<0.01$). Overall, there were no significant differences in the iron parameters between the two iron preparations Venofer® and ISS1. The gender specific serum iron results for each treatment group are depicted in Figure 1 and table 2 reports the statistical analysis of the different treatments for the different genders in time. This analysis gives insight into possible differences in gender responses on the treatments.

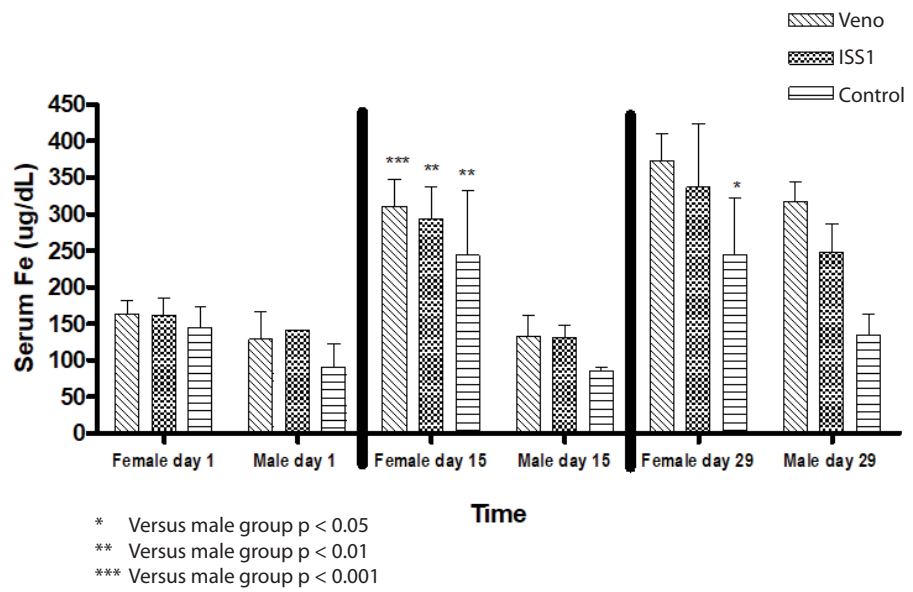

Figure 1. Gender differences for serum Fe concentrations in (µg/dL) within the treatment groups (female versus male animals) at the different time points. Results represent mean ± standard deviation of 4 animals per gender group.

Figure 1 shows that the female rats have a trend for higher serum iron values compared to males, being most prominent at day 15. On that day the female rats of all treatment groups including the control group displayed higher serum iron values compared to the male rats of the same treatment group (Venofer®, $p<0.001$; ISS1, $p<0.01$ and control $p<0.01$). Watanabe et al. (29), studied the iron content of rat serum ferritin in both genders and observed no differences between the genders for the iron concentrations in serum. However, the serum ferritin concentration in female rats was significantly higher than in male rats, suggesting that female rats had higher iron stores than male rats. Table 2 shows that at day 29, both female and male rats have statistically higher iron values compared to control rats that received saline injections. This indicates that in terms of iron measured in serum after multiple iron administration, both genders are susceptible to these iron treatments. Nevertheless, Table 2 shows no differences between the two iron preparations Venofer® and ISS1 within a gender throughout the experiment.

Serum Fe (µg/dL) Gender in time		Control	Veno	ISS1
Female	day 1	145 ± 24	122 ± 72	161 ± 21
Male	day 1	68 ± 45	96 ± 62	35 ± 61
Female	day 15	244 ± 76	233 ± 137	220 ± 131
Male	day 15	86 ± 4	100 ± 61	131 ± 14
Female	day 29	244 ± 68	280 ± 164	337 ± 75
Male	day 29	134 ± 25	238 ± 139	248 ± 34
Statistical analysis Gender in time		**Veno versus control P value**	**ISS1 versus control P value**	**Veno versus ISS1 P value**
Female	day 1	P > 0.05	P > 0.05	P > 0.05
Male	day 1	P > 0.05	P > 0.05	P > 0.05
Female	day 15	P > 0.05	P > 0.05	P > 0.05
Male	day 15	P > 0.05	P > 0.05	P > 0.05
Female	day 29	P < 0.01	P < 0.05	P > 0.05
Male	day 29	P < 0.001	P < 0.01	P > 0.05

Table 2. Serum iron in µg/dL specified for each gender in time and statistical analysis of serum iron within male/female groups between the treatments in time. Results represent mean ± standard deviation of 4 animals per gender in each treatment group.

Experiment 2 had an almost similar set-up as the first experiment but as described in Section 2.3, an extra time point for blood and urine collection was included at day 14 before the first intravenous administration. In addition, only male animals were used as we hypothesized that using only one gender, and more specifically male animals that do not have a hormonal cycle, will result in less variation within a treatment group.
In order to confirm that the animals were not anemic before the start of the experiment, hemoglobin (Figure 2) was measured 14 days prior the first iron administration and was also further monitored throughout the experiment.

The hemoglobin values were in the normal range of 14 - 20 g/dL for non-anemic rats (30).
The serum iron concentrations of experiment 2 are depicted in Table 3. It can be observed that at day 29, the serum iron levels of animals that received the iron treatments were significantly elevated compared to control animals that received saline. As compared to experiment 1, in which both male and female rats were used, the standard deviations per

treatment group are in general smaller. This means that for serum iron concentrations, there is indeed less variation within the treatment group when using only male animals. The total iron binding capacity data, likewise experiment 1, did not show differences between the treatments (Venofer®, ISS2 and saline control). On the other hand, the TSAT

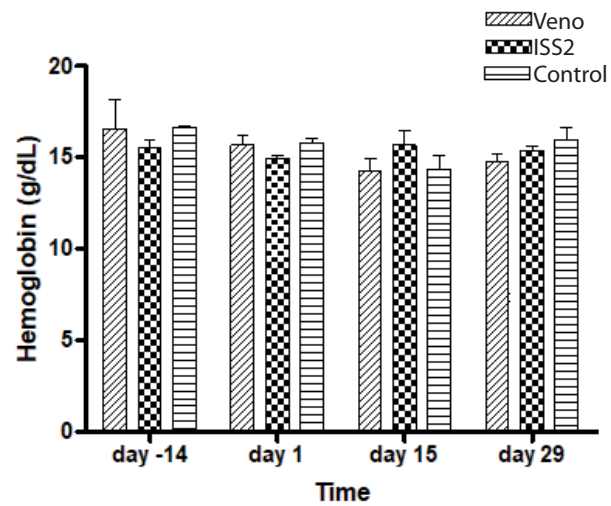

Figure 2. Hemoglobin (g/dL) measured in whole blood 14 days prior the first injections and after administration of iron treatments or saline as control. Results represent mean ± standard deviation of 3 male animals per treatment group.

values showed besides the significant difference between the iron treatment groups and control also a significant difference between the two iron treatments (Venofer® versus ISS2, $p<0.05$).

The results of the iron parameters measured in the two experiments clearly demonstrate a gender difference for these iron related parameters, while exposing the animals to the same experimental environment and treatment

Experiment 2

Day of exp	Veno	ISS2	Control
Serum iron (µg/dL)			
day-14	137 ± 40	91 ± 10	140 ± 25
day 1	237 ± 70	175 ± 33	128 ± 14
day 15	226 ± 20	262 ± 89	136 ± 27
day 29	331 ± 49	265 ± 32	104 ± 23
TIBC (µmol/L)			
day-14	93 ± 6	88 ± 4	85 ± 3
day 1	88 ± 11	79 ± 4	84 ± 8
day 15	109 ± 4	114 ± 6	109 ± 0
day 29	75 ± 2	80 ± 8	82 ± 3
TSAT (%)			
day-14	26 ± 6	19 ± 1	30 ± 6
day 1	48 ± 9	39 ± 5	28 ± 5
day 15	37 ± 4	40 ± 12	27 ± 0
day 29	79 ± 10	60 ± 6	23 ± 6

\+ Versus ISS2 group $p < 0.05$
* Versus control group $p < 0.05$
** Versus control group $p < 0.01$
*** Versus control group $p < 0.001$

Table 3. Serum Fe (µg/dL), total iron binding capacity (TIBC in µmol/L) and transferrin saturation (TSAT in %), in blood of rats collected at different time points upon administration of iron treatments or saline as control. Results represent mean ± standard deviation of 3 male animals per treatment group.

3.2 Biochemical analysis to evaluate liver and kidney function

3.2.1 Liver enzyme tests

In order to assess possible toxic effects that a high dose of iron may cause in the liver, the liver function was assessed by measuring the liver enzymes alkaline phosphatase (ALP), alanine aminotransferase (ALT) in experiment 1 and aspartate amino transferase (AST) in experiment 2. Toxicity of the formulations will result in release of these liver enzymes in the circulation and their concentrations were therefore measured in serum.

Experiment 1

Day of exp	Veno	ISS1	Control
ALP (U/L)			
day 1	61 ± 16	59 ± 14	48 ± 13
day 15	53 ± 14	63 ± 15	53 ± 16
day 29	52 ± 14	55 ± 11	37 ± 11
ALT (U/L)			
day 1	111 ± 28	105 ± 22	106 ± 30
day 15	74 ± 32	71 ± 22	79 ± 37
day 29	84 ± 34	71 ± 34	92 ± 25

Experiment 2

Day of exp	Veno	ISS2	Control
AST (U/L)			
day -14	82 ± 58	86 ± 38	69 ± 44
day 1	69 ± 27	55 ± 7	59 ± 2
day 15	45 ± 1	61 ± 20	73 ± 20
day 29	43 ± 4	56 ± 9	66 ± 12

Table 4. ALP, ALT and AST values in serum after administration of iron formulations or saline as control at different time points. Results represent mean ± standard deviation of 8 animals, female and male (ALP and ALT) or 3 animals, male (AST) per treatment group.

Table 4 shows ALP, ALT and AST values measured in serum of animals of experiment 1 and 2, and demonstrates that there were no differences between the treatment groups. Comparable studies carried out by Shah et al. (3) and Meier et al. (4), did also not find any statistical differences in the liver enzyme concentrations in serum of rats that received an ISS formulation (which) as compared to the originator Venofer®. However, more important is that we did not find a similar outcome to the extensive experiments conducted by Toblli et al., (1), even though we tested the same iron sucrose products. In the Toblli experiment, in which also mixed gender treatment groups were used, clear differences between the treatments were observed. They reported that animals that received the ISS showed much higher serum values of the liver enzymes as compared to the levels detected in saline control animals but also in animals that received Venofer®. Figure 3, displays the gender specific results for ALP (Figure 3A) and ALT (Figure 3B) for each treatment group and table 5 gives the statistical analysis per gender in time.

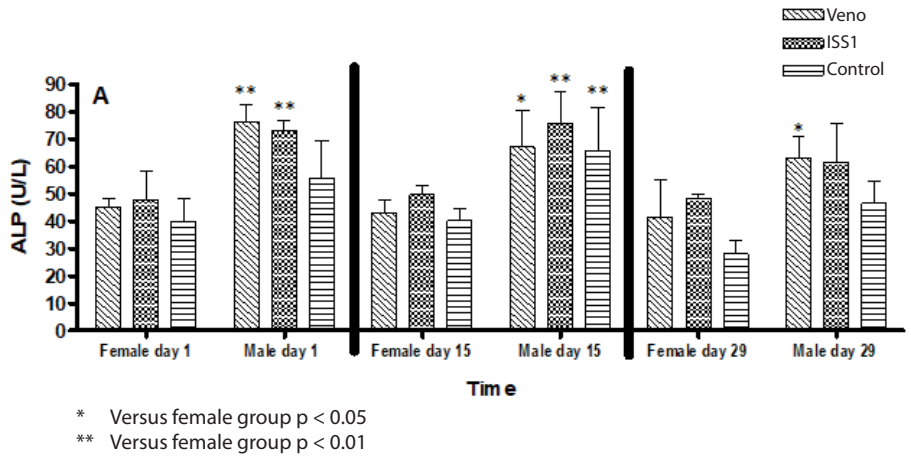

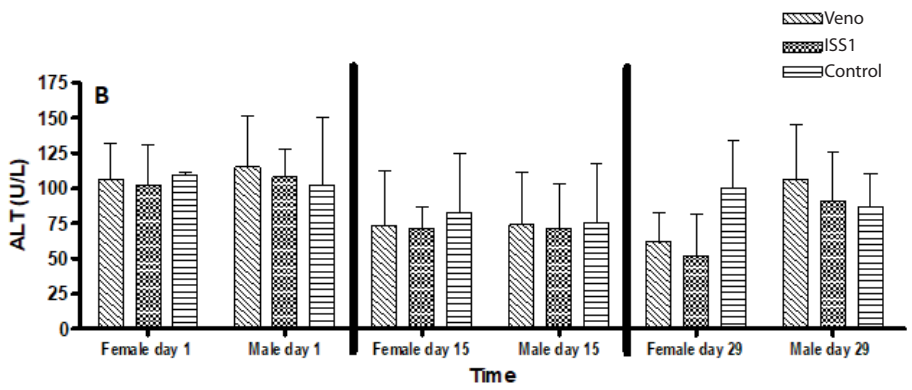

Figure 3. Gender differences within a treatment group (female versus male animals) for A; ALP (U/L) and B; ALT (U/L) serum levels at the different time points. Results represent mean ± standard deviation of 4 animals per gender in each treatment group.

The ALP serum levels of the male animals were statistically higher than the levels of the females. This was especially the case after one injection (day 1) and at day 15 after three injections. At day 15, it can also be seen that even the male rats of the control group gave higher ALP values than the female animals of the control group. This is in contrast with the results of the iron serum concentrations (Figure 1), where the females display more elevated values than the male animals. In addition table 5 shows that at day 1 there is a significant difference between ALP levels of male animals of the Venofer® group compared to male rats of the control group ($p < 0.05$) and at day 29 between females that received ISS1 and females of the control group ($p < 0.05$).

Figure 3B demonstrates that ALT was not different between the genders. In addition, there was also no statistical difference in ALT values within rats of the same gender in time.

ALP (U/L) Gender in time		Veno versus control P value	ISS1 versus control P value	Veno versus ISS1 P value
Femal	day 1	P > 0.05	P > 0.05	P > 0.05
Male	day 1	*P < 0.05*	P > 0.05	P > 0.05
Female	day 15	P > 0.05	P > 0.05	P > 0.05
Male	day 15	P > 0.05	P > 0.05	P > 0.05
Female	day 29	P > 0.05	*P < 0.05*	P > 0.05
Male	day 29	P > 0.05	P > 0.05	P > 0.05

Table 5. Statistical treatment difference within a gender group in time. Results represent mean ± standard deviation of 4 animals per gender in each treatment group.

3.2.2 Kidney function analysis

Proteinuria was measured for assessment of the kidney function (Table 6). At day 29 after five injections, both experiment 1 and 2 showed a statistical difference in proteinuria between the iron treatments. In experiment 1, proteinuria levels of animals that received ISS1 were significantly higher than levels of the Venofer® treated rats on day 29 ($P<0.05$). In experiment 2, the proteinuria was corrected for the amount of urine excreted per day. Here, elevated protein urine values of animals that received Venofer®, in comparison with the animals that received ISS2 ($P<0.01$) and saline ($P<0.05$), can be seen. Toblli et al., (1) observed statistical differences in proteinuria between the originator (Venofer®) and the iron sucrose similars already after one injection at day 1 and this difference remained after five injections, resulting in greater values for animals that received the ISS than those that received Venofer®.

Experiment 1

Day of exp	Veno	ISS1	Control
proteinuria (µg/ml)			
day 1	1,419 ± 248	2,037 ± 804	1,463 ± 293
day 15	1,185 ± 266	1,483 ± 489	1,190 ± 278
day 29	1,944 ± 547	2,684 ± 828^{+}	1,985 ± 618

Experiment 2

Day of exp	Veno	ISS2	Control
proteinuria (mg/day)			
day -14	9 ± 1	8 ± 1	8 ± 0
day 1	10 ± 1	9 ± 0	9 ± 1
day 15	9 ± 1	7 ± 2	8 ± 0
day 29	13 ± 2^{*++}	9 ± 2	9 ± 2

\+ Versus Veno group $p < 0.05$
* Versus control group $p < 0.05$
++ Versus ISS2 group $p < 0.01$

Table 6. Proteinuria values (experiment 1 in µg/ml; experiment 2 in mg/day) in urine after weekly administration of iron formulations or saline at different time points. Results represent mean ± standard deviation of 8 animals (experiment 1) or 3 animals (experiment 2) per treatment group.

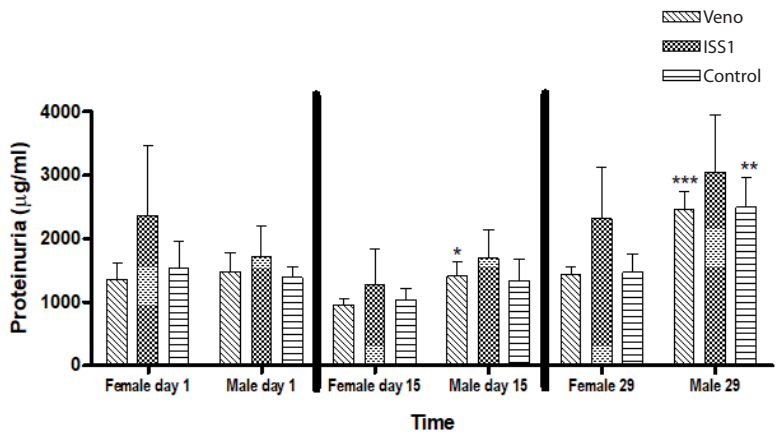

* Versus female group $p < 0.05$
** Versus female group $p < 0.01$
*** Versus female group $p < 0.001$

Figure 4. Gender differences within a treatment group (female versus male animals) for proteinuria (µg/ml) at the different time points. Results represent mean ± standard deviation of 4 animals per gender in each treatment group.

3.3 Oxidative stress in liver and kidney

Oxidative stress in the liver and kidney was assessed by measuring thiobarbituric acid reactive substances (TBARS), which are markers for cellular lipid peroxidation in the organs. TBARS are expressed in malondialdehyde (MDA) levels. The malondialdehyde (MDA) levels in livers (Figure 5A) were not significantly different between the treatments. However, MDA levels of the kidneys (Figure 5B) of animals that received Venofer® formulation were significantly higher ($p<0.05$) compared to animals that received saline as control, but not significantly different from animals that received ISS1. Figure 5C illustrates that the male animals are predominantly accountable for the significant difference in MDA levels of animals that received Venofer® compared to the control animals. During experiment 2 (Figure 6), in which MDA levels were corrected for the amount of organ protein, the iron treatments did not exhibit differences compared to the saline control but also not between the different iron treatments.

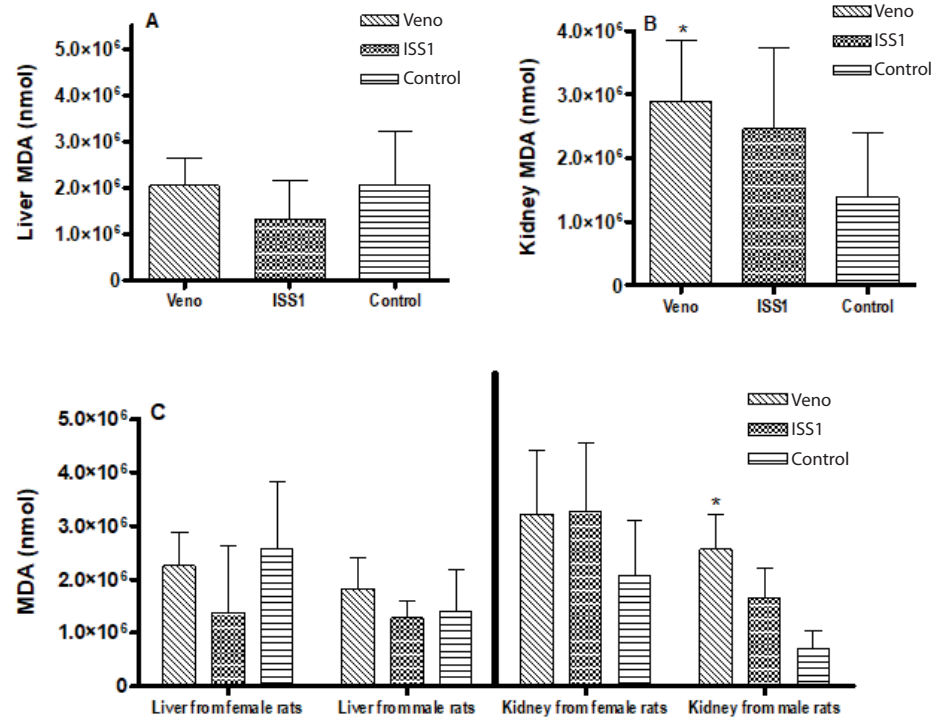

* Versus control group $p < 0.05$

Figure 5. Thiobarbituric acid reactive substances (TBARS) expressed in malondialdehyde levels in nmol (experiment 1), measured in A; liver, B; kidney and C; treatment difference within a gender in time in liver and kidney. Results represent mean ± standard deviation of 8 animals (A and B) or 4 animals per gender (C) per treatment group.

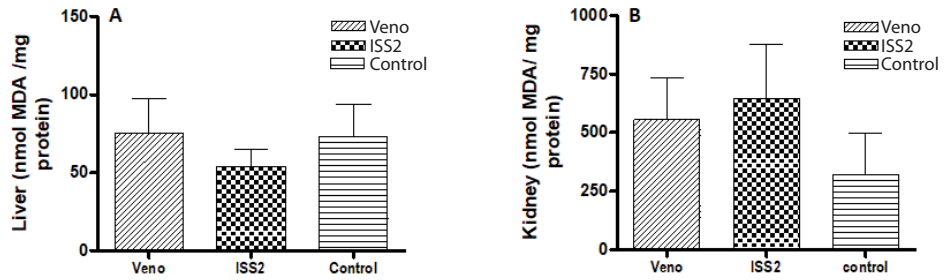

Figure 6. Thiobarbituric acid reactive substances (TBARS) expressed in malondialdehyde levels in nmol/mg protein (experiment 2), measured in liver (A) and kidney (B). Results represent mean ± standard deviation of 3 animals per treatment group.

The previously mentioned study by Toblli et al. (1), in which five weekly treatments were given, also no significant differences in MDA levels of animals that received ISS and Venofer® were found.

3.4 Prussian blue staining liver

The morphology of the liver of animals that received multiple injections of the various iron complexes or saline was analyzed (experiment 1 only). Figure 7A shows iron staining of the liver sections for the female and male rats together as a group and Figure 7B depicts the treatment results per gender.

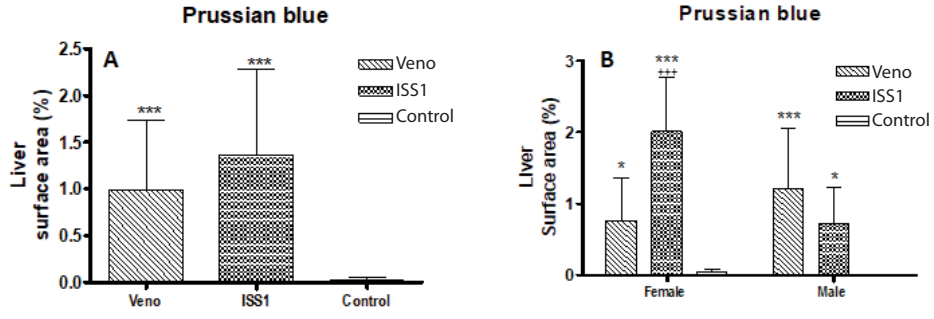

Figure 7. Prussian blue staining of the liver (expressed in % of stained surface) for A; the different treatments and B; treatment difference within a gender. Results represent mean ± standard deviation of 8 animals (A) or 4 animals (B) per gender in each treatment group.

Figure 7A, clearly portrays that there is iron disposition in the liver after multiple injections of the different iron formulations. Animals that received either Venofer® or ISS1 showed statistically higher iron staining levels compared to animals that received saline ($p<0.001$). This outcome is in accordance with the previous study of Toblli et al. (1). However, in the present study no distinction between the iron treatments was found while the results by Toblli et al. (1) suggested large and statistically significant differences between the iron treatments, where both the ISS treatments resulted in a higher Prussian blue staining areas as compared to Venofer®. Figure 7B, shows that both the male and female rats that received iron injections gave higher values than the animals of the control group. Interestingly, while no distinction between Venofer® and ISS1 can be seen when the rats are taken together (Figure 7A), Figure 7B suggests that there is large significant variation between the females that received ISS1 compared to those that received Venofer® ($p<0.01$).

The aim of this research was to assess whether results from studies in which the original iron sucrose product was compared to iron sucrose similars, are reproducible. This, as it is interesting to evaluate whether a frequently used model (Sprague Dawley rats), is sensitive enough to give insight into the potential differences in physiological and toxicological effects of the different iron sucrose formulations. It was disclosed after the collection and interpretation of the data that the two ISS examined during this research were the same iron sucrose similars evaluated by Toblli et al. (1). In contrast to the study performed by Toblli et al., our results demonstrate that there was no clear difference between the iron products (1). When comparing the outcomes of several studies with a similar experimental protocol, including our results and the studies performed by Toblli et al. (1, 2), Shah et al. (3) and Meier et al. (4), it can be concluded that there is no agreement in terms of demonstrating major differences between the original iron sucrose product Venofer® and the various generics.

In addition, the study presented here demonstrates clear differences between results obtained from female or male rats. When using mixed genders within a treatment, some parameters such as serum iron and proteinuria gave results with quite large standard deviations after multiple injections of the iron products. This reflects a large inter-variance within a treatment group. Therefore, if the aim is to test the overall effect of iron treatments in general and possible outcome differences between male and female, both genders should be included in the study. However, if the aim is to just compare toxicity and detect small differences between the iron treatments, one should consider if it is necessary to use both male and female animals during non-clinical experiments for iron based medicines. In case of using mixed genders in experimental set-ups, the treatment groups should consist of a sufficient population of males and females in order to minimize large deviations resulting from biological variation within the treatment group.

Accordingly, it should also be scrutinized whether the animal model itself is sensitive enough to exhibit effects after the different treatments.

4. CONCLUSION

The results presented in this chapter give insight into difficulties to reproduce animal studies. When conducting research on iron medicinal products, reproducibility of non-clinical studies is a requirement that should be carefully assessed.

5. ACKNOWLEDGEMENT

This research was financially supported by Vifor Pharma. Special thanks to Professor Jorge E. Toblli from the Hospital Alemán Buenos Aires Argentina, for his support and advice during this research.

6. CONFLICT OF INTEREST

The views expressed in this manuscript are the personal views of the authors. Vifor Pharma participated in meetings and financially supported the research.

7. REFERENCES

1. Toblli, JE, Cao, G, Oliveri, L, & Angerosa, M. Differences between original intravenous iron sucrose and iron sucrose similar preparations. Arzneimittelforschung. 2009;59:176-190.
2. Toblli JE, Cao G, Oliveri L, Angerosa M. Differences between the original iron sucrose complex Venofer® and the iron sucrose similar Generis®, and potential implications. Portuguese Journal of Nephrology and Hypertension. 2009;23:53-63.
3. Shah GB, Chorawala MC, Trivedi VR, Deshpande SS. Differences between the original iron sucrose complex Venofer and the iron sucrose similar Sucrofer. Research Journal of Pharmaceutical, Biological and Chemical Sciences. 2013;4:655-669.
4. Meier T, Schropp P, Pater C, Leoni AL, Khov-Tran VV, Elford P. Physicochemical and toxicological characterization of a new generic iron sucrose preparation. Arzneimittelforschung. 2011;61:112-119.
5. Benoist de B, McLean E, Egli Ines, Cogswell M. Worldwide prevalence of anaemia 1993-2005: WHO global database on anaemia. 2008.
6. Goldberg LA. Iron sucrose similars. Hospital pharmacy europe. 2010;48: 21-22.
7. Schrier SL, Auerbach M, Mentzer WC, Tirnauer JS. http://www.uptodate.com/contents/treatment-of-iron-deficiency-anemia-in-adults. Accessed Nov 2017.
8. Auerbach M, Ballard H. Clinical Use of Intravenous Iron: Administration, efficacy and safety. ASH Education Program Book. 2010;338-347.
9. Locatelli F, Aljama P, Bárány P, Canaud B, Carrera F, Eckardt KU, Hörl WH, Macdougal IC, Macleod A, Wiecek A, Cameron S. European Best Practice Guidelines Working Group. Revised European best practice guidelines for the management of anaemia in patients with chronic renal failure. Nephrology Dialysis Transplantation. 2004;19 Suppl 2:1-47.
10. Bailie GR, Clark JA, Lane CE, Lane PL. Hypersensitivity reactions and deaths associated with intravenous iron preparations. Nephrology Dialysis Transplantation. 2005;20:1443-1449.
11. Critchley J. Adverse events associated with intravenous iron infusion (low-molecular weight iron dextran and iron sucrose): a systematic review. Transfusion Alternatives in Transfusion Medicine. 2007;9:8-36.
12. Chertow GM, Mason PD, Vaage-Nilsen O, Ahlmén J. Update on adverse drug events associated with parenteral iron. Nephrology Dialysis Transplantation. 2006;21(2):378-82.
13. Yee J, Besarab A. Iron sucrose: The oldest iron therapy becomes new. American Journal of Kidney Diseases. 2002;40(6):1111-21.
14. Fütterer S, Andrusenko I, Kolb U, Hofmeister W, Langguth P. Structural characterization of iron oxide/hydroxide nanoparticles in nine different parenteral drugs for the treatment of iron deficiency anaemia by electron diffraction (ED) and X-ray powder diffraction (XRPD). Journal of Pharmaceutical and Biomedical Analysis. 2013;86:151-60.
15. Kudasheva DS, Lai J, Ulman A, Cowman MK. Structure of carbohydrate-bound polynuclear iron oxyhydroxide nanoparticles in parenteral formulations. Journal of Inorganic Biochemistry. 2004;98(11):1757-69.

16. Crichton RR, Danielson BG, Geisser P. Iron therapy: With special emphasis on intravenous administration. Uni-Med, Bremen. 2008; 4th Edition: 81-2.
17. Nissim J, Robson JM. Preparation and standardization of saccharated iron oxide for intravenous administration. The Lancet. 1949;253(6556):686-9.
18. https://www.accessdata.fda.gov/drugsatfda_docs/nda/2000/21135_Venofer.cfm
19. Elford P, Bouchard J, Jaillet L, Pearson N, Rogue A, Sabadie C, Forster R. Biodistribution and predictive hepatic gene expression of intravenous iron sucrose. Journal of Pharmacological and Toxicological Methods. 2013;68(3):374-83.
20. Koskenkorva-Frank TS, Weiss G, Koppenol WH, Burckhardt S. The complex interplay of iron metabolism, reactive oxygen species, and reactive nitrogen species: insights into the potential of various iron therapies to induce oxidative and nitrosative stress. Free Radical Biology & Medicine. 2013;65:1174-94.
21. Schellekens U, Klinger E, Muhlebach S, Brin JF, Storm G, Crommelin DJ. The therapeutic equivalence of complex drugs. Regulatory Toxicology and Pharmacology. 2011;59:176-183
22. EMA, 2015. Reflection Paper on the Data Requirements for Intravenous Iron-based Nano-colloidal Products Developed with Reference to an Innovator Medicinal Product. 2015; EMA/CHMP/SWP/620008/2012. http://www.ema.europa.eu/docs/en_GB/document_library/Scientific_guideline/2015/03/WC500184922.pdf
23. Van der Meer PJK. The scientific value of non-clinical animal studies in drug development (PhD Dissertation). Utrecht University, 2013
24. Kacew, S. Role of rat strain in the differential sensitivity to pharmaceutical agents and naturally occurring substances. Journal of Toxicology and Environmental Health. 1996;47:1-1.
25. Hedrich HJ. Chapter 1 - History, Strains and Models A2 - Krinke, Georg J. The Laboratory Rat. 2000;3-16. London: Academic Press.
26. Soldin OP, Mattison DR. Sex differences in pharmacokinetics and pharmacodynamics. Clinical Pharmacokinetics. 2009;48(3):143-57.
27. Soldin OP, Chung SH, Mattison DR. Sex differences in drug disposition. Journal of Biomedicine and Biotechnology. 2011;Article ID 187103: 14 pages. doi:10.1155/2011/187103
28. Schröder O, Mickisch O, Seidler U, De Weerth A, Dignass AU, Herfarth H, Reinshagen M, Schreiber S, Junge U, Schrott M. Intravenous iron sucrose versus oral iron supplementation for the treatment of iron deficiency anemia in patients with inflammatory bowel disease a randomized, controlled, open-label, multicenter study. The American Journal of Gastroenterology. 2005;100(11):2503-9.
29. Watanabe K, Yamashita Y, Ohgawara H, Sekiguchi M, Satake N, Orino K, et al. Iron Content of Rat Serum Ferritin. Journal of Veterinary Medical Science. 2001;63(5):587-9.
30. van Zutphen LFM, Baumans V, Ohl F. Handboek proefdierkunde : proefdieren, dierproeven, alternatieven en ethiek. 2012. Amsterdam : Reed Business.

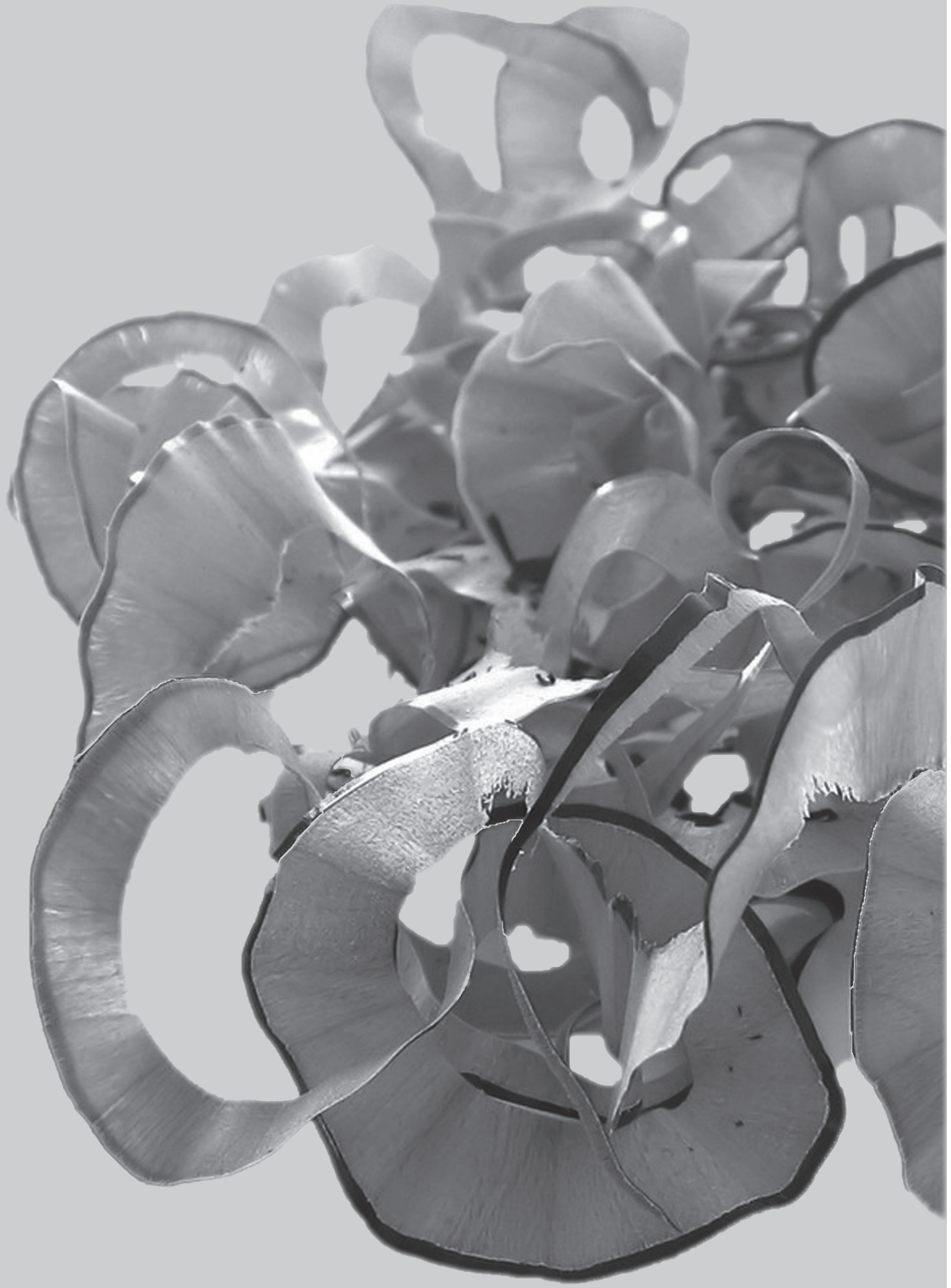

CHAPTER 4

Evaluation of the suitability of a Sprague Dawley rat model to assess intravenous iron preparations

Kimberley Span, Ebel H.E. Pieters, Vera Brinks, Wim E. Hennink, and Huub Schellekens

Published in Journal of Pharmacological and Toxicological Methods
2018; 91: 7-17

Abstract

The aim of the study was to examine the reproducibility of a rat model to assess the preclinical similarity in safety profiles and tissue accumulation of iron products. Accordingly, the effect of several doses of intravenously administered Venofer® and of Ferrlecit® on blood parameters, and on kidney and particularly liver toxicity were examined in non-anemic Sprague Dawley rats. The different analysis showed neither a clear treatment nor a dose effect after multiple injections. The parameters measured in this rat strain showed some iron induced adverse effects, but these could not be correlated to treatment specific differences. The findings presented in this paper indicate the difficulty to define a useful preclinical model to evaluate iron-based nano-colloidal preparations.

KEYWORDS

Anemia, Bio-distribution, Intravenous iron, methods, Rats, Toxicity

1. INTRODUCTION

Intravenous iron products are given as standard of care to treat iron deficiency anemia in patients suffering from various diseases such as chronic renal failure. Common clinically used intravenous iron products consist of colloidal particles consisting of a polynuclear iron(III) oxyhydroxide core surrounded by a carbohydrate shell in order to stabilize the core and delay the release of iron from the complex (1). All iron preparations contain a similar core, but have distinct molecular weight and compositions of the carbohydrate shell (2). The older types of intravenous iron complexes such as high molecular weight iron dextran, iron sucrose and sodium ferric (iron) gluconate are categorized by their kinetic and thermodynamic properties (3). However, the more recent generation of intravenous iron products like ferumoxytol and iron isomaltoside 1000 (4) cannot be classified by the above mentioned parameters as these complexes do not demonstrate evident correlation between molecular weight of the complex and degradation kinetics as is the case for the first types of iron products. The type of carbohydrate used to stabilize the iron compound is an important factor for the amount of iron that is rapidly released from these iron complexes, and may affect the subsequent processing of the iron complex by the reticuloendothelial system (5, 4). Non-complex-bound iron is either transferrin or non-transferrin bound (NTBI, non-transferrin bound iron). NTBI is taken up rapidly by parenchymal cells resulting in an increase of the labile iron pool (LIP) concentration, which has been suggested to have an important role in the formation of reactive oxygen species (ROS) (6-8). ROS cause oxidative stress and ultimately result in cell and tissue damage (9-11). As a result, a series of preclinical studies with iron complexes focused on oxidative stress induced cell and tissue damage has been performed. These studies have demonstrated a variable increase in oxidative stress biomarkers, dependent on the type of complex being used (12). Therefore, it is of utmost importance to properly characterize the iron preparations in terms of physicochemical properties and toxicology. Moreover, it is important to develop robust and reproducible manufacturing processes to secure product quality, and therefore ensure optimal pharmacokinetics and bio-distribution of the products. These non-clinical studies are now considered an essential component for the market approval of new or of follow up generic iron based nanoparticle products (13). To this end, it is essential to select an appropriate experimental model that is able to properly represent or measure iron accumulation in the organs. Several *in-vivo* models including the use of avian embryos (5, 12, 14-16) have been used to evaluate the iron tissue distribution and/or possible toxic effects of intravenous iron therapy. The Sprague Dawley (SD) rat, which is an outbred animal model, is used for multiple purposes including safety and efficacy testing (17) as well as comparative studies between generics and original iron preparations (18, 19). The aim of the present study is to investigate whether the Sprague Dawley rat, in an almost comparable experimental set-up as described by Toblli et al. (20), Shah et al. (19) and Meier et al. (17), is a reproducible and appropriate

model to evaluate the tissue iron accumulation and possible iron related toxicity of iron products after intravenous administration. This was done by studying the dose effect of Venofer® (iron sucrose) and of Ferrlecit® (sodium ferric gluconate). Ferrlecit® is included as positive control since this product is regarded as less stable with a higher content of labile iron compared to Venofer® (21-23).

2. MATERIALS AND METHODS

2.1 Materials

Venofer® (iron sucrose; 20 mg Fe/ml) lot number 118101 was obtained from Vifor (International) Ltd, St. Gallen, Switzerland. Ferrlecit® (ferric sodium gluconate; 12.5 mg Fe/ml) lot number D1C300A, from Sanofi-Aventis U.S. LLC. and saline solution (sodium chloride 0.9% w/v) was purchased from Braun Melsungen AG, Oss, The Netherlands. Isoflurane was purchased from Teva Pharmachemie B.V., Haarlem, The Netherlands, and pentobarbital (sodium) 60 mg/ml (charge number 12042302) was provided by the pharmacy of Veterinary Medicine at Utrecht University, the Netherlands. Formalin solution neutral buffered 10% (HT501128-4L) and protein quantification kit-rapid for protein quantification in tissue, urine and serum samples were both purchased from Sigma-Aldrich Chemie B.V., Zwijndrecht, The Netherlands. Sarstedt S-monovettes tubes containing clotting activator silica beads or EDTA for blood collection were obtained from Sarstedt B.V, Etten Leur, The Netherlands and heparin LEO, 5000 U.I./ml from Leo Pharma B.V, Amsterdam, The Netherlands. Iron-related parameters hemoglobin (Hb), total serum iron (Fe), total iron binding capacity (TIBC) and transferrin saturation (TSAT), were measured using an ADVIA 120 Siemens hematology analyzer and a Ferrentest (Diagnostic Chemicals Ltd, Charlottetown, Canada). Creatinine in serum and urine was measured via the colorimetric Jaffe method using SYNCHRON® Systems (24-26). Aspartate transaminase (AST) assay kit was obtained from Bioo Scientific, catalog #3460-02, (Austin, USA), the antibiotic antimycotic solution (A5955) was from Sigma-Aldrich Chemie B.V., Zwijndrecht, The Netherlands. Thiobarbituric acid reactive substance (TBARS) measurements were performed using the Oxiselect™ TBARS assay kit MDA Quantification (Cell Biolabs Inc., San Diego, USA). Anti-ferritin light chain antibody (ab69090) and anti-IL6 antibody (ab6672) were purchased from Abcam plc, Cambridge, United Kingdom. Iron staining via the Prussian blue method was done with the iron stain kit (product number HT20-1KT) from Sigma-Aldrich Chemie B.V., Zwijndrecht, The Netherlands. Vectastain Biotinylated Universal Anti-Mouse IgG/Rabbit IgG was purchased from Vectastain ABC kit Cat.No. PK-6200, Universal Elite, Vector Lab., Burlingame, Ca, USA). Phosphate buffered saline (PBS) pH 7.4 containing per liter 8.2 g NaCl, 3.1 g $Na_2HPO_4 \cdot 12H_2O$ and 0.3 g $NaH_2PO_4.2H_2O$ was obtained from Braun Melsungen AG (Melsungen, Germany). Bovine serum albumin lyophilized powder (BSA), hydrogen

peroxidase solution 30% and 3,3-diaminobenzidine (DAB) tetrahydrochloride tablets were purchased from Sigma-Aldrich Chemie B.V., Zwijndrecht, The Netherlands. All iron related parameters, the liver enzyme AST, TBARS assay and protein measurement in serum and urine samples were performed as described by assay manuals unless stated otherwise.

2.2 Animals

The animal experiment was performed according to Institutional Ethical Committee Regulations of Utrecht University, The Netherlands. Male HSd: Sprague Dawley rats (Harlan laboratories, The Netherlands) were housed in standard perspex cages and fed standard rat chow (rat and mouse breeder and grower diet from Special Diets Services, United Kingdom) and (acidified) water *ad libitum* unless stated otherwise. The animals were acclimatized for 4 weeks prior to the experiment and subjected to a 12 hours light/dark cycle. Each treatment group consisted of 4 animals weighing around 300 grams (10 weeks old) at the beginning of the experiment.

2.3 Experimental setup

Animals received one single intravenous injection or five injections of the different treatments in a time span of four weeks, with one injection per week. The treatments were: 40 mg Fe/kg, 60 mg Fe/kg and 80 mg Fe/kg of Venofer® (Veno) or 40 mg Fe/kg, 60 mg Fe/kg of Ferrlecit® (Ferr) and saline solution as control. The dose and volume to be administered to each animal were calculated using the iron concentration in Venofer® and Ferrlecit® and the weight of the animals. The control group received saline solution also according to their weight in equal volumes as animals that received 60 mg (Fe)/kg of Ferrlecit®. The clinically used dose is around 7 mg/kg. Therefore, in order to be able to induce iron accumulation in the organs, high doses of ≥ 40 mg/kg and multiple administrations of the two different therapeutic iron complexes were administered. The starting dose of 40 mg Fe/kg was chosen because this is also the dose used in similar studies to evaluate possible toxic effects of iron preparations. The rats receiving the Ferrlecit® treatments were not injected with a higher dose than 60 mg/kg, as adverse effects in rats have been reported when higher concentrations of this formulation were administered (27). The animals were placed in metabolic cages immediately after injection and deprived from food for 19 hours and had access to (acidified) water *ad libitum*. Twenty four hours after injection of the iron formulations or saline, the animals were taken out of the metabolic cages, blood was collected via the tail vein and urine was taken out of the container. Depending on whether the animals received one or five injections, blood and urine were collected twice (pretreatment and at day 1 of the experiment) or a total of four times (pretreatment, and at day 1, 15 and 29 of the

experiment). The volume of the urine was assessed and stored at – 20°C until analysis. Following the last blood collection the animals were sacrificed by an overdose of pentobarbital (1 - 2 ml) via intraperitoneal injection followed by saline perfusion until they were completely blood depleted. The liver and kidneys were collected for oxidative stress analysis and histochemistry.

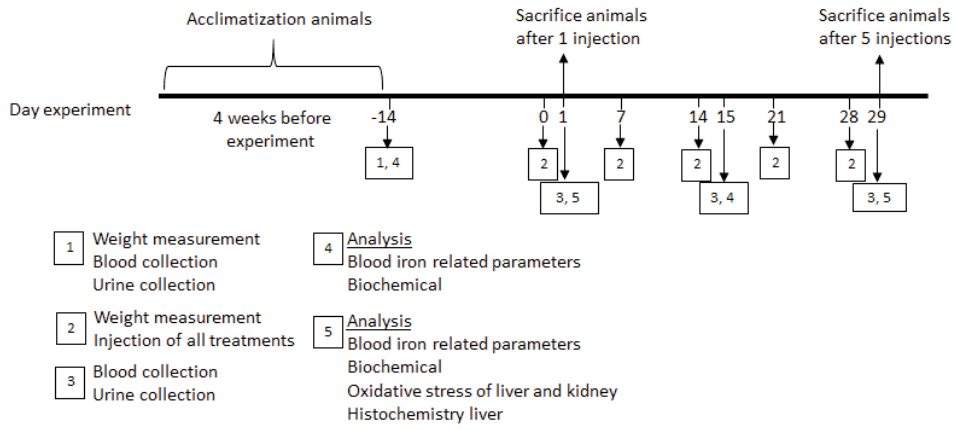

Fig. 1. Experimental schedule with time points; 4 weeks prior experiment and day -14, 0, 1, 7, 14, 15, 21, 28 and 29 of experiment.

The experimental setup used in the study described in this publication had a staggered setup, where part of the rats were included in every "run", and each "run" had a different starting date. In order to avoid a bias in the results due to this staggered setup, we included one rat from every treatment group in each "run".

2.3.1 General well-being of the animals

The general well-being of the animals was assessed by examining (1) the weight of the animals throughout the study and overall appearance of the rats, (2) the iron parameters pretreatment and (3) the organs for any anomalies at the end of the study. The weight of the rats was measured every week. In the weeks that the animals were scheduled to receive an iron treatment, the weight of the animals was measured before treatment injection (thus at day 0, 7, 14 and 28 of the experiment). In order to establish that the animals were not anemic prior starting the experiment, hemoglobin, serum iron (Fe), and total iron binding capacity (TIBC) were measured at 14 days before start of the experiment. Finally, antecedent to the organ collection for further analysis, the tissues of the different organs were visually examined for any anomalies.

2.3.2 Blood and urine collection

Fourteen days preceding the experiment, blood was collected via the tail vein to obtain the pretreatment iron related parameters, to assess the animals' general well-being and to confirm that they were non-anemic. During the experiments blood was drawn 24 hours after the iron products or saline were administered. The blood was collected in EDTA blood collecting vials for the measurement of whole blood hemoglobin or in vials containing clotting activating silica to obtain serum for serum Fe, Total Iron Binding Capacity (TIBC), serum creatinine and aspartate transaminase (AST) determinations. The vials were centrifuged at 4°C for 10 minutes at 3000 rpm. The serum was then collected and kept at -20°C until analyzed. The serum Fe and TIBC were used to calculate transferrin saturation (TSAT), which is the ratio of serum iron and TIBC (formula 1).

TSAT (%) = (Serum iron (µmol/L) / TIBC (µmol/L)) x 100% (1)

The activity measurement of the liver enzyme aspartate transaminase (AST), to detect any liver deterioration, was performed as described by the assay manual as supplied by the manufacturer. The urine was collected in measurement cylinders containing 1 ml of the antibiotic antimycotic solution and subsequently diluted 5 times with deionized water. The volume was recorded and the urine was kept at -20°C until analysis. Proteinuria in urine was measured using a protein quantification kit based on the coomassie brilliant blue G technique as described in the assay kit manual. Creatinine in serum and urine were determined as described by the manufacturer's manual. In order to calculate the creatinine clearance rate (Ccr) the following equation (2) was used:

Ccr = (Urine creatinine x 24 hour volume (ml)) / (Serum creatinine x 24 x 60 (minutes)) (2)

2.3.3 Oxidative stress markers in organs

The rodents were sacrificed and the organs were drained from blood by saline perfusion. The liver and kidneys were collected and immediately frozen in liquid nitrogen and subsequently stored at -80 °C until investigated. Oxidative stress markers in the liver and kidney after only one injection or multiple injections was determined by measuring the degree of cellular damage after lipid peroxidation. Here, the reactive compound malondialdehyde (MDA), formed from the decomposition of unstable peroxides derived from polyunsaturated fatty acids, was determined via a reaction with thiobarbituric acid (TBARS). The TBARS assay was corrected for the protein amount in the organ. The protein content in the livers and kidney was quantified using a protein kit for proteinuria.

2.3.4 Immunohistochemistry of liver

To perform immunohistochemistry studies, the first liver lobe of each animal was collected. The liver was cut longitudinal in order to obtain an average of 3-5 sections per liver. Next, the liver tissue sections were mounted on a glass slide and five regions with comparable surface were chosen to assess stain surface using ImageJ software. The average stained surface was then calculated. The analysis of the tissue sections was performed using a Keyence microscope BZ-9000 series (Keyence Corporation of America, Itasca, IL, USA) at a magnification of 200x.

Interleukin-6 and ferritin labeling

Livers were assessed for IL-6 and ferritin. After collection, livers of the animals were fixed for 48 hours in 10% formalin and subsequently embedded in paraffin. The livers were cut in five micron sections using a microtome for paraffin embedded tissue sections. The tissue sections were deparaffinized by subsequently placing them in xylene and thereafter in ethanol/water mixtures with decreasing ethanol concentrations ranging from 100 to 50% and finally rinsing the tissue sections in running cold tap water. In case of the IL-6 assay, after deparaffinization, an antigen retrieval step was performed by placing the tissue sections in an antigen retrieval buffer (10 mM citrate buffer, pH 6). Subsequently, the tissue sections were placed in a microwave for 10 minutes. Next, for both the IL-6 and the ferritin assay, the tissue sections were washed 3 times for 5 minutes with PBS- 1% Tween 20 (PBS-Tween), followed by addition of 150 µL blocking serum (normal horse serum) supplied with the Vectastain kit on each tissue section and incubated for 20 minutes. The sections were subsequently rinsed twice for 5 minutes with PBS-Tween and incubated with 300 µL primary antibody as follows. For IL-6 staining a rabbit polyclonal to IL-6, 1:400 dilution in 1% BSA in PBS was incubated for 2 hours at room temperature and for the ferritin labeling a polyclonal antibody to ferritin light chain, 1:200 dilution in 1% BSA in PBS was used and incubated overnight at 4°C. Subsequently, the tissue sections were rinsed for 5 minutes with PBS-Tween and quenching was achieved by incubating the sections with 1.6% v/v H_2O_2 (30% hydrogen peroxidase in deionized water). IL-6 and ferritin were visualized utilizing Vectastain Biotinylated Universal Anti-Mouse IgG/Rabbit IgG as a secondary antibody. The tissue sections were rinsed twice with PBS-Tween for 5 minutes and subsequently incubated with 200 µL of the secondary antibody for 30 minutes. Next, the tissue sections were washed twice for 3 minutes with only PBS and the Vectastain ABC reagent was added and incubated for 30 minutes. PBS-Tween was then used to wash off the ABC reagent followed by addition of 1 drop, to cover each tissue section completely, of 3,3-ddiaminobenzidine (DAB) tetrahydrochloride solution (1 DAB tablet was dissolved in 15 ml PBS and filtered on a 0.2 µM filter; subsequently 12 µL of 30% H_2O_2 (in deionized water) was added to the 15

ml solution). After 2-3 minutes of incubation with the DAB solution, the tissue sections were rinsed with tap water and counterstained with hematoxyline. The hematoxyline dye solution was filtered using a 0.2 µm filter and the tissue sections were then placed in the filtered hematoxyline stain for 30 seconds. Next, the sections were washed with tap water twice for 3 minutes and dehydrated by placing them for 30 seconds in 70% ethanol, 1 minute in 100% ethanol and finally 2 minutes in xylene. Subsequently, the tissue sections were left to dry completely overnight at room temperature.

Prussian blue staining of liver

Prussian blue was used to assess iron present in the livers of all animals that received either one or five injections of the different formulations. After deparaffinization of the tissue sections as described for interleukin-6 and ferritin labeling, the tissues were placed for 10 minutes in iron staining working solution which was supplied and prepared according to supplier manual (iron stain kit, procedure No.HT20). After rinsing with deionized water, the sections were placed for 3 minutes in pararosaniline working solution, which was also supplied and prepared according to supplier manual (iron stain kit procedure No.HT20). Next, hematoxyline dye solution was filtered using a 0.2 µm filter. The tissue sections were subsequently stained with the filtered hematoxylin solution for 30 seconds and thereafter with eosin-Y solution (1 gram in 1 liter 70% ethanol containing 5 ml glacial acid) for 5 seconds and the sections were dehydrated by placing them in ethanol/water mixtures with increasing ethanol concentrations ranging from 50 to 100% ethanol and finally in xylene. The tissue sections were then dried overnight at room temperature.

2.4 Statistical methods

The bodyweight, iron parameters in blood, biochemical data as well as the immunohistochemistry results are all expressed as mean ± standard deviation. First a Gaussian distribution test was performed using the D'Agostino & Pearson normality test. Further analysis was done using a Two-way ANOVA with Bonferroni post hoc test. The threshold for significance was an alpha of 0.05, with $p \leq 0.05$ regarded as significant. In the manuscript significance is indicated with a symbol when $p \leq 0.05$, independent of the actual p-value. Both tests were performed with GraphPad Prism version 4.02 for Windows, GraphPad Software, San Diego California USA.

3. RESULTS

3.1 General well-being of animals

Figure 2 shows the weight of the animals in time after administration of the different iron formulations. The animals gained weight in time according to their age.

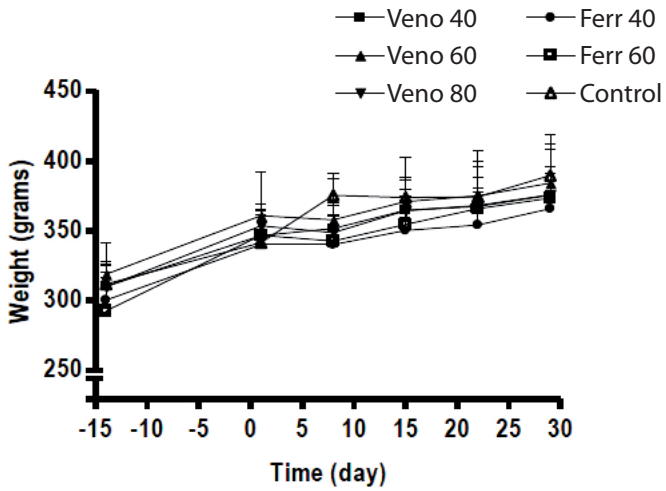

Fig. 2. Weight of animals throughout the study (starting 14 days prior the first injection until day 28 of the experiment). Results represent mean ± standard deviation of four animals per treatment group.

3.1.1 Iron related blood values in rats after administration of the iron formulations: hemoglobin, serum iron, total iron binding capacity and transferrin saturation

Figure 3 shows the hemoglobin values in time after administration of the various treatments. The pretreatment results for hemoglobin obtained at 14 days before the start of the experiment showed values in the normal expected range of 14 - 20 g/dL (28), demonstrating that the rats were not anemic. The hemoglobin concentrations in blood remained unchanged throughout the experiment even after multiple injections of the formulations.

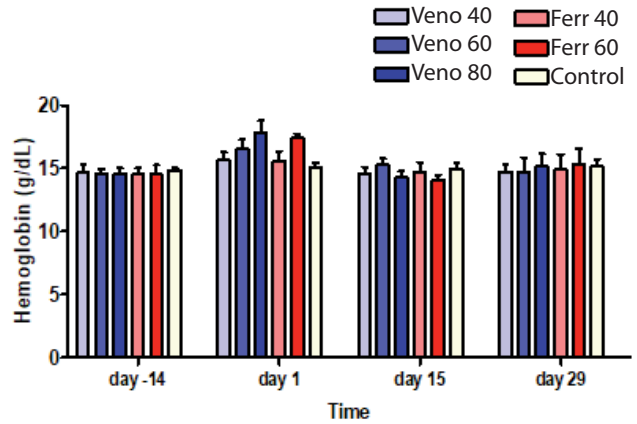

Fig. 3. Hemoglobin concentrations (g/dL) in blood of rats as a function of time after administration of iron treatments or saline as control. Results represent mean ± standard deviation of four animals per treatment group.

Table 1 shows the serum iron and TIBC values, measured in serum at different time points after administration of the iron preparations. An increase in serum iron was observed for all treatment groups, except the control group, throughout the study. On the other hand TIBC values remained stable for all the treatments.

Table 1. Serum Fe in (µg/dL) and total iron binding capacity (TIBC in µmol/L)

Serum Fe

Day of exp.	Veno 40	Veno 60	Veno 80	Ferr 40	Ferr 60	Control
day -14	104 ± 35	99 ± 39	63 ± 11	56 ± 6	100 ± 52	113 ± 86
day 1	186 ± 31	164 ± 36	186 ± 16	193 ± 21	166 ± 16	144 ± 31
day 15	359 ± 106	250 ± 63	277 ± 51	206 ± 83	192 ± 31	154 ± 21
day 29	462 ± 105	315 ± 23	312 ± 100	244 ± 38	221 ± 27	183 ± 39

TIBC

Day of exp.	Veno 40	Veno 60	Veno 80	Ferr 40	Ferr 60	Control
day -14	78 ± 8	79 ± 2	76 ± 3	72 ± 3	76 ± 4	80 ± 9
day 1	97 ± 13	71 ± 9	73 ± 5	87 ± 7	75 ± 12	101 ± 8
day 15	110 ± 17	78 ± 9	83 ± 12	71 ± 8	87 ± 12	92 ± 8
day 29	97 ± 21	71 ± 6	79 ± 16	71 ± 3	72 ± 11	90 ± 13

Serum Fe and TIBC measured in serum derived from blood of rats collected at different time points upon administration of iron treatments or saline as control. Results represent mean ± standard deviation of four animals per treatment group.

Figure 4 shows, after administration of the different iron formulations, significant increases in transferrin saturation (TSAT) total values in serum of animals that received an iron complex compared to rats in the control group.

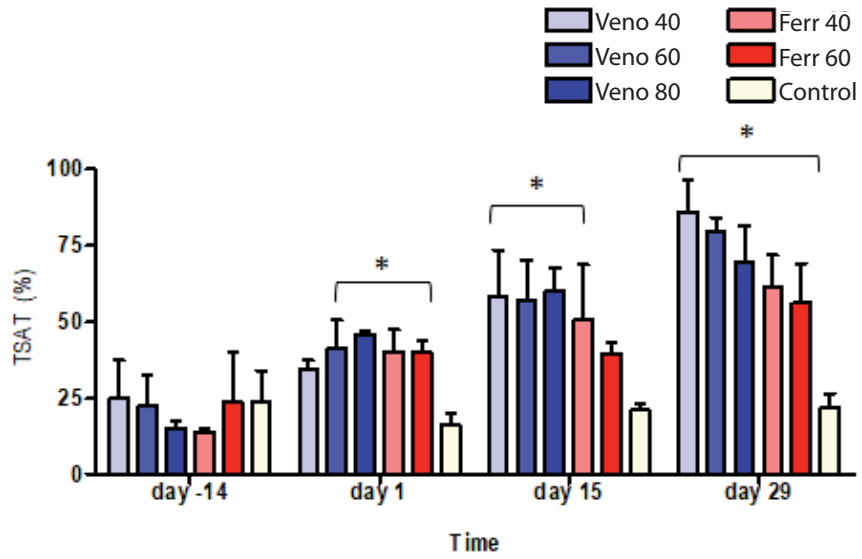

* Versus control

Fig. 4. Transferrin saturation (TSAT) in %, calculated as the ratio of serum iron and total iron binding capacity, as function of time after administration of iron treatments or saline as control. Results represent mean ± standard deviation of four animals per treatment group.

The serum iron parameters (Serum Fe, TIBC and TSAT) showed no statistical differences between animals that received the different iron treatments. However, multiple applications of the same iron preparation in the same group of animals, resulted in greater serum iron levels and TSAT values in time.

3.1.2 Visual observation of abdominal organs after intravenous administration of various iron treatments.

Photographs of the abdomen of the rats that received the different formulations were taken. Figures 5 and 6 are a representation of the appearance of the livers and intestines from animals in the various sample groups.

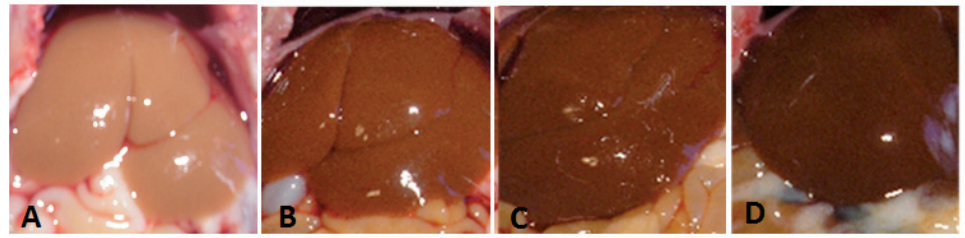

Fig. 5. Liver appearance of (A) control group (saline solution); (B) Venofer® 40 mg/kg; (C) Venofer® 60 mg/kg; (D) Venofer® 80 mg/kg at day 29 after animals were sacrificed and saline perfused.

Both the liver and intestines of animals that received an iron complex showed a brownish coloration. Figure 5 also demonstrates that rats that received a higher iron dose had a stronger discolored liver (brownish color).

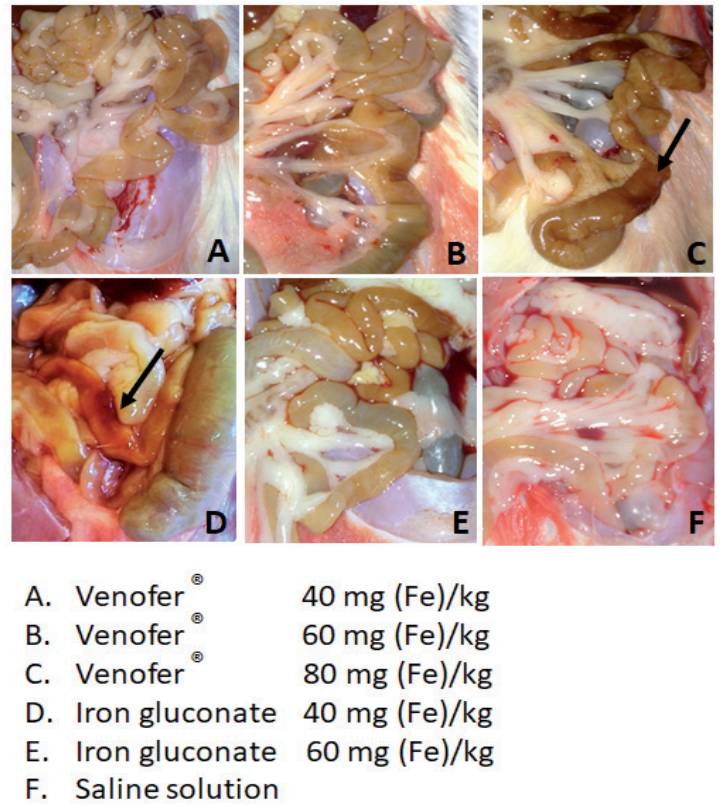

Fig. 6. Intestine appearance of animals that received the different treatments at day 29 after animals were sacrificed and saline perfused.

The intestines of the iron treated animals which also showed a brownish color however, did not demonstrate a dose-effect correlation as observed for the liver (Figure 5). Furthermore, also a reddish discoloration can be seen in the intestines in iron treated rats compared to control in Figure 6 marked with an arrow.

3.2 Biochemical analysis of liver and kidney

Table 2 shows the results of the liver enzyme aspartate transaminase (AST) as biomarker to evaluate the liver function. The average AST values of the animals 14 days prior the start of the experiment was 65 ± 12 U/L.

Table 2. Aspartate transaminase (AST) in (U/L)

Day of exp.	Veno 40	Veno 60	Veno 80	Ferr 40	Ferr 60	Control
day -14	68 ± 7	78 ± 16	72 ± 10	63 ± 11	64 ± 10	59 ± 9
day 1	118 ± 39	143 ± 51	75 ± 10 #	95 ± 26 #	92 ± 21	73 ± 10 #
day 15	84 ± 7	66 ± 7	63 ± 11	75 ± 13	61 ± 5	58 ± 6
day 29	86 ± 10	93 ± 20	90 ± 13	84 ± 4	126 ± 94*	73 ± 13

* Versus Control $p < 0.05$

\# Versus Veno 60 $p < 0.05$

AST values in serum after administration of iron formulations or saline as control at different time points. Results represent mean ± standard deviation of four animals per treatment group.

The AST values depicted in Table 2, demonstrate that at day 1, there was an increased mean value for Venofer® 60 mg/kg compared to other treatment groups including the Venofer® 80 mg/kg group. Furthermore at day 29, the Ferrlecit® 60 mg/kg group showed a higher AST value than rats that received saline as control.

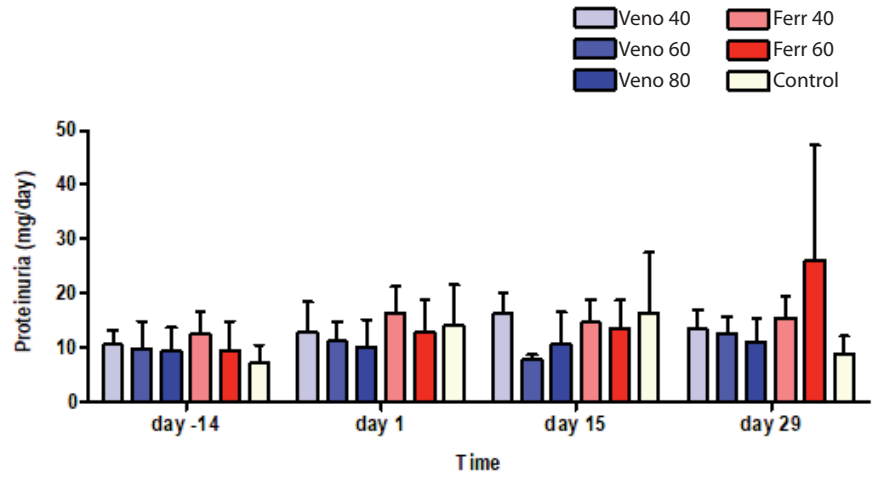

Fig. 7. Proteinuria as function of time after administration of iron treatments or saline as control. Results represent mean ± standard deviation of four animals per treatment group.

When assessing the kidney function, neither the proteinuria levels in urine (Figure 7) nor creatinine clearance (Figure 8) resulted in significant differences between the two iron formulations as well as compared to controls at any time.

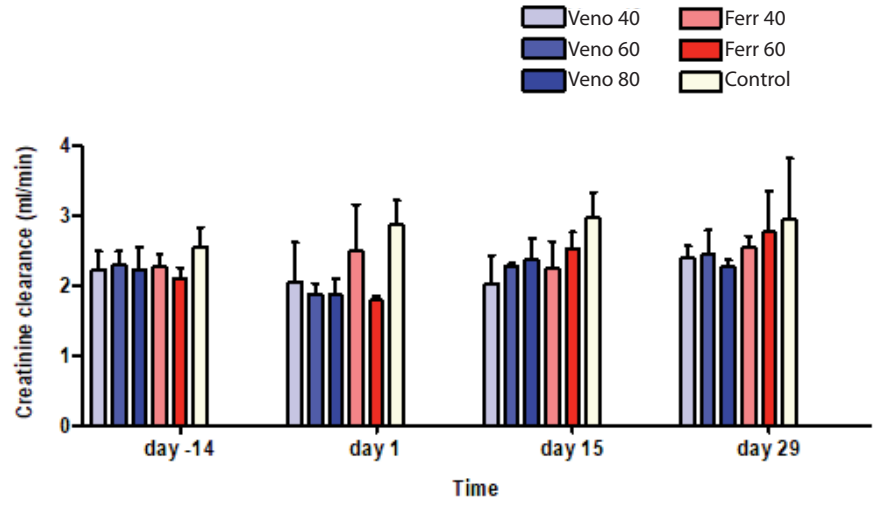

Fig. 8. Creatinine clearance values of animals that received iron treatments or saline as function of time. Results represent mean ± standard deviation of four animals per treatment group.

3.3 Oxidative stress in liver and kidney

Table 3 illustrates the thiobarbituric acid reactive substance (TBARS) measurements for the iron complex treatment groups and control group. At day 1 after one single injection, the lipid peroxidation in the kidneys of the animals that received an iron formulation were significantly higher compared to the animals that received saline solution. Moreover, at day 29 after multiple injections, the mean value of the iron sample groups also evidently increased as compared to the control group, but the extent of lipid peroxidation was lower than at day 1. The latter was also observed by Toblli et al. (18). The livers of rats that received an iron formulation displayed time dependent changes for the same iron treatment. Higher average lipid peroxidation values were observed in livers of animals that received multiple injections of the same formulation in time when comparing the results of day 1 with day 29 for both Venofer® and Ferrlecit®.

Table 3. Thiobarbituric acid reactive substance (TBARS) in nmol/mg

Day of exp.	Veno 40	Veno 60	Veno 80	Ferr 40	Ferr 60	Control
Kidney						
day 1	1,756 ± 278 *	1,665 ± 424 *	2,134 ± 463 *	2,340 ± 261 *	2,172 ± 274 *	692 ± 166
day 29	1,391 ± 455	1,030 ± 186	1,279 ± 248	1,604 ± 69	1,389 ± 123	715 ± 149
Liver						
day 1	158 ± 32	297 ± 23	257 ± 8	312 ± 20	289 ± 32	308 ± 116
day 29	503 ± 94	507 ± 95	550 ± 179	583 ± 186	344 ± 288	457 ± 212

* Versus control $p < 0.05$

TBARS measurement to monitor lipid peroxidation in kidney and liver at day 1 and day 29 after administration of the two iron formulations or saline. Results represent mean ± standard deviation of four animals per treatment group.

3.4 Histology of the liver of rats after multiple treatment injections

Figure 9 shows iron staining of the liver sections as well as the results of the Prussian blue analysis for the different treatments. The results demonstrate that administration of both Venofer® and Ferrlecit® results in an increase in iron deposit in the liver.

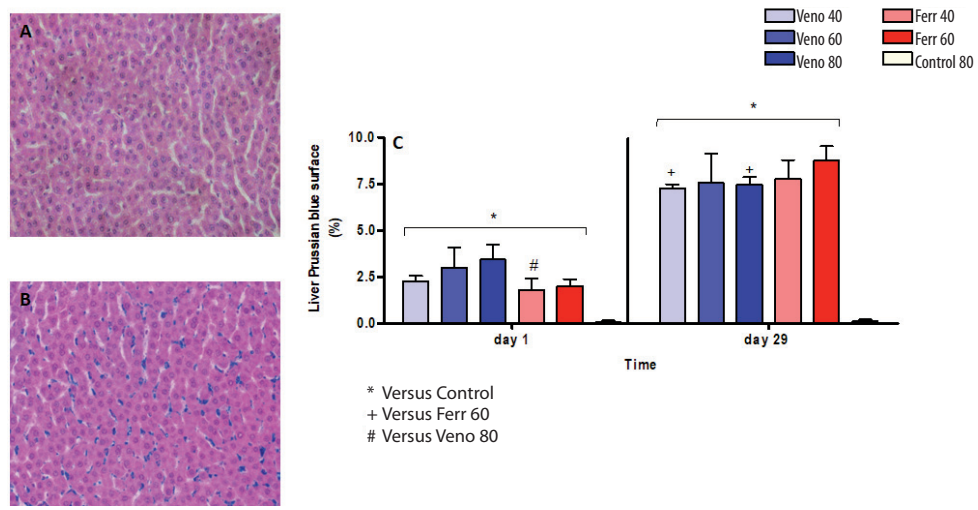

Fig. 9. Prussian blue staining of A) liver section of control group; B) liver section of Venofer® 40 mg/kg at day 29 of experiment C) Prussian blue staining surface area (%). Results represent mean ± standard deviation of four animals per treatment group.

After only one injection of the various iron formulations, the liver tissue already showed positive staining for iron (Prussian blue). At day 1 the animals injected with Venofer® 80 mg/kg showed increased iron staining compared to animals that received one injection of Ferrlecit® 40 mg/kg, while at day 29 the animals of the Ferrlecit® 60 mg/kg group showed more iron staining compared to the Venofer® 40 and 80 mg/kg groups. Following multiple injections of the iron preparations, some of the Prussian blue images obtained, indicate that there was iron present in the Kupffer cells but also in the hepatocytes which implies iron overload (images are not shown).

Measurement of the pro-inflammatory marker Interleukin-6 (IL-6) after administration of the different treatments to rats, showed elevated IL-6 levels at day 29 but not at day 1. Figure 10 shows that after one single injection the values of the different sample groups are similar. In contrast, at day 29 the animals that received the various doses of Venofer® resulted in an evident increase compared to control animals. Furthermore, after multiple injections, animals treated with the highest iron concentration (Venofer® 80 mg/kg) resulted also in higher IL-6 values compared to Venofer® 40 mg/kg and Ferlecit® 40- and 60 mg/kg treated groups. The liver IL-6 values from the animals that received Ferrlecit®

40 and 60 mg/kg portrayed high variability within the treatment group and higher mean levels at day 29 compared to the animals that received these treatments on day 1, but there was no significant difference with the control group.

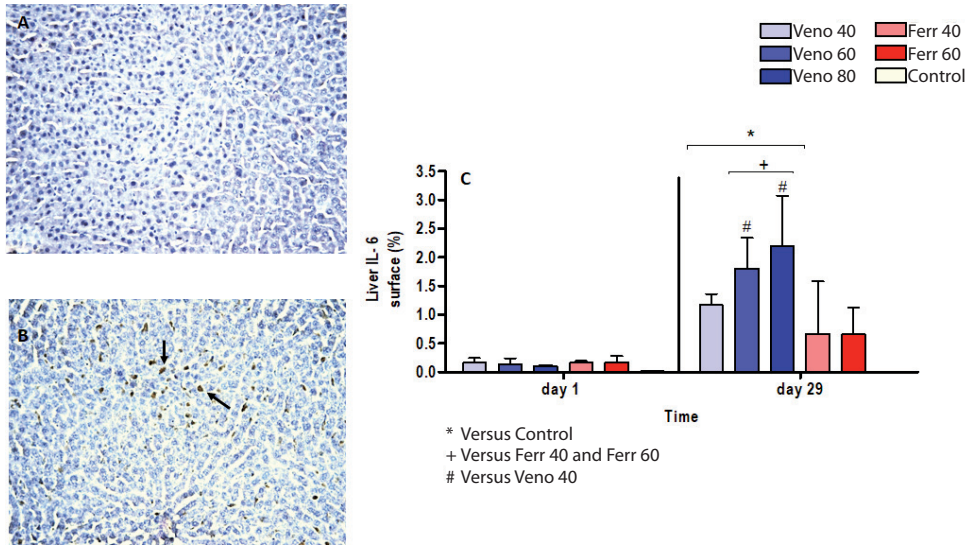

Fig. 10. IL-6 analysis of A) liver section of control group; B) liver section of Venofer® 40 mg/kg at day 29 of experiment C) IL-6 staining surface area (%). Results represent mean ± standard deviation of four animals per treatment group.

In addition, Table 5 compares results of the IL-6 marker after one single injection (day 1) and after multiple administrations (day 29).

Table 5. Interleukin-6 (IL-6) variance analysis in %.

Treatment	day 1	day 29	P-values
Veno 40	0.161 ± 0.070	1.168 ± 0.166	P < 0.05
Veno 60	0.139 ± 0.089	1.808 ± 0.459	P < 0.01
Veno 80	0.105 ± 0.019	2.200 ± 0.752	P < 0.001
Iron gluco 40	0.165 ± 0.025	0.670 ± 0.744	ns
Iron gluco 60	0.173 ± 0.090	0.657 ± 0.384	ns
Control	0.014 ± 0.006	0.000 ± 0.000	ns

IL-6 variance analysis (%). Results represent mean ± standard deviation of four animals per treatment group.

Figure 11 shows representative histological pictures of liver tissue of a control and an iron treated rat, and illustrates the surface area (%) of ferritin positive staining following one and five injections. At day 1, ferritin levels in the liver demonstrate a clear dose effect

where Venofer® 60- and 80 mg/kg give significant higher values than results obtained from control treated animals. After multiple injections at day 29, this dose effect disappears and all iron treated rats give ferritin levels significantly higher compared to controls.

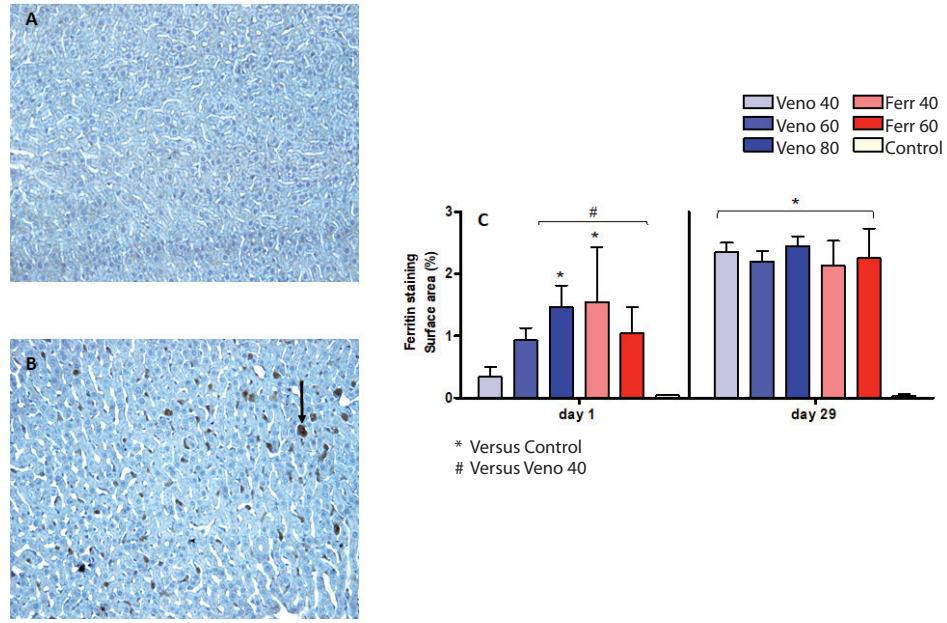

Fig. 11. Ferritin immunostaining of A) representative liver section of control group; B) representative liver section of Venofer® 40 mg/kg at day 29 of experiment; C) Ferritin staining surface area (%). Results represent mean ± standard deviation of four animals per treatment group.

4. DISCUSSION

The animals were subjected to high doses of ≥ 40 mg/kg and multiple administrations of two different therapeutic iron complexes (Venofer® and Ferrlecit®) of which the latter has been described to cause iron related oxidative stress both in clinical studies (29, 30) and in preclinical studies (31). It was opted not to submit animals with Ferrlecit® doses higher than 60 mg Fe/kg, as administration above this concentration resulted in adverse effects in rats (27). The other treatments began at a dose of 40 mg Fe/kg, which was the dose used in similar studies to evaluate possible toxic effects of iron preparations (17, 19, 20).

Throughout the study, the weight of the animals was monitored, as weight loss is often an indication of declining health of animals. It can be observed that independent of the formulation they received, the rats gained weight and the animals did not show any signs of distress or disease. Furthermore, the rats showed during the whole experiment

hemoglobin values in the normal expected range of 14 - 20 g/dL (28).
To get further insight into the blood iron related parameters, the serum iron and Total Iron Binding Capacity (TIBC) were measured in order to calculate the transferrin saturation (TSAT). Serum iron is known to be a variable parameter that can fluctuate depending on the time of day and thus on the time of blood sampling (32, 33). Therefore, during this study the blood collection for each animal was performed as accurate as possible exactly 24 hours after injection. The pretreatment and control serum iron values were similar to values obtained by Meier et al. (17). Even though no statistical differences between animals that received the different iron treatments was observed, multiple applications of the same iron preparation resulted in the same group of animals in time dependent changes resulting in greater serum iron levels and TSAT values. These results do not correspond to previous results obtained in relatively similar experiments performed by Toblli et al. (20, 31). In the Toblli experiments, different iron compounds were studied and administered in a dose of 40 mg (Fe)/kg. Multiple injections of the same iron complex did not result in an increase of serum iron levels over time but gave stable values throughout the experiment.
The abdominal organs of the rats that received 5 injections of the different iron formulations were examined to assess whether organs had irregularities as compared to the organs of the animals of the control group. Especially the liver and intestines depicted anomalies. The liver shows a dose-effect related brownish discoloration but in the intestines which also showed a brown color, a dose-effect was not apparent. Meier et al. (17), likewise also reported a change in liver color after supplying Sprague Dawley rats with two intravenous injections of iron sucrose complex at two different time points. In addition, Figure 6 suggests that the intestines of the majority of the rats treated with iron, portray signs of inflammation as depicted by the reddish area.
The toxic effects that might occur in the liver and kidney in case of excessive iron disposition in the organ tissue as well as the organ function were evaluated by performing a set of assays. The results from the liver enzyme aspartate transaminase (AST) which was measured as biomarker to evaluate the liver function, demonstrated no pattern in the significant differences between the different treatments. It can be concluded that the AST values during this study are neither dose nor time dependent and therefore are not considered of toxicological relevance.
The kidney function was evaluated by measuring proteinuria (Figure 7) and the creatinine clearance (Figure 8). The results demonstrate no evidence of renal failure as there was no significant differences between the iron treatments nor compared to control and there was no decrease in creatinine clearance as would be expected in the case of declining glomerular filtration function.
Elevated oxidative stress was observed in the kidney after one injection but remarkably after multiple injections of the iron treatments there was no significant differences. Interestingly, even though the liver is probably one of the primary organs to depict

any oxidative stress in case of iron overload, this organ did not exhibit any apparent differences in lipid peroxidation between the different groups.
The morphology of the liver tissue after administration of the various iron formulations or saline as control, was analyzed by performing iron staining, immunocytochemistry for the pro-inflammatory marker Interleukin-6 (IL-6) and ferritin immunostaining. The liver was assessed as the hepatic macrophages (Kupffer cells) comprise around 15% of the liver cells (34) and are an important absorptive cellular site for intravenous iron. Prussian blue staining in the liver was observed for all iron treatments already after one injection, indicating immediate iron disposition in the organ. The extent of Prussian blue staining was much higher on day 29 than on day 1 for the same iron treatment. This means that, even though the results on day 1 and day 29 are from a different subset of animals, there is most likely a gradual iron accumulation in the liver after multiple injections. The results of day 29, however, did not reflect a dose dependent effect which was expected as the livers displayed in Figure 5 showed somewhat a correlation between the given dose and brownish discoloration of the organ.
The immunohistochemistry studies also revealed clear signs of liver inflammation after multiple injections of the iron treatments. When assessing the pro-inflammatory marker Interleukin-6 (IL-6) at day 29, elevated values were obtained compared to control. In addition, table 5, showed that the pro-inflammatory (IL-6) marker is more prominent in time after multiple dosing of the same Venofer® treatment. This was however not the case for the Ferrlecit® treated animals and the control group.
In contrast to results obtained at day 1 for the IL-6 marker, the ferritin levels in the liver already depict at day 1 a clear dose effect. Compared to day 1, after multiple injections at day 29, there was no treatment nor dose effect and all iron treated groups gave significant elevated ferritin values compared to control. Interestingly, at day 29 after multiple injections of both formulations no treatment effect was found for the liver ferritin concentrations. Ferritin is normally considered to be a useful biomarker when determining iron accumulation in tissue and thus it was expected to obtain different ferritin levels in the liver tissue after administration of the various iron doses. It was also expected to detect different effects from the two iron preparations as they have different physicochemical characteristics (21).
The various assays did not show a clear pattern in neither the toxicological effects nor tissue accumulation. This unexpected outcome could be due to inter-variance of the treatment groups. The Sprague Dawley rat, which is widely used for medical research, is an out-bred strain with higher genetic variability compared to inbred strains and is hence expected to give a higher variability in individual results (35, 36). Already in early studies in which tumors in six sources of Sprague Dawley rats was investigated, the authors emphasized how important it was to be careful when assessing findings using this model especially when performing research in different facilities or using animals from different sources (37). Therefore when performing experiments with this

rat strain, using larger group sizes could be recommended when the aim is to detect small differences in markers in animals that received different iron doses or formulations. It should be noted that, generally speaking, toxicological effects are very dependent on the dose administered. Thus, even though a relatively small group size was used in our study, by administrating different doses of two different iron formulations, we lowered the risk of failing to observe and detect possible toxicological effects. The results obtained however demonstrate neither a dose effect after multiple injections of the iron formulations administered, nor an effect of the type of formulation. Thus, the sensitivity of this frequently used model to give a good indication of the similarity in iron tissue distribution and possible toxic effects of two different types of iron formulations, remains questionable. In order to conduct good preclinical studies, a good evaluation model and method should therefore be established. The results of this study reflect the difficulty to setup proper preclinical research to carry out comparison studies for iron products and potentially even more when analyzing iron based nano-particle similar.

5. ACKNOWLEDGEMENT

Special thanks to Professor Jorge E. Toblli from the Hospital Alemán Buenos Aires Argentina, for his support and advice during this research.

6. FUNDING SOURCES

This research was financially supported by Vifor (International) Ltd.

7. CONFLICT OF INTEREST

The views expressed in this manuscript are the personal views of the authors. Vifor participated in meetings and financially supported the research.

8. REFERENCES

1. Auerbach M. & Ballard H. Clinical Use of Intravenous Iron: Administration, Efficacy, and Safety. ASH Education Program Book. 2010;338-347.
2. Danielson BG. Structure, Chemistry, and Pharmacokinetics of Intravenous Iron Agents. Journal of the American Society of Nephrology. 2004;15:S93-S98.
3. Funk F, Ryle P, Canclini C, Neiser S, Geisser P. The new generation of intravenous iron: chemistry, pharmacology, and toxicology of ferric carboxymaltose. Arzneimittelforschung. 2010;60:345-353.
4. Neiser S, Rentsch D, Dippon U, Kappler A. Weidler P G, Gottlicher J, Steininger R, Wilhelm M, Braitsch M, Funk F, Philipp E, Burckhardt S. Physico-chemical properties of the new generation IV iron preparations ferumoxytol, iron isomaltoside 1000 and ferric carboxymaltose. Biometals. 2015;28:615-635.
5. Elford P, Bouchard J, Jaillet L, Pearson N, Rogue A, Sabadie C, Forster R. Biodistribution and predictive hepatic gene expression of intravenous iron sucrose. Journal of Pharmacological and Toxicological Methods 2013;68;374-383.
6. Koskenkorva-Frank TS, Weiss G, Koppenol WH, Burckhardt S. The complex interplay of iron metabolism, reactive oxygen species, and reactive nitrogen species: insights into the potential of various iron therapies to induce oxidative and nitrosative stress. Free Radic Biol Med. 2013;65:1174-1194.
7. Brissot P, Ropert M, Le Lan C, Loréal,O. Non-transferrin bound iron: A key role in iron overload and iron toxicity. Biochimica et Biophysica Acta (BBA) - General Subjects. 2012;1820:403-410.
8. Kruszewski M. Labile iron pool: the main determinant of cellular response to oxidative stress. Mutation Research/Fundamental and Molecular Mechanisms of Mutagenesis. 2003;531: 81-92.
9. Kaul N, Siveski-Iliskovic N, Hill M, Slezak J, Singal P K. Free radicals and the heart. Journal of Pharmacological and Toxicological Methods. 1993;30:55-67.
10. Bishu K, Agarwal R. Acute Injury with Intravenous Iron and Concerns Regarding Long-Term Safety. Clinical Journal of the American Society of Nephrology. 2006; 1:S19-S23.
11. Geisser P, Burckhardt S. The pharmacokinetics and pharmacodynamics of iron preparations. Pharmaceutics. 2011;3:12-33.
12. Bailie GR, Schuler C, Leggett RE, Li H, Li HD, Patadia H, Levin R. Oxidative effect of several intravenous iron complexes in the rat. BioMetals. 2013;26:473-478.
13. EMA. Reflection Paper on the Data Requirements for Intravenous Iron-based Nano-colloidal Products Developed with Reference to an Innovator Medicinal Product. 2015; EMA/CHMP/SWP/620008/2012. http://www.ema.europa.eu/docs/en_GB/document_library/Scientific_guideline/2015/03/WC500184922.pdf
14. Spicher K, Brendler-Schwaab S, Schlosser C, Catarinolo M, Futterer S, Langguth P, Enzmann H. Differences in tissue distribution of iron from various clinically used intravenous iron

complexes in fetal avian heart and liver. Regul Toxicol Pharmacol. 2015;73:65-72
15. Geisser P., Baer M, Schaub E. Structure/histotoxicity relationship of parenteral iron preparations. Arzneimittelforschung.1992;42:1439-1452.
16. Bailie G R, Schuler C, Leggett RE, Levin R. Oxidative effect ferumoxytol and iron dextran on urinary bladder contraction and impact of antioxidants. Free Radicals and Antioxidants. 2013;3:7-10.
17. Meier T, Schropp P, Pater C, Leoni AL, Khov-Tran VV, Elford P. Physicochemical and toxicological characterization of a new generic iron sucrose preparation. Arzneimittelforschung. 2011;61:112-119.
18. Toblli JE, Cao G, Oliveri L, Angerosa M. Differences Between Original Intravenous Iron Sucrose and Iron Sucrose Similar Preparations. Arzneimittelforschung. 2009;59:176-190.
19. Shah GB, Chorawala MC, Trivedi VR, Deshpande SS. Differences between the original iron sucrose complex Venofer® and the iron sucrose similar Sucrofer. Research Journal of Pharmaceutical, Biological and Chemical Sciences. 2013;4:655-669.
20. Toblli JE, Cao G, Oliveri L, Angerosa M. Differences between the original iron sucrose complex Venofer® and the iron sucrose similar Generis®, and potential implications. Portuguese Journal of Nephrology and Hypertension. 2009;23:53-63.
21. Jahn MR, Andreasen HB, Fütterer S, Nawroth T, Schünemann V, Kolb U, Hofmeister W, Muñoz M, Bock K, Meldal M, Langguth P. A comparative study of the physicochemical properties of iron isomaltoside 1000 (Monofer®), a new intravenous iron preparation and its clinical implications. European Journal of Pharmaceutics and Biopharmaceutics 2011;78: 480-491.
22. Espósito BP, Breuer W, Slotki I, Cabantchik ZI. Labile iron in parenteral iron formulations and its potential for generating plasma nontransferrin-bound iron in dialysis patients. European Journal of Clinical Investigation. 2002;32:42-49.
23. Van Wyck D, Anderson J, Johnson K. Labile iron in parenteral iron formulations: a quantitative and comparative study. Nephrology Dialysis Transplantation. 2004;19:561-565.
24. Jaffe M. Ueber den Niederschlag welchen Pikrinsäure in normalen Harn erzeugt und über eine neue reaction des Kreatinins. Hoppe-Seyler's Zeitschrift fur physiologische Chemie. 1886;10:391–400.
25. Vasiliades J. Reaction of alkaline sodium picrate with creatinine: I. Kinetics and mechanism of formation of the mono-creatinine picric acid complex. Clinical Chemistry. 1976;22:1664-1671.
26. Heinegard D, Tiderstrom G. Determination of serum creatinine by a direct colorimetric method. Clinica Chimica Acta. 1973;43:305-310.
27. U.S. Food and Drug Administration, Center for Drug Evaluation and Research. Ferrlecit, Pharmacological Review(s), NDA 020955, April 7, 1998. Retrieved March16 2017. www.accessdata.fda.gov/drugsatfda_docs/nda/99/20955_Ferrlecit_pharmr.pdf
28. Van Zutphen LFM, Baumans V, Ohl F. Handboek proefdierkunde : proefdieren, dierproeven, alternatieven en ethiek (5e druk). Amsterdam : Reed Business. 2012.
29. Leehey DJ, Palubiak DJ, Chebrolu S, Agarwal R. Sodium ferric gluconate causes oxidative stress but not acute renal injury in patients with chronic kidney disease: a pilot study. Nephrology Dialysis Transplantation. 2005;20:135-140.
30. Pai AB, Boyd AV, McQuade CR, Harford A, Norenberg JP, Zager P. Comparison of oxidative stress markers after intravenous administration of iron dextran, sodium ferric gluconate, and iron sucrose in patients undergoing hemodialysis. Pharmacotherapy: The Journal of Human Pharmacology and Drug Therapy. 2007;27:343-350.
31. Toblli JE, Cao G, Olivieri L, Angerosa,M. Comparison of the renal, cardiovascular and hepatic toxicity data of original intravenous iron compounds. Nephrology Dialysis Transplantation. 2010;25:3631-3640.
32. Walter Bowie EJ, Newlon Taux, W, Sjoberg JWE, Yamaguchi MY. Daily Variation in the Concentration of Iron in Serum. American Journal of Clinical Pathology. 1963;40:491-494.
33. Sennels HP, Jørgensen HL, Hansen ALS, Goetze JP, Fahrenkrug J. Diurnal variation of hematology parameters in healthy young males: The Bispebjerg study of diurnal variations. Scandinavian Journal of Clinical and Laboratory Investigation. 2011;71:532-541.
34. Sitia G, Iannacone M, Aiolfi R, Isogawa M, van Rooijen N, Scozzesi C, Bianchi M E, von Andrian UH, Chisari FV, Guidotti LG. Kupffer Cells Hasten Resolution of Liver Immunopathology in Mouse Models of Viral Hepatitis. PLOS Pathogens. 2011;7:e1002061.
35. Kacew S. Role of Rat Strain in the Differential Sensitivity to Pharmaceutical Agents and Naturally Occurring Substances. Journal of Toxicology and Environmental Health. 1996;47:1-1.
36. Hedrich HJ. Chapter 1 - History, Strains and Models A2 - Krinke, Georg J. In The Laboratory Rat. London: Academic Press. 2000;3-16.
37. Mac Kenzie WF, Garner FM. Comparison of Neoplasms in Six Sources of Rats. JNCI: Journal of the National Cancer Institute. 1973;50:1243-1257.

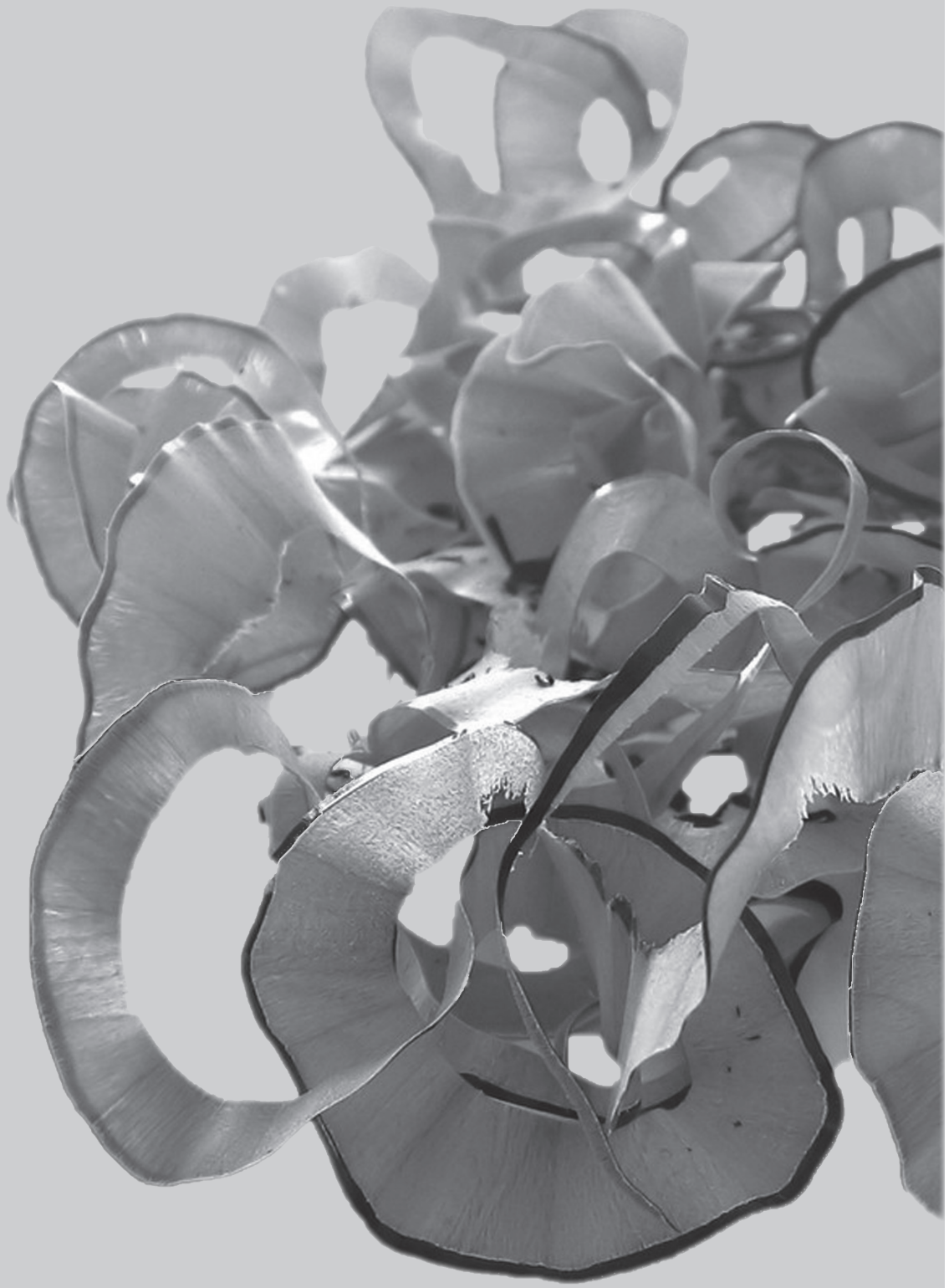

CHAPTER 5

The use of Magnetic Resonance Imaging for non-invasive assessment of Venofer® biodistribution in rats

Kimberley Span, Ebel H.E. Pieters, Wim E. Hennink, Annette van der Toorn, Vera Brinks, Rick M. Dijkhuizen, Geralda A.F. van Tilborg

Accepted for publication in Pharmaceutical Research
(January 2018)

Abstract

Purpose The aim of this study was to determine the potential of Magnetic Resonance Imaging to evaluate the biodistribution of exogenous iron within 24 hours after one single injection of Venofer® (iron sucrose).

Methods Venofer® was evaluated *in-vitro* for its ability to generate contrast in MR images. Subsequently, iron disposition was assessed in rats with MRI, *in-vivo* up to 3 hours and post mortem at 24 hours after injection of Venofer®, at doses of 10- and 40 mg/kg body weight (n=2x4), or saline (n=4).

Results Within 10-20 min after injection of Venofer®, transverse relaxation rates (R_2) clearly increased, representative of a local increase in iron concentration, in liver, spleen and kidney, including the kidney medulla and cortex. In liver and spleen R_2values remained elevated up to 3 hours post injection, while the initial R_2 increase in the kidney was followed by gradual decrease towards baseline levels. Bone marrow and muscle tissue did not show significant increases in R_2 values.

Whole-body post mortem MRI showed most prominent iron accumulation in the liver and spleen at 24 hours post injection, which corroborated the *in-vivo* results.

Conclusion MR imaging is a powerful imaging modality for non-invasive assessment of iron distribution in organs. It is recommended to use this whole-body imaging approach complementary to other techniques that allow quantification of iron disposition at a cellular/ subcellular level.

KEYWORDS

Iron · Intravenous · Biodistribution · Oxidative stress · MRI

ABBREVIATIONS

EMA	European medicine agency
HB	Hemoglobin
Hct	Hematocrite
ICP-MS	Plasma mass spectrometry
MCH	Mean corpuscular hemoglobin
MCHC	Mean corpuscular hemoglobin concentration
MCV	Mean corpuscular volume
MEMS	Multi-slice multi-spin echo sequence
MGE3D	Multi-gradient-echo 3D
MGEMS	Multi-echo gradient-echo sequence
MRI	Magnetic resonance imaging
PET	Positron emisssion tomography
r_1, r_2, r_2*	relaxivities
R_2	Transverse relaxation rate
ROIs	Regions of interest
Serum Fe	Serum iron
SPIONs	Superparamagnetic iron oxide nanoparticles
T1/2	Blood half life
T1	Longitudinal relaxation rate
T2	Transverse relaxation rate
TE	Echo time
TIBC	Total iron binding capacity
TR	Repetition time

1. INTRODUCTION

Iron is an essential nutrient for the transport of oxygen in the body. It is mainly present in heme, which is an important component of the oxygen-transporting protein hemoglobin that is present in erythrocytes. Insufficient intake and/or uptake can result in iron deficiency or anemia. In particular patients suffering from disorders such as chronic kidney disease (CDK) are in need of treatments such as erythropoietin and/or intravenous iron to enhance the number of erythrocytes (1-3). Several FDA-approved iron products are presently used in clinical practice, of which particularly iron sucrose has been widely used because this complex has shown to induce less side effects compared to other first generation intravenous iron complexes such as high molecular weight iron dextran (4, 5). Although these iron complexes have been shown to be therapeutically beneficial for patients suffering from iron deficiency, there are some concerns that these iron products can also cause short- and long-term complications (6, 7). After administration, the iron

complexes which are colloidal dispersions of polynuclear ferric-oxyhydroxide cores stabilized by a carbohydrate shell, are taken up by phagocytosis by macrophages of the mononuclear phagocyte system (previously termed reticuloendothelial system (RES)) (8). In this respect, the colloidal iron particles follow the same fate of other nanoparticles based on for example synthetic polymers or lipids (9-12). In the macrophages, the complexes are degraded and the iron can be stored in ferritin or it can be released to bind to the blood plasma glycoprotein transferrin. The amount of iron released, relies on the physiological iron need and is speculated to also depend in part on the properties of the iron product, specifically related to the type of carbohydrate used to stabilize the iron complex (4, 8, 13). In case of iron overload, accumulation of iron in macrophages represents a safety concern as this might result in oxidative stress, inflammation, kidney- and heart disorders (6, 14). Because of these safety concerns, there is a great need for insight into the distribution of iron after intravenous administration of iron-based medicinal products. In the reflection paper published by the European Medicine Agency concerning data requirements for the development of iron colloidal products for parenteral administration, a minimum requirement for biodistribution studies is outlined. This paper states that studies of iron distribution, retention and accumulation *in-vivo*, should at least comprise analyzing the blood plasma, reticuloendothelial system and organ tissue (15). Furthermore, it is also desirable to examine the early iron distribution, meaning within twenty-four hours after iron administration, preferably in a non-invasive manner. Beshara et al. studied the long-term kinetics and distribution of iron after an intravenous injection, with a particular focus on iron distribution and the production of erythrocytes within 3-4 weeks after administration (16).

There is, however, no comprehensive knowledge available regarding the possible distribution of iron in the different organs within 24 hours after administration. Giving insight into the iron distribution shortly after administration of the iron complexes, elucidates on the early iron pharmacokinetics which is useful when for example comparing two iron formulations. Several methods have been described to assess the distribution of iron complexes and quantitative disposition in different organs. Such methods mainly consisted of using radio isotopes, as for example ^{52}Fe or ^{59}Fe in positron emission tomography (PET) studies or using whole body counters (17-19). Previous studies using this approach to investigate iron disposition in several organs within a twenty-four-hour span after administration of the iron complexes, demonstrated that these methods allow qualitative assessment of iron biodistribution (16, 18, 19). Nevertheless, the use of radioactive labeling has its pitfalls such as safety and ethical issues and the need of excessive numbers of animals in the case of pre-clinical *in-vivo* studies (20). Therefore, it is interesting to assess other methods to study the biodistribution of iron complexes. In a recent *in-vivo* study, we investigated the toxicity effects and *in-vivo* disposition of iron after intravenous administration by measuring iron parameters such as hemoglobin, serum iron and liver enzymes in blood serum, but also by performing histochemical

studies to determine the tissue iron content and tissue inflammatory markers in rats. However, these parameters measured in the Sprague Dawley rat model did not give sufficient insight into the iron accumulation and adverse iron related effects after intravenous administration of different doses of iron products (manuscript submitted for publication).

Rostoker et al. (21) reported that it is feasible to study iron content in transfusion dependent patients suffering from iron overload or in hemochromatosis patients by using magnetic resonance imaging. In the past, the MRI technique has been used to investigate the delivery of iron nanoparticles such as liposomal SPION (superparamagnetic iron oxide nanoparticles) formulations (22). Thus, it would be of interest to investigate whether intravenously injected complex – bound iron can also be monitored with *in-vivo* MRI. A study by Vinitski et al. reported that ferric hydroxide sucrose was successfully used as a MR contrast agent to image pulmonary embolism, suggesting the potential use of MRI for imaging of iron sucrose distribution (23). Iron has paramagnetic properties and can therefore reduce the magnetic resonance signal as the iron concentration increases (24). Therefore, the aim of this study was to determine the potential of magnetic resonance imaging (MRI) to non-invasively and accurately monitor iron disposition within twenty four hours after one single injection of iron sucrose (Venofer®).

2. MATERIALS AND METHODS

2.1 Materials

Venofer® (lot number: 118101) was obtained from Vifor (International) Ltd., St. Gallen, Switzerland. Saline (sodium chloride 0.9% w/v) was purchased from Fresenius Kabi Nederland B.V. (Zeist, The Netherlands). Heparin, 5000 U.I. (dissolved in water), was a product of Leo Pharma B.V, Amsterdam. Isoflurane was obtained from Teva Pharmachemie B.V., Haarlem, The Netherlands, and sodium pentobarbital 60 mg/ml in water, charge number 12042302, was provided by the pharmacy of Veterinary Medicine at Utrecht University, The Netherlands. Formalin solution neutral buffered 10% (HT501128-4L), antibiotic antimycotic solution and sodium azide were purchased from Sigma-Aldrich Chemie B.V., Zwijndrecht, The Netherlands. Phosphate buffered saline (PBS) was from J.T. Baker (Avantor Performance materials B.V., Deventer, The Netherlands). Sarstedt S-monovettes tubes containing clotting activator silica beads for serum collection or EDTA for whole blood collection were purchased from Sarstedt B.V, Etten Leur, The Netherlands.

2.2 Animals

All experiments were performed according to Institutional Ethical Committee Regulations of Utrecht University, The Netherlands.

MRI:
Twelve male HSd: Sprague Dawley rats of 8 weeks old (Harlan laboratories, The Netherlands) were housed in standard perspex cages and were fed standard rat chow (Special Diets Services, United Kingdom) and (acidified) water *ad libitum* unless stated otherwise. The animals were housed for 4 weeks prior to the experiment and were subjected to a 12 hours light/dark cycle. Each treatment group consisted of four animals per group (n=4), weighing 325-400 grams. The rats were randomly assigned to the different treatment groups, which were saline solution (control group) or Venofer® (20 mg (Fe)/ml) given in two different doses, namely: 10 mg (Fe)/kg and 40 mg (Fe) /kg. Each animal received one single intravenous bolus, instead of a drip infusion or slow injection as done in the clinic. The injection consisted of the volume Venofer® needed to reach 10 or 40 mg/kg, replenished with saline (sodium chloride 0.9% w/v) up to 1.5 ml.

Urine iron content measurement
For the iron measurement in urine a total of eight Male HSd: Sprague Dawley rats weighing 325-400 grams were used. The animals were divided in two treatment groups (n=4 per group), specifically: the control group (saline solution) and 40 mg/kg of Venofer®. The experimental set-up for the measurement of iron content in urine is described in more detail further on in materials and methods in the section for iron measurement in urine.

Blood half-life
For the blood half-life experiment, eighteen male HSd: Sprague Dawley rats weighing 325-400 grams were used. The animals were randomly assigned to different treatment and time-point groups for blood collection as described more in detail in the section; blood half-life of Venofer® in Sprague Dawley rats. Each animal received one single intravenous injection of (40 mg/kg) Venofer® or saline solution. The animals were housed and fed under the same conditions as described above.

2.3 Blood collection

In order to assess that the animals were healthy and non-anemic, 14 days prior to the MRI measurement blood was collected via the tail vein to measure the preteatment blood iron parameters. Rats were deprived from food for 19 hours in order to avoid interference of iron present in food and had access to (acidified) water *ad libitum* before blood collection. The iron related blood parameters measured were: hemoglobin (HB),

hematocrite (Hct), mean corpuscular volume (MCV), mean corpuscular hemoglobin (MCH), mean corpuscular hemoglobin concentration (MCHC), serum Fe (iron) and total iron binding capacity (TIBC) using an ADVIA 120 Siemens hematology analyzer and a Ferrentest (Diagnostic Chemicals Ltd, Charlottetown Canada).

2.4 Iron measurement in urine after a single intravenous injection

Animals received a single intravenous injection with a volume ranging from 650 to 750 µl conform to the weight of the rat, of Venofer® (40 mg/kg) or ~1.5 ml saline (control). Next, rats were placed in metabolic cages for 24 hours, in which they had free access to (acidified) water *ad libitum* and 5 hours to food. The aliment was then removed, resulting in a fasting period of 19 hours. The urine of the different animals was collected for 24 hours in a measuring cylinder containing 1 ml of antibiotic antimycotic solution diluted 1:5 with deionized water and the volume for each animal was recorded. Next, the urine was kept at -20°C until further assessment of the iron content which was determined using a Ferrentest (Diagnostic Chemicals Ltd, Charlottetown Canada).

2.5 *In-vitro* assessment of Venofer® as contrast agent for MRI

Venofer® was diluted in saline to obtain samples with different iron concentrations, ranging from 0.00125 – 0.04 M. MRI of the samples was conducted on a 4.7 T horizontal bore MR system (Varian, Palo Alto, CA, USA), using a home-built solenoid coil with a diameter of 3 cm. All measurements were performed at room temperature, using freshly prepared samples. T_1 was measured using a Look Locker inversion recovery sequence, (Total Repetition Time = 10 s, Repetition time per image =25 ms, Echo Time (TE) = 4.2ms, flip angle 5º, 100 images per inversion pulse, 2 averages, slice thickness 1 mm, field of view 30 mm x 30 mm, matrix 256 x 256). T_2 values were assessed using a multi-slice multi spin-echo (MEMS) sequence with the following parameters: Repetition Time (TR) = 3 s, TE = 8.52 ms, 100 echoes, 4 averages, slice thickness 1 mm, field of view 30 mm x 30 mm, matrix 256 x 256. T_2^* values were obtained using a multi echo gradient-echo sequence (MGEMS) with the following settings TR = 500 ms, TE = 5 ms, 25 echoes, flip angle 70°, 16 averages, slice thickness 1 mm, field of view 30 mm x 30 mm, matrix 256 x 256. Average T_1, T_2 and T_2^* values for each individual sample were established using non-linear fitting routines in Matlab. Next, relaxation rates R_1 ($1/T_1$), R_2 ($1/T_2$) and R_2^* ($1/T_2^*$) were calculated, and used to determine relaxivities r_1, r_2 and r_2^* based on the linear correlation between concentration and relaxation rate.

2.6 Blood half-life of Venofer® in Sprague Dawley rats

The blood half-life ($t_{1/2}$) of Venofer® was obtained by MRI analysis of blood samples taken

from the animals at several time points after a single intravenous injection of Venofer® as described above. In short, for each time point 2-3 Sprague Dawley rats received one single injection of Venofer® (40 mg/kg) or saline via the tail vein. Each rat was used to draw blood samples at two subsequent time points. For example, blood was collected from one rat at 30 minutes and 2 hours post injection and the rat was then euthanized by an overdose pentobarbital administered intraperitoneally. Blood was collected in heparin coated Eppendorf tubes at time points 0 (pre-injection), and at 30 minutes, 1, 2, 3 and 24 hours after injection of the formulation. The heparin coated Eppendorf tubes were prepared by pipetting 10 µl of heparin (5000 U.I) into 1.5 ml Eppendorf tubes and then allowing the heparin to concentrate overnight at 37°C. Next, blood was diluted 1:4 with saline and the samples were transferred into 250 µl PCR tubes for Magnetic Resonance Imaging (MRI). Blood samples were stored at 4 °C, and MRI was performed within 1-3 days after blood collection. MRI analysis of the blood samples was performed on a 9.4 T horizontal bore MR system (Varian, Palo Alto, CA, USA), using a Millipede™ coil (Varian Inc.). Shortly before the MRI measurements were carried out, the blood samples were vortexed for 30 seconds. T_2-weighted images of blood samples were acquired, using a multi-slice multi-spin echo sequence (MEMS) with the following parameters: TR = 5 s, TE = 9 ms, 200 echoes, 4 averages, field-of-view 30mm×30mm, matrix size 256×256 and slice thickness 1 mm. Regions of interest were drawn within each tube, and average signal intensities at the different echo times were used to fit the average T_2 value in each blood sample, using a non-linear fitting routine in Matlab. Subsequently, average T_2 values were used to calculate the average relaxation rate R_2 ($1/T_2$) of each blood sample, as R_2 scales linearly with contrast agent concentration. Next, blood half-life ($t_{1/2}$) of Venofer® was obtained from the R_2 values using a mono-exponential fitting routine in Matlab, according to the following function:

$$R_2(t) = R_2(0) * e^{\frac{-\ln(2)*t}{t_{\frac{1}{2}}}}$$

where R_2 (t) is the relaxation rate at each time point, R_2 (0) is the relaxation rate at time zero, t is time and $t_{1/2}$ is the blood half-life (24). R_2 values used for fitting were corrected for the average R_2 value in blood samples from animals that did not receive any injections, resulting in a baseline R_2 value of 0.

2.7 Iron disposition in Sprague Dawley rats

2.7.1 In-vivo MRI of iron distribution after one single intravenous Venofer® injection

Venofer® was intravenously administered via the tail vein to non-anemic Sprague Dawley rats. A total volume of 1.5 ml was administered consisting of a mixture of Venofer®, to obtain a dose of 10 or 40 mg/kg, supplemented with saline. As a control,

1.5 ml saline solution was injected into the rats. Shortly before MRI analysis, the animals were anesthetized with 3% isoflurane in air/O_2 (1:2) and endotracheally intubated for mechanical ventilation. During MRI, the animals were mechanically ventilated and anesthetized with 2% isoflurane in air/O_2 (4:1). Temperature, respiration, end-tidal CO_2 levels, O_2 saturation and heart rate were continuously monitored and kept within physiological range. *In-vivo* MRI measurements were conducted on a 4.7 T horizontal bore MR system (Varian, Palo Alto, CA, USA), using a home-built Helmholtz volume coil with a diameter of 8 cm. Serial respiratory-triggered T_2-weighted images of the rat abdomen were acquired over a period of 3.25 hours using a multi-slice multi spin-echo sequence (MEMS) with the following parameters: TR=500 ms, TE=4.1 ms, 9 echoes, 2 averages, field-of-view 64 mm×64 mm, matrix size 128×128, 10 slices, 1 mm slice gap and slice thickness 1.5 mm. Total scan time per MEMS acquisition varied between 4.7 and 5.5 minutes for the different animals depending on the respiration rate. A total of 4 MEMS scans were acquired before intravenous injection of Venofer®, followed by approximately 3 hours of repetitive MEMS acquisitions after injection. Following MRI, the animals were allowed to recover from anesthesia, transferred into normal cages and provided with *ad libitum* standard rat chow and (acidified) water until sacrificed 24 hours after injection.

2.7.2 Postmortem MRI of iron distribution in rats euthanized at 24 hours after one single intravenous injection of Venofer®

For analysis of whole-body iron distribution at 24 hours after a single intravenous injection of Venofer®, the rats described above in the *in-vivo* MRI section, were prepared for postmortem MRI. Twenty four hours post injection, the rats were sacrificed using an overdose of pentobarbital that was administered intraperitoneally. Next, the animals were perfused with PBS followed by a 4% formaldehyde in water solution until they were completely blood depleted, and subsequently placed for further fixation in 4% formaldehyde for 7 days at 4 °C. Subsequently, the formaldehyde solution was replaced by a PBS/ 0.1% azide solution, and the animals were stored at 4°C for postmortem MRI. Postmortem MRI measurements were conducted on a 4.7 T horizontal bore MR system (Varian, Palo Alto, CA, USA), using a home-built Helmholtz coil with a diameter of 8 cm. In order to cover the whole rat from head-to-toe, the animal was manually shifted by approximately 7 cm in between acquisitions, resulting in three acquisitions per rat. T_2^*-weighted images were acquired using a multi gradient-echo 3D sequence (MGE3D) with the following parameters: TR=100 ms, TE=5 ms, flip angle = 25°, 8 echoes, 2 averages, field-of-view 100mm × 90mm x 60 mm and matrix size 250×226 x150.

2.8 MR image analysis *in-vivo* and postmortem

For analysis of *in-vivo* MRI data, regions of interest (ROIs) were manually outlined on the first MEMS acquisition of the time series in FSLView (FMRIB Software Library, 26, 27). Next, ROI positioning was verified for the entire time series, and ROIs were manually adjusted to correct for motion. ROIs involved the liver, kidney, spleen, spine and muscle. Next, a non-linear fitting routine in Matlab was used to assess the average T_2 value in each specific ROI at each individual time point. Venofer® -induced changes in R_2 ($1/T_2$) values, representative of Venofer® concentration, were used to evaluate Venofer® distribution. Afterwards, the area under the curve (AUC) for the different treatments in each organ was calculated, starting at baseline R_2 at t=0 until the end of the measurement of every individual rat, using GraphPad Prism version 4.02 for Windows. Subsequently, the average AUC of 4 rats within the different treatment groups was then calculated and statistical analysis was done to evaluate any differences *in-vivo* between the treatments. For analysis of postmortem MRI data, a predefined subset of organs, including the abdominal organs; liver, spleen, kidney, stomach and intestines and additional organs such as the heart, lungs, spine (bone marrow tissue), muscle, testis and brain, were manually outlined in the MGE3D images using FslView. Next, a non-linear fitting routine in Matlab was used to assess the average T_2* value in each specific organ. T_2* values were used to calculate relaxation rates R_2*, as described in the *in-vitro* assessment of Venofer® section. In addition, the average signal intensity in the first T2*-weighted image (TE = 5 ms) of the MGE3D acquisition was calculated in the liver and spleen, and normalized to the average signal intensity in muscle tissue in the corresponding T2*-weighted image.

2.9 Statistical methods

The *in-vivo* and postmortem data are expressed as mean ± standard deviation (st.dev). A two-way ANOVA with Bonferroni post-hoc testing was used to test the effects of the different Venofer® treatments on the Area Under the Curve from *in-vivo* R_2 values, postmortem R_2* values and postmortem normalized signal intensity. Statistics was performed in GraphPad Prism version 4.02 for Windows, GraphPad Software, San Diego California USA. $P<0.05$ was considered statistically significant.

3. RESULTS AND DISCUSSION

3.1 Pretreatment blood collection

To assure that the rats were healthy and not anemic prior the MRI experiment, blood was collected via the tail vein 2 weeks prior to the start date of the experiment and several blood iron related parameters were measured (Table 1).

Table I Iron related blood parameters

Sample mg/kg	HB (g/dL)	Hct (%)	MCV (fL)	MCH (pg)	MCHC (g/dL)	Serum Fe (µg/dL)	TIBC (umol/L)
10	15.6	46	50.8	17.1	33.7	69.8	74.1
10	15.3	45	51.2	17.4	34.0	74.2	69.3
10	15.1	44	51.2	17.6	34.5	85.4	84.3
10	14.8	43	51.8	18.0	34.8	113.3	69.6
40	14.8	45	54.1	17.7	32.9	79.2	73.2
40	14.8	43	53.1	18.2	34.3	75.3	83.7
40	15.3	44	48.7	16.8	34.5	95.4	86.1
40	15.5	44	48.7	16.9	34.8	93.7	80.4
saline	15.0	43	52.8	18.4	34.6	153.5	77.1
saline	14.8	44	50.9	17.4	34.0	82.0	69.3
saline	15.5	45	51.1	18.4	34.8	87.6	80.4
saline	15.9	46	51.2	17.9	34.8	102.7	76.5

Iron related parameters for the individual rats in the different sample groups 14 days before the first injection.

The parameter values shown in Table I were within normal physiological range of non-iron deficient rats as described in the manual for animal experiments, and as indicated by the animal supplier (28). The serum iron and total iron binding capacity values were in accordance with previously obtained results within our department (manuscript submitted for publication).

3.2 Iron measurement in urine 24 hours after a single intravenous injection

Urine samples were collected in measuring cylinders for 24 hours after one single Venofer® intravenous injection, as described in the section materials and methods for iron measurement in urine. A brownish color was observed in the urine collected at 3 hours after administration in all rats receiving Venofer®, which was not observed in animals that received saline solution or in urine collected at 24 hours post Venofer® injection (Figure 1). This suggests that the exogenous iron is partly excreted via the urine within 24 hours after administration.

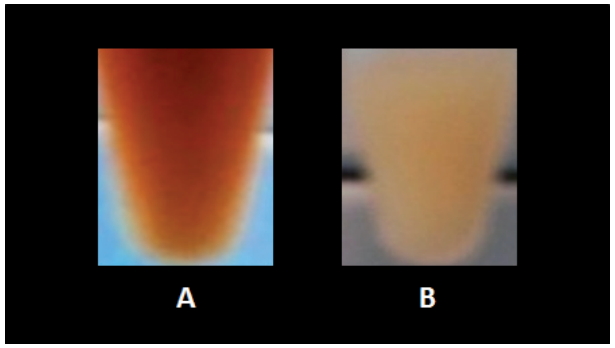

Fig. 1 Photographs of urine collected 3 hours (**A**) and 24 hours (**B**) after one single intravenous injection of 40 mg/kg Venofer®

In order to verify whether the brown color was indeed caused by iron, its concentration was measured in urine collected for twenty-four hours from animals receiving 40 mg/kg Venofer® or saline.

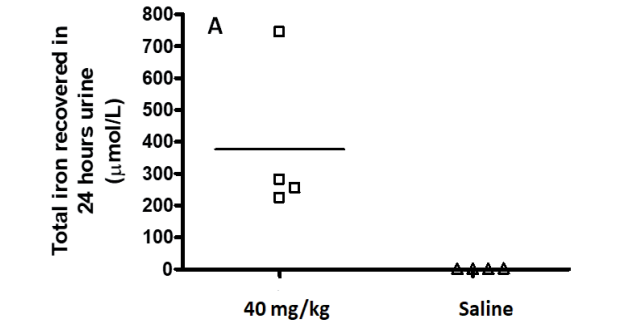

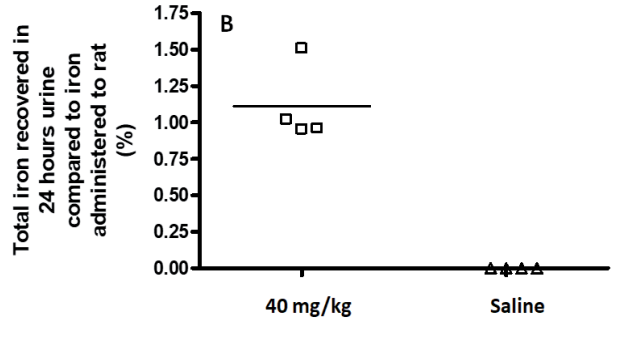

Fig. 2 Total iron (µmol/L) in urine collected for 24 hours for each individual animal. Figure (**A**) depicts the concentration of iron in µmol/L and (**B**) shows the percentage of total amount of iron present in the urine compared to the administered iron dose per animal

Figure 2 shows the total iron recovered in urine for the individual rats. The animals excreted an average of 20 ml urine in 24 hours (range was 10 – 40 ml). For the rats that received saline solution, no iron was detected in the urine. This in contrast to the animals receiving 40 mg/kg Venofer®, which showed an average iron concentration of 380 ± 215 µmol/L. Urine-collected iron accounted for 1.1 ± 0.2 % of the administered iron dose. This indicates that to some extent there is renal elimination of iron originating from the Venofer® injection. Danielson *et al.* also reported renal excretion in humans after receiving one intravenous Venofer® injection containing 100 mg Fe 5% iron and 68% sucrose of the injected dose were excreted respectively after 4 hours (29). A brown coloration of urine indicative of iron renal elimination, has also been reported for animals that received low molecular iron preparations (< MW 18 kD) (30). Venofer® has a molecular weight in the range of 34-60 kD and further research demonstrated that the average particle core size is smaller than 10 nm (31-33). Renal filtration is thought to be limited to 30-50 kD (around 5 nm) for proteins (34-36) making it plausible, that to some extent smaller iron complexes are filtered by the kidneys.

3.3 *In-vitro* MRI assessment of Venofer®

Venofer® was evaluated as a contrast agent for MRI prior to the *in-vivo* experiment. Both the longitudinal (T_1) and transverse (T_2 or T_2^*) relaxation times for several Venofer® (iron) concentrations were measured to determine the relaxation rates ($R_1 = 1/T_1$ (s^{-1}); $R_2 = 1/T_2$(s^{-1}) and $R_2^* = 1/T_2^*$ (s^{-1})) as described in the materials and methods section for *in-vitro* assessment of Venofer®. The slope obtained from linear regression analysis with iron concentration as the independent variable (x) and relaxation rate (R) as the dependent variable (y), provided the corresponding relaxivities r_1, r_2 and r_2^*, which give an indication of the efficiency of Venofer® to generate contrast on T_1-weighted, T_2-weighted or T_2^*-weighted magnetic resonance images, respectively.

Table II Relaxivities

Contrast agent	r_1 ($mM^{-1}s^{-1}$)	r_2 ($mM^{-1}s^{-1}$)	r_2^* ($mM^{-1}s^{-1}$)
Venofer®	0.45	3.24	3.63

Relaxivities r_1, r_2, r_2^* of Venofer® in saline solution at room temperature obtained from relaxation times measured at 4.7 Tesla magnetic field strength.

The r_1, r_2 and r_2^* relaxivities of Venofer® in saline solution at room temperature and 4.7 Tmagnetic field strength were respectively 0.45 $mM^{-1}s^{-1}$, 3.24 $mM^{-1}s^{-1}$ and 3.63 $mM^{-1}s^{-1}$ (Table II). These values indicate that Venofer® generates more efficient contrast on $T_2^{(*)}$-weighted magnetic resonance (MR) images than T_1-weighted images. When compared to the relaxivities of a commonly clinically used T_1 contrast agent at 4.7 T, such as Gadovist

(Gd-DO3A-butrol), it can be concluded that Venofer® is less efficient as a contrast agent (relaxivities Gd-DO3A-butrol, r_1 = 3.43 $mM^{-1}s^{-1}$; r_2 = 4.69 $mM^{-1}s^{-1}$ (unpublished results). However, the iron complex does generate sufficient MRI contrast as it clearly generates a decrease in signal intensity on T_2-weighted images, i.e. darker images, with increasing concentrations and increasing echo time (TE) as shown in Figure 3A. This decrease in signal intensity is caused by the fact that iron shortens the intrinsic T_2 relaxation time according to its paramagnetic properties (24, 37). Quantitative T_2- and T_2^*-maps are shown in Figure 3B to visualize the effect of increasing iron concentrations on T_2 and T_2^* relaxation times. Furthermore, R_2- and R_2^*-maps ($1/T_2$ and $1/T_2^*$) are shown in Figure 3C to visualize the effect of increasing iron concentrations on R_2 and R_2^* relaxation rates. These maps clearly demonstrate that the highest concentration of Venofer® (0.04 M) most strongly reduced T_2 and T_2* values, whereas the lowest concentration (0.00125 M) had a smaller effect on T_2 and T_2* values. Moreover, these maps show that Venofer® affects T_2 and T_2^* relaxation times in a similar fashion, which was expected as relaxivities r_2 and r_2^* are comparable (Table II). Consequently, both T_2- and T_2^*-weighted MR imaging sequences qualified for non-invasive monitoring of Venofer® biodistribution. *In-vivo* experiments were performed using T_2-weighted imaging (MEMS), whereas T_2^*-weighted imaging (MGE3D) was used for postmortem MRI.

3.4 Blood half-life of Venofer® and *in-vivo* MRI of iron distribution

3.4.1 Blood half-life of Venofer®

The blood half-life ($t_{1/2}$) of Venofer® was determined as described in the section materials and methods for blood half-life of Venofer® in Sprague Dawley rats. Here, T_2 relaxation times of blood samples collected at 0, 30 minutes, 1, 2, 3 or 24 hours after one single injection of 40 mg/kg Venofer® were measured at 9.4 T. The calculated blood half-life ($t_{1/2}$) of Venofer®, based on a mono-exponential fit of the R_2 (i.e. 1/ $T_{1/2}$) values as a function of time, was 2.3 ± 0.6 hours. In humans, a terminal blood half-life of $t_{1/2}$ of 5.3 hours was reported, based on the decay in iron concentration in the terminal phase (3-12 hours post injection) (29). Longer elimination half-life, in humans compared to rodents, has also been reported for other types of nano-based medicines such as pegylated liposomal doxorubicin formulations (38).

3.4.2 In-vivo MRI of iron distribution

Axial multi-slice T_2-weighted multi-spin-echo images were acquired to monitor iron distribution over different abdominal organs following Venofer® injection. Examples of resulting axial R_2 ($1/T_2$) maps of the abdominal region of animals pre- and post- one single injection of saline solution (control), 10 mg/kg or 40 mg/kg Venofer® are shown in Figure 4. Changes observed in R_2 values compared to pre-injection R_2 values are proportional

to the concentration of iron present in the organs, meaning that an increase of the relaxation rate R_2 reflects more iron (see Figure 3).
For further quantitative assessment of the *in-vivo* distribution of Venofer®, average R_2 values were calculated in several regions of interest (ROIs), i.e. liver, spleen, kidney, spine (bone marrow) and muscle (Figure 5).

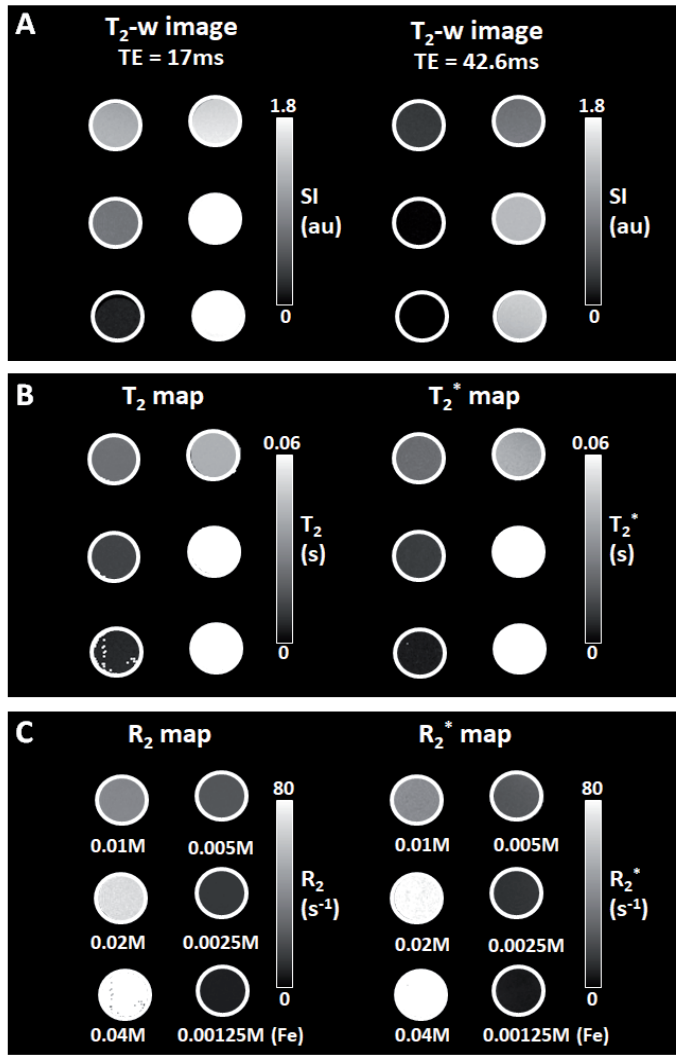

Fig. 3 Effect of Venofer® at increasing iron concentrations on (**A**) T_2-weighted images with two different echo times (TE), and its corresponding (**B**) T_2 and T_2^* maps and (**C**) R_2 and R_2^* maps. The concentrations are similar for Figures A, B and C

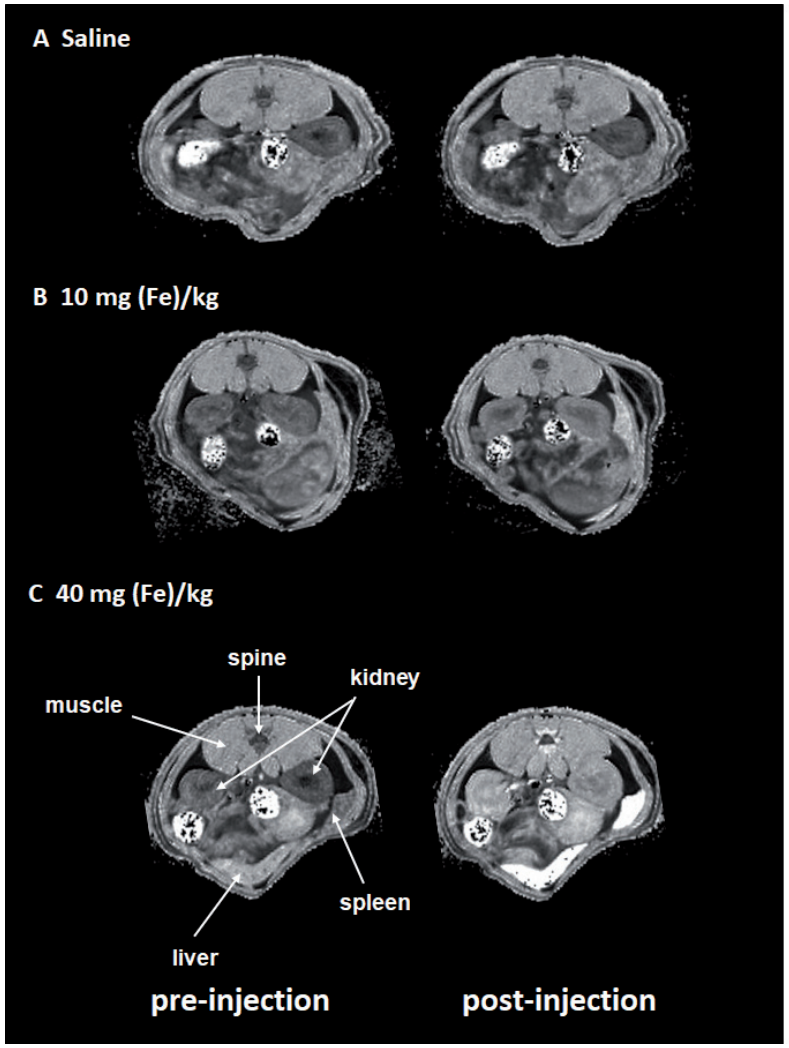

Fig. 4 Representative examples of axial *in-vivo* R_2 maps of the rat abdomen depicting the organs pre- (left column) and post- (right column) intravenous injection of (**A**) saline; (**B**) 10 mg/kg Venofer® and (**C**) 40 mg/kg of Venofer®. Only one representative slice out of the 10 acquired slices is shown

In the liver (Fig 5A), an injection of the frequently used dose for preclinical toxicity studies of 40 mg/kg, induced a rapid increase in R_2 values that slowly continued to elevate reaching a plateau with an average R_2 of 95 s^{-1} around 50 minutes post injection (57 s^{-1} higher compared to saline-treated control). Administration of 10 mg/kg of Venofer®, which is close to the maximum clinical dose of 7 mg/kg (39), also resulted in a fast increase of R_2 values followed by a slow increase in R_2 to reach maximum values of ~ 63 s^{-1} around 100 minutes after administration.

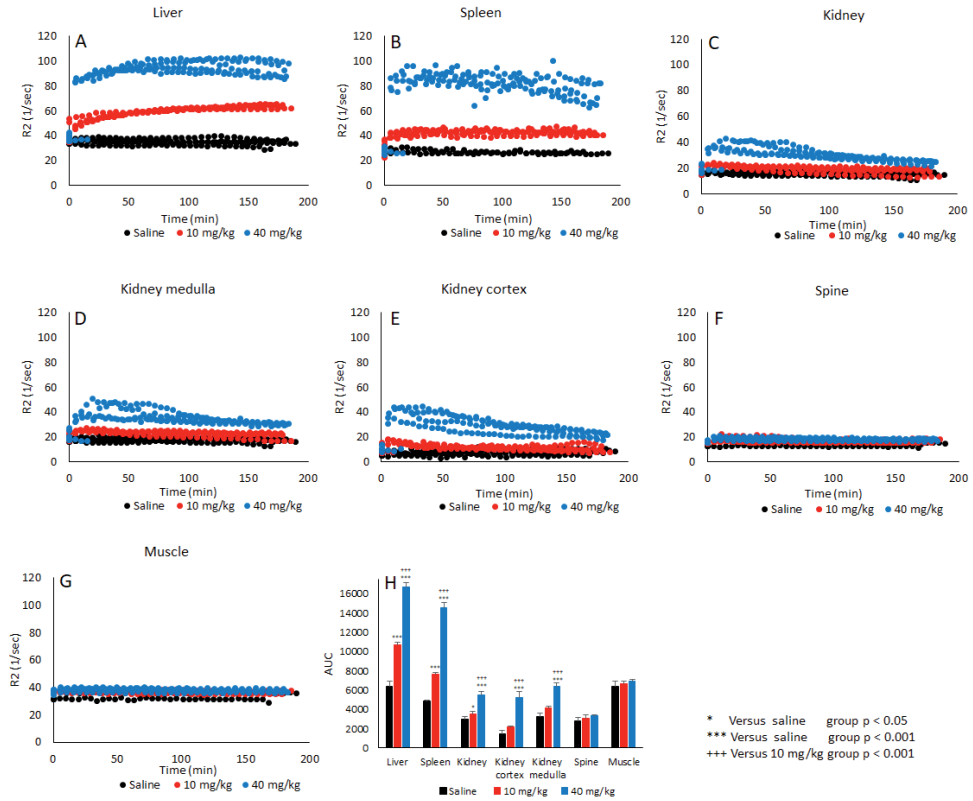

Fig. 5. *In-vivo* R_2 values (s^{-1}) of the different organs (**A**–**G**) as a function of time after one injection of saline (black), 10 mg/kg (red) or 40 mg/kg (blue) (n=4 per group). Results are shown for each individual rat. R_2 values at time zero are the average values of the 4 acquisitions that were acquired before injection for each individual rat. Figure **H** shows the area under the curve (AUC) for Figures **A** to **G**. The results represent AUC mean ± st.dev of 4 rats

Similar to the liver, the spleen (Fig. 5B) demonstrated a steady increase in R_2 values reaching maximum values at 30 minutes post injection that remained stable (low dose Venofer®) or showed a modest decrease (high dose Venofer®) towards the end of the *in-vivo* measurements. Animals that received 40 mg/kg Venofer® showed an increase reaching maximum R_2 values of 82 s^{-1} (54 s^{-1} higher than saline-treated control), while animals treated with 10 mg/kg Venofer® reached maximum R_2 values of 43 s^{-1} (14 s^{-1} higher than saline-treated control).

The kidney also showed a rapid increment in R_2 after administration of 40 mg/kg Venofer®. However, unlike the liver and spleen, the initial increase in R_2 was followed by a more obvious gradual decrease over time (Fig 5C). Three hours post-injection, R_2 values of the whole kidney, as well as for the separate compartments (Fig 5D, Fig 5E; cortex and medulla), decreased to values not different from the pretreatment or saline values both

at high and low dose Venofer®. In addition, there was no distinction between the two sections of the kidney (cortex and medulla) during the *in-vivo* measurements at either dose. Compared to all other regions of interest, spine, which served as a measure for bone marrow, and muscle tissues showed only modest changes in R_2 after injection with the iron complex (Fig 5F, Fig 5G). Figure 5H depicts the area under the curve (AUC) for the R_2 values over time in each organ. The AUC in the liver, spleen and kidney (including both the compartments cortex and medulla) of animals that received 40 mg/kg Venofer®, was significantly increased compared to animals in the 10 mg/kg and saline (control) treated groups ($p<0.001$). Furthermore, also the 10 mg/kg Venofer dose, which is comparable to the maximum clinical dose, significantly increased the AUC compared to saline-treated control animals in liver, spleen ($p<0.001$) and kidney ($p<0.05$).

This clearly demonstrates the potential of MRI to measure the *in-vivo* distribution of the iron sucrose complex at relatively high dose.

Absolute concentrations of deposited iron in the organs of interest cannot be quantified because the r_2 relaxivity of Venofer®, as assessed *in-vitro*, may change *in-vivo*. For instance due to release of iron from the sucrose complex or due to internalization of the iron complex by cells of the RES (8). Moreover, changes in R_2 values do not only originate from deposited iron, but may partly originate from Venofer® that is circulating in the blood, particularly in highly vascularized tissues such as spleen and liver. The blood half-life of Venofer® in rats is 2.3 ± 0.6 hours, meaning that the contribution of vascular Venofer® to the measured R_2 values should gradually decrease over the time course of the longitudinal *in-vivo* MRI experiment, and only round 40% of the injected dose will be present in the blood at the final acquisition 3 hours post-injection. Nevertheless, R_2 values remained constantly elevated over the time course of 3 hours in the liver and spleen, indicating that these organs are the main organs of exogenous iron disposition after a single injection of the iron complex.

3.5 Post mortem MRI of iron distribution in rats euthanized 24 hours after one single injection of Venofer®

Postmortem T_2*-based MRI (multi-gradient-echo 3D (MGE3D)) was performed to evaluate whole-body iron disposition, 24 hours post Venofer® injection. Three postmortem imaging sessions were performed for each rat to allow whole-body coverage with an 8 cm diameter Helmholtz volume coil (Figure 6), and ROIs were manually drawn in different organs of interest to calculate mean R_2* values from the MGE3D images (Figure 7).

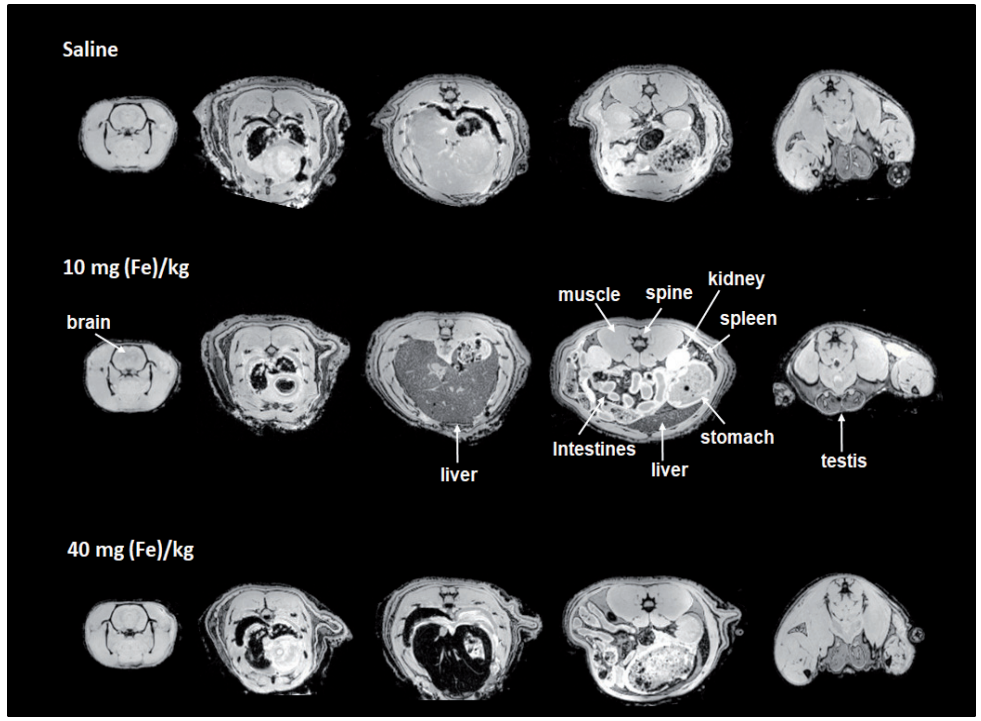

Fig. 6 Representative T2*-weighted images (TE = 5 ms) of the whole rat, from head (left) to toe (right), after administration of saline, 10 - or 40 mg/kg Venofer®

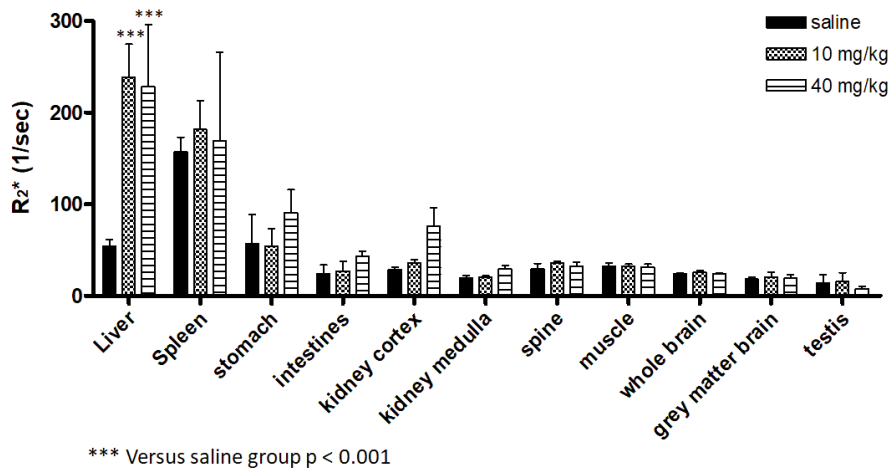

Fig. 7 Average R_2^* values (s^{-1}) for different organs measured post mortem in rats euthanized 24 hours post injection of 10 - or 40 mg/kg Venofer® or saline solution (n=4 per group). Results represent mean ± st.dev for 4 rats

ROI-based analysis in rats that received Venofer® showed increased R_2^* values compared to saline-treated control animals, indicative of iron uptake in the liver (Figure 7). R_2^* values from organs such as the lungs and the heart, which are also considered target organs for iron accumulation, are not depicted in Figure 7 as these values may be affected by the presence of air and should therefore be treated with care.

The observed R_2^* values in the liver and spleen suggest that there is no significant difference in iron accumulation between animals treated with 10 or 40 mg/kg (Figure 7). However, this outcome is not in accordance with Figure 6, where a clear decrease in signal intensity was observed in these organs with increasing dose from 10 to 40 mg/kg. This discrepancy may be explained by substantial iron accumulation in these organs, resulting in T_2^* values that were too low for accurate T_2^* quantification. Therefore iron accumulation in the liver and spleen was also studied by quantification of the average signal intensity in these organs in the T_2^*-weighted images (TE=5 ms), after normalization to the average signal intensity of muscle tissue in the corresponding images (Figure 8). Both in liver and spleen, the normalized signal intensity was significantly lower in the animals that received the 40 mg/kg dose as compared to the saline-treated controls (Figure 8). Moreover, both organs demonstrated a significant decrease in signal intensity with increasing Venofer® dose.

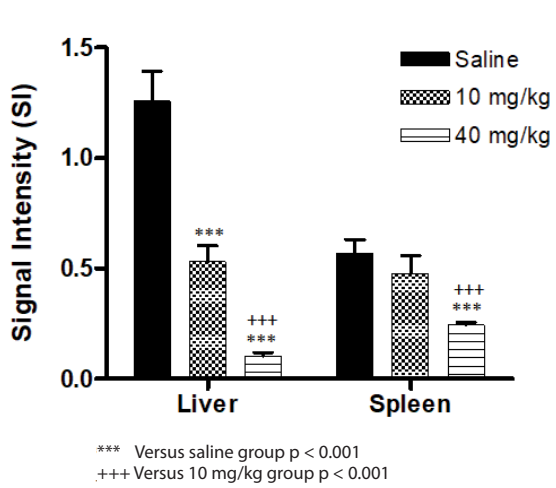

Fig. 8 Average signal intensity in the liver and spleen, normalized to the signal intensity in muscle tissue in the corresponding MR acquisition. Results represent mean ± st.dev for 4 rats

The outcomes of this MRI experiment demonstrate that within 24 hours of one single administration of two different doses of Venofer®, the liver and spleen are the main organs for exogenous iron disposition. This coincides with previous reports describing the most adopted mechanism, in which intravenously injected iron complexes are taken up by the mono nuclear phagocyte system and engulfed by macrophages to next dissociate the iron from the complex. Subsequently, the iron is then presumably mainly absorbed by the liver,

spleen and bone marrow. (8, 13).

Besides chemical and physical characterization of the iron nano-colloidal complexes, a biodistribution study is necessary in order to perform a proper comparison between different iron products. PET imaging with radioisotope-labeled iron and inductively coupled plasma mass spectrometry (ICP-MS) techniques have been demonstrated to allow assessment of iron content in different organs (3,16). Nevertheless, an MRI-based method that allows longitudinal non-invasive monitoring of iron distribution is considered more advantageous, as this imaging modality does not require modifications of the iron complex with radioactive labels, as needed for PET. Moreover, there is no need to sacrifice animals at several time points such as in the case of ICP-MS measurements, and it is hence expected to be easily translated to the clinic.

The present study shows that T_2-based MRI allows continuous and non-invasive monitoring of iron distribution over various organs of interest. Despite the obvious advantages, there are some limitations to the present method. First, iron complexes such as Venofer® induce relatively low MRI contrast, which limits its detection to relatively high iron concentrations. It should also be taken into account that due to differences between the various iron complexes, each iron product should be separately evaluated for their ability to generate sufficient MR contrast. Second, the spatial resolution of MRI only allows monitoring iron disposition at macroscopic level but cannot be used when interested in cellular iron disposition which can be studied with microscopy techniques (40). Third, R_2^* changes in organs cannot be directly converted into iron concentrations, as intracellular iron accumulation may alter its relaxivities (24, 41).

Therefore, in order to scrutinize differences in biodistribution and fate of the various iron preparations as proposed by the European Medicines Agency (EMA) (15), a multimodal study should be carried out. Several evaluation techniques have to be combined to encompass the full scope of iron accumulation in plasma, mononuclear phagocyte system and organ tissues, after administration of iron-based medicines.

4. CONCLUSION

MRI was successfully used for non-invasive monitoring of iron distribution up to twenty-four hours after one single intravenous injection of Venofer® in rats. The present method is considered complementary to existing iron quantification techniques, and could therefore be a valuable whole-body imaging approach for biodistribution measurements to compare iron-based medicines in preclinical studies.

5. ACKNOWLEDGMENT

This research was financially supported by Vifor (International) Ltd., St. Gallen, Switzerland.

6. REFERENCES

1. Macdougall IC, Geisser P. Use of intravenous iron supplementation in chronic kidney disease: an update. Iranian Journal of Kidney Diseases. 2013;7(1):9-22.
2. Schiesser D, Binet I, Tsinalis D, Dickenmann M, Keusch G, Schmidli M, Ambühl PM, Lüthi L, Wüthrich RP. Weekly low-dose treatment with intravenous iron sucrose maintains iron status and decreases epoetin requirement in iron-replete haemodialysis patients. Nephrology Dialysis Transplantation. 2006;21(10):2841-5.
3. Elford P, Bouchard J, Jaillet L, Pearson N, Rogue A, Sabadie C, Forster R. Biodistribution and predictive hepatic gene expression of intravenous iron sucrose. Journal of Pharmacological and Toxicological Methods. 2013;68(3):374-83.
4. Chertow GM, Mason PD, Vaage-Nilsen O, Ahlmén J. Update on adverse drug events associated with parenteral iron. Nephrology Dialysis Transplantation. 2006;21(2):378-82.
5. Fishbane S. Safety in iron management. American Journal of Kidney Diseases. 2003;41:18-26.
6. Agarwal R, Vasavada N, Sachs NG, Chase S. Oxidative stress and renal injury with intravenous iron in patients with chronic kidney disease. Kidney International. 2004;65(6):2279-89.
7. Faich G, Strobos J. Sodium ferric gluconate complex in sucrose: Safer intravenous iron therapy than iron dextrans. American Journal of Kidney Diseases. 1999;33(3):464-70.
8. Danielson BG. Structure, Chemistry, and Pharmacokinetics of Intravenous Iron Agents. Journal of the American Society of Nephrology. 2004;15(suppl 2): S93-S8.
9. Storm G, Belliot SO, Daemen T, Lasic DD. Surface modification of nanoparticles to oppose uptake by the mononuclear phagocyte system. Advanced Drug Delivery Reviews. 17:31-48 (1995).
10. Romberg B, Oussoren C, Snel CJ, Hennink WE, Storm G. Effect of Liposome characteristics and dose on the pharmacokinetics of liposomes coated with ppoly(amino acid). Pharmaceutical Research. 2007;24:2394-2401.
11. Duan X and Duan Y. Physicochemical characteristics of nanoparticles affect circulation, biodistribution, cellular internalization and trafficking. Small. 2013;9:1521-1532.
12. Gustafson HH, Holt-Casper D, Grainger DW, Ghandehari H. Nanoparticle uptake: The phagocyte problem. Nano Today. 2015;10(4):487-510.
13. Koskenkorva-Frank TS, Weiss G, Koppenol WH, Burckhardt S. The complex interplay of iron metabolism, reactive oxygen species, and reactive nitrogen species: insights into the potential of various iron therapies to induce oxidative and nitrosative stress. Free Radical Biology & Medicine. 2013; 65:1174-94.
14. Bishu K, Agarwal R. Acute iinjury with iiintravenous iron and crltsconcerns regarding long-term safety. Clinical Journal of the American Society of Nephrology. 2006 September 1, 2006;1(Suppl 1): S19-S23.
15. EMA, 2015. Reflection Paper on the Data Requirements for Intravenous Iron-based Nano-colloidal Products Developed with Reference to an Innovator Medicinal Product. 2015; EMA/CHMP/SWP/620008/2012. http://www.ema.europa.eu/docs/en_GB/document_library/Scientific_guideline/2015/03/WC500184922.pdf
16. Beshara S, Lundqvist H, Sundin J, Lubberink M, Tolmachev V, Valind S, Antoni G, Långström B, Danielson BG. Kinetic analysis of ^{52}Fe-labelled iron(III) hydroxide–sucrose complex following bolus administration using positron emission tomography. British Journal of Haematology. 1999;104(2):288-95.
17. Schümann K, Szegner B, Kohler B, Pfaffl MW, Ettle T. A method to assess ^{59}Fe in residual tissue blood content in mice and its use to correct ^{59}Fe-distribution kinetics accordingly. Toxicology. 2007;241(1-2):19-32.
18. Beshara S, Lundqvist H, Sundin J, Lubberink M, Tolmachev V, Valind S, Antoni G, Långström B, Danielson BG. Pharmacokinetics and red cell utilization of iron(III) hydroxide–sucrose complex in anaemic patients: a study using positron emission tomography. British Journal of Haematology. 1999;104(2):296-302.
19. Beshara S, Sörensen J, Lubberink M, Tolmachev V, Långström B, Antoni G, Danielson BG, Lundqvist H. Pharmacokinetics and red cell utilization of 52Fe/59Fe-labelled iron polymaltose in anaemic patients using positron emission tomography. British Journal of Haematology. 2003;120(5):853-9.
20. Walczyk T, Davidsson L, Zavaleta N, Hurrell RF. Stable isotope labels as a tool to determine the iron absorption by Peruvian school children from a breakfast meal. Fresenius Journal of Analytical Chemistry. 1997;359(4):445-9.
21. Rostoker G, Cohen Y. Magnetic resonance imaging repercussions of intravenous iron products used for iron-deficiency anemia and dialysis-associated anemia. Journal of Computer Assisted Tomography. 2014;38(6):843-4.
22. Kato Y, Zhu W, Backer MV, Neoh CC, Hapuarachchige S, Sarkar SK, Backer JM, Artemov D. Noninvasive imaging of liposomal delivery of superparamagnetic iron oxide nanoparticles to orthotopic human breast tumor in mice. Pharmaceutical Research. 2015;32:3746-55.
23. Vinitski S, Thakur ML, Consigny PM, Mitchell DG, Mohamed FB, Ortega HV. Use of ferrum in MRI of lung parenchyma and pulmonary embolism. Magnetic Resonance Imaging. 1993;11(4):499-508.
24. Gandon Y, Olivie D, Guyader D, Aube C, Oberti F, Sebille V, Deugnier Y. Non-invasive assessment of hepatic iron stores by MRI. Lancet (London, England). 2004;363(9406):357-62.
25. Liu L, Hitchens TK, Ye Q, Wu Y, Barbe B, Prior DE, Li WF, Yeh FC, Foley LM, Bain DJ, Ho C. Decreased reticuloendothelial system clearance and increased blood half-life and immune cell labeling for nano- and micron-sized superparamagnetic iron-oxide particles upon pre-treatment with Intralipid. Biochimica et Biophysica Acta. 2013;1830(6):3447-53.
26. Smith SM, Jenkinson M, Woolrich MW, Beckmann CF, Behrens TE, Johansen-Berg H, Bannister PR, DE Luca M, Drobnjak I, Flitney D, Niazy RK, Saunders J, Vickers J, Zhang Y, De Stefano N, Brady JM, Matthews PM. Advances in functional and structural MR image

analysis and implementation as FSL. Neuroimage. 2004;23(Suppl 1): S208-19.
27. Jenkinson M, Beckmann CF, Behrens TE, Woolrich MW, Smith SM. FSL. Neuroimage. 2012;62(2):782-90.
28. van Zutphen LFM, Baumans V, Ohl F. Handboek proefdierkunde : proefdieren, dierproeven, alternatieven en ethiek (5e dr., 2e opl. ed.). Amsterdam : Reed Business; 2012.
29. Danielson BG, Salmonson T, Derendorf H, Geisser P. Pharmacokinetics of iron(III)-hydroxide sucrose complex after a single intravenous dose in healthy volunteers. Arzneimittel-Forschung. 1996;46(6):615-21.
30. Geisser P, Baer M, Schaub E. Structure/histotoxicity relationship of parenteral iron preparations. Arzneimittel-Forschung. 1992;42(12):1439-52.
31. Venofer® (iron sucrose injection, USP) NDA 21-135/S-017 https://www.accessdata.fda.gov/drugsatfda_docs/label/2007/021135s017lbl.pdf
32. Fütterer S, Andrusenko I, Kolb U, Hofmeister W, Langguth P. Structural characterization of iron oxide/hydroxide nanoparticles in nine different parenteral drugs for the treatment of iron deficiency anaemia by electron diffraction (ED) and X-ray powder diffraction (XRPD). Journal of Pharmaceutical and Biomedical Analysis. 201386:151-60.
33. Kudasheva DS, Lai J, Ulman A, Cowman MK. Structure of carbohydrate-bound polynuclear iron oxyhydroxide nanoparticles in parenteral formulations. Journal of Inorganic Biochemistry. 2004;98(11):1757-69.
34. Liu J, Yu M, Zhou C, Zheng J. Renal clearable inorganic nanoparticles: a new frontier of bionanotechnology. Materials Today. 2013;16(12):477-86.
35. Ruggiero A, Villa CH, Bander E, Rey DA, Bergkvist M, Batt CA, Manova-Todorova K, Deen WM, Scheinberg DA, McDevitt MR. Paradoxical glomerular filtration of carbon nanotubes. Proceedings of the National Academy of Sciences of the United States of America. 2010;107(27):12369-74.
36. Choi HS, Liu W, Misra P, Tanaka E, Zimmer JP, Ipe BI, Bawendi MG, Frangioni JV. Renal Clearance of Nanoparticles. Nature Biotechnology. 2007;25(10):1165-70.
37. Wood JC, Enriquez C, Ghugre N, Tyzka JM, Carson S, Nelson MD, Coates TD. MRI R2 and R2* mapping accurately estimates hepatic iron concentration in transfusion-dependent thalassemia and sickle cell disease patients. Blood. 2005;106(4):1460-5.
38. Gabizon A, Shmeeda H, Barenholz Y. Pharmacokinetics of Pegylated Liposomal Doxorubicin. Clinical Pharmacokinetics. 2003 April 01;42(5):419-36.
39. Schröder O, Mickisch O, Seidler U, De Weerth A, Dignass AU, Herfarth H, Reinshagen M, Schreiber S, Junge U, Schrott M. Intravenous iron sucrose versus oral iron supplementation for the treatment of iron deficiency anemia in patients with inflammatory bowel disease a randomized, controlled, open-label, multicenter study. The American Journal of Gastroenterology. 2005;100(11):2503-9.
40. Richter GW. The cellular transformation of injected colloidal iron complexes into ferritin and hemosiderin in experimental animals: a study with the aid of electron microscopy. The Journal of Experimental Medicine. 1959;109(2):197–216.

41. Tanimoto A, Oshio K, Suematsu M, Pouliquen D, Stark DD. Relaxation effects of clustered particles. Journal of Magnetic Resonance Imaging. 2001;14(1):72-7.

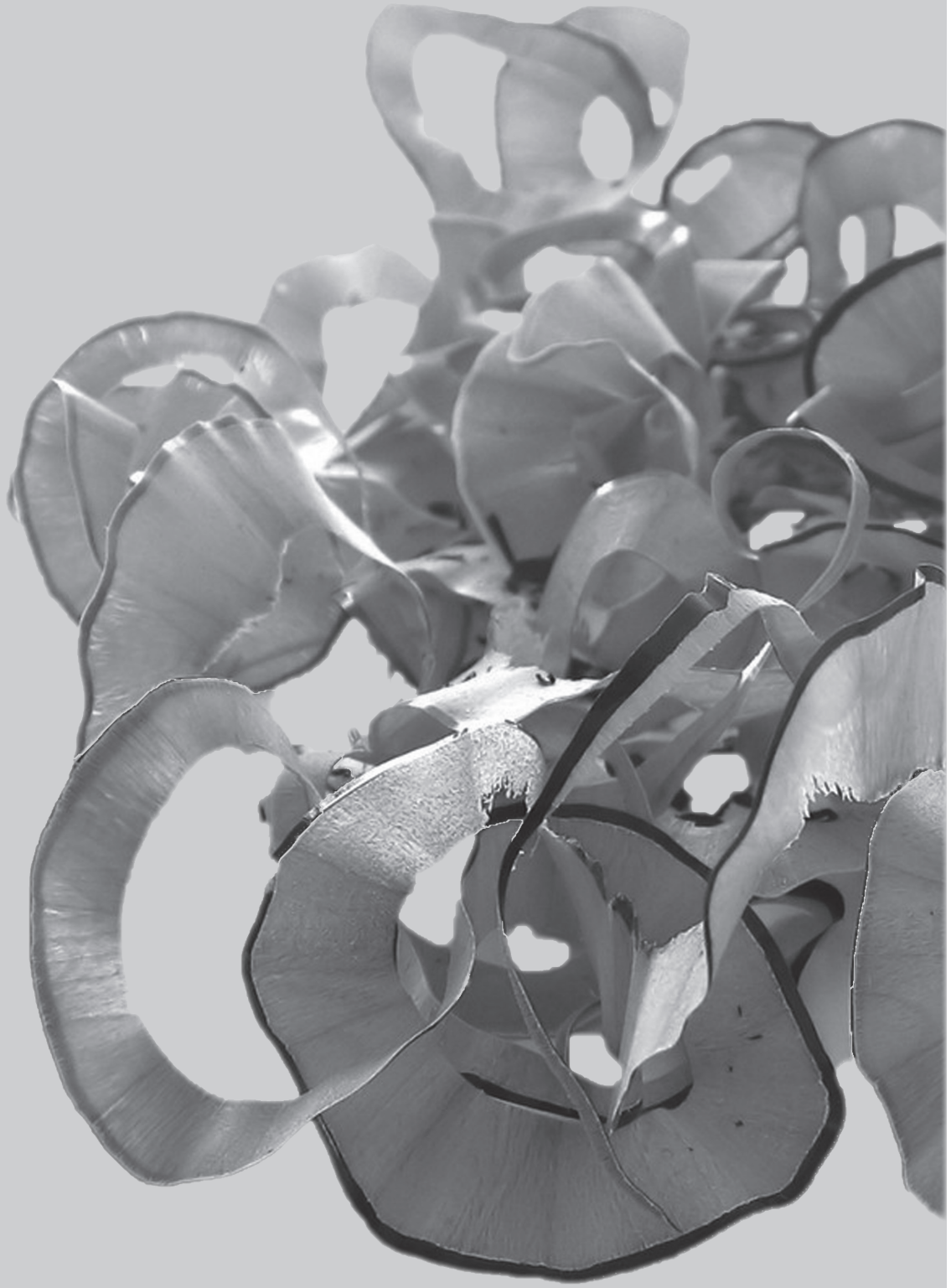

CHAPTER 6

Summary and Discussion

1. SUMMARY

Iron treatment is necessary to replenish iron deficit due to several clinical conditions such as chronic diseases. However, as an excess of iron can result in redox imbalance resulting in oxidative stress and thus severe damage to tissue and organs, it is of utmost importance to develop iron therapies that are effective and yet safe to not induce iron overload (1). Especially in the case of intravenous iron formulations, which are complexes consisting of a polynuclear iron(III) oxyhydroxide core and a carbohydrate shell, several factors such as the physicochemical properties and manufacturing processes have demonstrated to impact their efficiency and safety *in-vivo* (2). Up to date it has been a challenge to develop evaluation methods, particularly suitable *in-vivo* pre-clinical models to perform proper comparisons and in-depth assessment studies of iron therapeutics.

In **Chapter 1**, we gave a general introduction describing the importance of iron as a nutrient and the significance of keeping a healthy iron metabolism. Furthermore, the different iron treatment modalities, oral and intravenous, are described as well as their possible impact on iron overload. Iron plays an important role in the Fenton reaction which can result in oxidative stress in organs and tissues. Therefore, assessing the various iron products for safety and efficacy is essential, especially when evaluating the similarity of an original iron product and its generics. In **chapter 2**, we designed an iron-complex formulation for oral iron treatment, based on hemin-loaded polymeric micelles, with the aim to develop an oral supplement with better bioavailability and possible less side effects than the commonly used iron sulfate. As heme has a superior bioavailability to non-heme iron, the heme analogue hemin was encapsulated in the biodegradable and thermosensitive polymer, methoxy-poly(ethylene glycol)-b-poly[*N*-(2-hydroxypropyl) methacrylamide-dilactate], to form hemin-micelles. The highest loading capacity for hemin in mPEG-*b*-p(HPMAm-Lac_2) micelles was 3.9% and the average particle diameter of the hemin-micelles, depending on the hemin concentration, ranged from 75 to 140 nm. Furthermore, the hemin micelles demonstrated to be stable at pH 2 for approximately 3 hours and up to 17 hours at a more neutral pH of 7.4. More importantly, after incubation of Caco-2 cells with hemin-micelles, ferritin values of 2500 ng/mg protein were observed. These values are 10 fold higher compared to ferritin levels obtained with iron sulfate. The results presented in chapter 2 demonstrate that hemin-loaded micelles are a promising novel iron formulation for oral delivery. In **Chapter 3**, the reproducibility of non-clinical studies was assessed. Here, the original iron sucrose product Venofer® was compared with two iron sucrose similars (ISS) in an almost comparable set-up, using Sprague Dawley rats, as has been previously described in literature. During this study a similar dose of the originator and the similars was administered weekly to male and female animals for 4 weeks. Blood and urine were collected in order to measure blood related parameters and to perform biochemical analysis that give insights in possible

toxic effects of the formulations for particularly the liver and kidneys. Post mortem, oxidative stress of the liver and kidney as well as iron disposition in the liver were established. The results presented in chapter 3 did not show clear differences between the original iron sucrose Venofer® and the two iron sucrose similars. This in contrast to results described in a previous study in which the same iron products were evaluated. In addition, differences in results of male and female rats that were exposed to the same treatments and experimental circumstances were shown. Chapter 3, illustrates the difficulties to compare, standardize and reproduce results from various pre-clinical iron related comparison studies that were performed with similar experimental design. As it was interesting to scrutinize whether the animal model used for these investigations is sensitive enough to give appropriate insight into potential toxicity differences of the iron medicinal products, in **chapter 4**, we conducted a dose-response study. During these investigations doses much higher (> 40 mg iron/kg; Venofer® and Ferrlecit®) than the clinical administered dose (7 mg/kg) were injected in male Sprague Dawley rats. The assessed biomarkers, were similar to those presented in chapter 3. The blood related iron parameters, namely serum iron and transferrin saturation (TSAT), showed no statistical differences between the iron treatments, but did display higher levels in the same group of animals after multiple injections in time. Furthermore, the abdominal organs in particular the liver, showed a dose-effect related brownish color. However, this was not reflected in other parameters measured such as oxidative stress levels and Prussian blue staining of the liver. In addition, the results from the liver enzyme aspartate transaminase (AST), demonstrated no significant differences between the different treatments. Moreover, evaluation of the kidney function also did not show signs of renal toxicity which was expected after injecting such high doses of iron. The different analysis in chapter 4, demonstrated neither a clear treatment nor a dose effect after multiple injections of the two different iron formulations. Therefore, it is questionable whether this frequently used model is sensitive enough to give proper insight into possible toxic effects of the two iron formulations investigated.

Characterization of the physicochemical properties (e.g. size, charge, stability) of an intravenous iron preparation is not predictive for the clinical effect of the injected iron formulation. Therefore, a thorough assessment of the iron distribution *in-vivo* should be done. **Chapter 5**, sheds light onto the possibility of using imaging techniques such as magnetic resonance imaging (MRI) for these purposes. The results showed that Venofer®(iron sucrose) generated sufficient contrast in order to evaluate its disposition in organs using MRI. Sprague Dawley rats were assessed *in-vivo* up to 3 hours and post mortem at 24 hours after injections of both 10- and 40 mg/kg Venofer®. As a control, animals that received saline were included in this study. Within 10 to 20 minutes after injection an increase in iron disposition, in the liver, spleen and kidney (including kidney medulla and cortex) were observed. Post mortem analysis 24 hours after one

administration of the iron preparation showed, that as expected, iron accumulation was essentially observed in the liver and spleen. The results of this Chapter demonstrates that the MRI technique has proven to be a powerful non-invasive modality to monitor iron distribution after administering exogenous iron.

2. DISCUSSION AND PERSPECTIVES

2.1 Iron deficiency

The adverse effects of iron deficiency on the overall health of living organisms is well known. It is important to eradicate the circumstances that induce this disorder and to investigate treatment modalities while of course continuously assuring efficacy and safety of these treatments.

The first step in treatment of iron deficiency is to have good diagnostic tools. In order to be able to diagnose iron deficiency, it is imperative to understand the three stages of iron deficit. The first stage is depletion of iron stores (low levels of ferritin). It should be mentioned that in this stage hemoglobin (Hb) levels and red blood cell parameters such as mean corpuscular volume (MCV), mean corpuscular hemoglobin (MCH) and mean corpuscular hemoglobin concentration (MCHC) are still normal (3). To detect deficiency in this stage one should check for low levels of serum ferritin and low hepcidin serum values (4). The second stage is iron deficiency without anemia. During this stage, the hemoglobin levels are within normal ranges. However, deviating other iron related blood parameters such as decreased serum transferrin saturation (TSAT) levels or higher transferrin receptor (TfR) levels are observed (5). The last stage is iron deficiency anemia. When this stage is reached it is relatively easy to diagnose, because the well-established iron related biomarkers, as mentioned in the two previous stages, will show levels characteristic for iron deficiency (6).

Iron metabolism is mainly regulated by the hormone hepcidin (7). As hepcidin production is upregulated by inflammatory stimuli, patients suffering from a wide range of chronic diseases such as chronic kidney disease (CKD), inflammatory bowel disease (IBD) and rheumatoid arthritis develop iron anemia (8, 9).

2.2 Iron deficiency treatments

Oral iron therapy is the most accessible and economical modality for iron replacement treatment. Iron salts are mainly used for oral therapy but they are also associated with gastrointestinal adverse reactions, which occur more frequently with increasing dose

(9). With the aim to lower the symptoms, other preparations with slow iron release properties, such as ferrous fumarate as well as oral iron complexes like iron polymaltose complex (IPC), have been developed (10-13). In addition, several alterations of the most commonly used iron salt, iron sulfate, have also been developed in the form of enteric/ film- coated tablets and extended release capsules (14). However, the occurrence of less side effects with these products is not evident (14). More recently, ferric citrate (Auryxia) obtained FDA approval after a clinical study in which significant increases in hemoglobin values were shown in patients that were unresponsive for other oral iron preparations (15,16). Besides iron salts, other products including the previously mentioned IPC but also carbonyl iron which consists of micro-particles with purified elemental iron, have been developed and clinically evaluated. Carbonyl iron has been reported to have a comparable bioavailability as ferrous sulfate but it induces less toxicity (17). All above mentioned oral supplementations consist of non-heme iron even though it is known that this type of iron has a lower bioavailability than heme iron. As the uptake of heme, unlike non-heme iron, occurs probably through receptors, this will lead to less iron overload (18). At present, the most prominent heme-based oral supplementation is the heme-iron polypeptide (HIP) that has proven to be a well-tolerated, effective and safe oral supplement (19-21). Nagaraju et al. reported that the efficacy of HIP was similar to that of intravenous iron sucrose in terms of maintaining the hemoglobin levels in patients with chronic kidney disease (non-dialysis), but patients receiving IV formulation had greater serum ferritin levels, indicating increased iron stores (22). In a review of three clinical studies in which HIP was applied for the management of anemia, it was observed that this product resulted in lower ferritin levels as compared to other iron treatments. Moreover, the effect on the iron related blood parameters as well as adverse effects were equal to non-heme iron preparations and intravenous iron treatment (23). In chapter 2, we discuss the development of a novel oral heme-based therapy. To this end, we encapsulated hemin in micelles consisting of thermosensitive biodegradable block copolymer based on methoxy-poly(ethylene glycol)-b-poly[*N*-(2-hydroxypropyl) methacrylamide-dilactate] (mPEG-*b*-p(HPMAm-Lac_2). Micelles based on this polymer, have proven to be water dispersible and an effective tool to deliver drugs (24-26). The amount of iron normally given to patients is approximately 325 mg with 65 mg being elemental iron for ferrous sulfate, even though this iron quantity administered has been debated in the past (27-29). The main challenge with the developed hemin micelles would be to increase the iron loading or to concentrate the micellar dispersion in order to deliver a sufficient dose of iron. Adding 0.1 ml of 120 µg/ml hemin solution to 0.9 ml polymer solution to form 1 ml hemin-micellar formulation, resulted in a loading capacity of 3.9% and an encapsulation efficiency of 61.4%, thus a micellar hemin concentration of ~ 70 µg/ml. This means that impracticable large volumes would be needed to deliver sufficient iron to the patients. Within our Department polymers have been developed that due to $\pi - \pi$ stacking and a more hydrophobic core, resulted in an increase in

loading and stability of poorly soluble drugs (30). It would be interesting to investigate these novel polymers for loading of hemin. Suitable formulations should be evaluated *in-vivo* to establish the bioavailibilty of hemin and their safety.
When intravenous iron is the modality treatment of choice, there are other factors that should be considered when developing new iron complexes/formulations. Chapter 3 and 4 illustrate difficulties to properly assess the toxicological differences between various iron formulations. The introduction of this thesis describes that even though iron is essential for the human physiology, it can also cause toxic effects to tissues and organs due to its ability to react with oxygen and to catalyze the production of reactive oxygen species (ROS) (6). Iron overload has been associated with several clinical conditions such as secondary hemochromatosis cancer by DNA mutation, neurodegenerative diseases, colorectal adenoma and diabetes mellitus (31,32). Therefore, one of the main concerns regarding iron therapy, especially in the case of intravenous iron treatment, is that products are efficient, stable and safe enough to not result in excessive iron overload.

2.3 Efficacy and safety of intravenous iron therapy

Primary and secondary iron overload has been clinically successfully managed with iron chelators (33,34). However, these products are associated with a number of adverse reactions such as decrease in liver- and kidney functioning and hypersensitivity reactions (35). It is therefore a must to assess intravenous iron therapy meticulously in regards to iron disposition, safety and efficacy, in order to avoid possible secondary iron overload. It is assumed that the carbohydrate surface properties play a main role in iron disposition and thus in safety and efficacy profiles of the iron formulations. Importantly, it has been reported that small variations in manufacturing processes might result in significant clinical differences between original iron preparations and their generics (36,37). Therefore, for a proper assessment of the original and generic versions of iron-based nano-colloidal products, the evaluation should include physicochemical characterization, preclinical studies with an emphasis on *in-vivo* biodistribution studies as well as clinical evaluations regarding pharmacokinetics, efficacy and safety (38). The focus of this dissertation is on the non-clinical assessment and this will therefore be further discussed.

The main site of action and thus the parameter of interest for iron preparations is the incorporation of iron in red blood cells. The amount of serum iron is only a small portion as compared to the total amount of iron, and also to the quantity incorporated hemoglobin present in the red blood cells. This in combination with the fact that serum iron levels fluctuate during the day, makes the generally used technique of measuring the area under the curve in serum to test efficacy of the drug, not applicable for iron preparations (9). Iron related blood parameters that need to be measured after iron

treatments are; 1) total iron binding capacity which together with the serum iron levels reflects whether there is oversaturation of transferrin; 2) serum ferritin to assess body iron stores; 3) hemoglobin and the red cell indices which give information of the amount of iron for erythropoiesis (9). However, the mentioned blood parameters are not sufficient to show differences in iron distribution of two iron formulations and thus further iron disposition studies on a cellular and organ level should be done. *In-vitro* studies are generally carried out under circumstances that are very different from the physiological condition. Therefore, it is advised to perform *in-vivo* iron distribution studies evaluating the following three compartments; 1) Serum or plasma and red blood cells, 2) mononuclear phagocyte system of macrophages (e.g. Kupffer cells in the liver) and 3) target tissues, which include the pharmacological target tissue such as bone marrow and tissue susceptible for toxicological effects such as liver, kidney, heart and lungs (38). In addition, the extent in which different formulations induce oxidative stress should be established. Here, levels of secondary antioxidants like super oxide dismutase (SOD), catalase and glutathione peroxidase should be measured, but also the more direct consequence of reactive oxygen species, particularly on lipid peroxidation should be investigated (39,40). Several *in-vivo* models have been used to evaluate iron tissue disposition and possible toxic effects of intravenous iron therapy (41-46). However, up to date there is no standardized *in-vivo* model to evaluate iron-based medicinal products. As described in chapter 3 and 4 of this thesis, outcomes of the different studies are very difficult to reproduce. Different analytical techniques and different sample preparation methods can lead to different *in-vivo* results (2, 47). Moreover, there are several other factors that can influence the outcome of these *in-vivo* studies. For instance, standard rat chow also contains small but varying amounts of iron. Housing and environment when not being proper, can be stress factors for the animals influencing their behavior and thus how they react on the drugs administered. The source of animals has also demonstrated to have a big impact on the outcome of *in-vivo* studies (48). As discussed in Chapter 3 and 4, other factors should also be taken into account such as variations in tissue sample processing as well as the gender of the animals. By using mixed genders, the biological variations of the animals is taken into account. However it should be considered whether this is really necessary for non-clinical toxicity comparison studies of iron complexes. The reason is that using both genders will result in larger variations within treatment groups and therefore larger group sizes are needed in order to be able to detect small differences between iron complexes. Finally, when using other assessment techniques, the significant biopharmaceutical properties of the different iron formulations for that specific technique should be defined, such as the ability of the iron complex to generate contrast in MR images, as described in chapter 5.

3. CONCLUSION

The results described in this thesis demonstrate the importance to develop and define a proper pre-clinical comparative evaluation model for intravenous iron preparations. It is recommended to establish and validate physicochemical analytical methods and to define and develop a sensitive robust animal model that can be used to evaluate the efficacy and particularly the safety of existing and novel intravenous iron formulations.

4. REFERENCES

1. Koskenkorva-Frank TS, Weiss G, Koppenol WH, Burckhardt S. The complex interplay of iron metabolism, reactive oxygen species, and reactive nitrogen species: insights into the potential of various iron therapies to induce oxidative and nitrosative stress. Free Radical Biology & Medicine. 2013; 65:1174-94.
2. Mühlebach S, Flühmann B. Iron Carbohydrate Complexes: Characteristics and Regulatory Challenges. In: Crommelin D, de Vlieger J. Non-Biological Complex Drugs. AAPS Advances in the pharmaceutical sciences series. Springer. 2015:(20);149-170.
3. Bugnara C, Beris P. ESH Handbook on Disorders of Iron Metabolism; 2009 Edition: 513-529
4. Ganz T, Olbina G, Girelli D, Nemeth E, Westerman M. Immunoassay for human serum hepcidin. Blood. 2008;112(10):4292-7.
5. Brugnara C. A Hematologic "Gold Standard" for Iron-deficient States? Clinical Chemistry. 2002;48(7):981-2.
6. Brugnara C. Iron Deficiency and Erythropoiesis: New Diagnostic Approaches. Clinical Chemistry. 2003;49(10):1573-8.
7. Fuqua BK, Vulpe CD, Anderson GJ, Intestinal iron absorption. Journal of trace elements in medicine and biology. 2012;26:115-119.
8. Beaumont C, Vaulont S. ESH Handbook on Disorders of Iron Metabolism; 2009 Edition: 488-511.
9. Crichton RR, Danielson BG, Geisser P. Iron therapy: With special emphasis on intravenous administration. Uni-Med, Bremen. 2008; 4th Edition: 81-2.
10. Harrington M, Hotz C, Zeder C, Polvo GO, Villalpando S, Zimmermann MB, et al. A comparison of the bioavailability of ferrous fumarate and ferrous sulfate in non-anemic Mexican women and children consuming a sweetened maize and milk drink. European journal of clinical nutrition. 2010;65:20.
11. Geisser P. Safety and Efficacy of Iron(III)-hydroxide Polymaltose Complex. Arzneimittelforschung. 2007; 57(6): 439-452
12. Funk F, Canclini C, Geisser P. Interactions between Iron(III)-hydroxide Polymaltose Complex and Commonly Used Medications. Arzneimittelforschung. 2007;57(6): 370-375.
13. Jacobs P, Wood L, Bird AR. Better Tolerance of Iron Polymaltose Complex Compared with Ferrous Sulphate in the Treatment of Anaemia. Hematology. 2000;5(1):77-83.
14. Comparison of oral iron supplements. Pharmacist's Letter/Prescriber's Letter 2008;24 (8):240811.
15. www.accessdata.fda.gov/drugsatfda_docs/nda/2014/205874Orig1s000TOC.cfm
16. Fishbane S, Block GA, Loram L, Neylan J, Pergola PE, Uhlig K, Chertow GM. Effects of Ferric Citrate in Patients with Nondialysis-Dependent CKD and Iron Deficiency Anemia. Journals of the American Society of Nephrology. 2017;28 (6):1851-1858.
17. Nagpal J, Choudhury P. Iron formulations in pediatric practice. Indian Pediatrics. 2004:41:807-15.

18. Nam T, Shim JY, Kim B, Rah SY, Park K, Kim S, Mun EG, Jeong YJ, Han MK, Cha YS, Chae SW, Im MJ, Kim UH. Clinical Study on the Iron Absorption from Heme-Iron Polypeptide and Nonheme-Iron. Nutritional Sciences. 2006; 9:295-300.
19. Pal B, Deshpande H, Sundari T, Biniwale P, Shah K, Goel S, Khurana AS, Qamra A, Motlekar S, Barkate H. Heme Iron Polypeptide in Iron Deficiency Anemia of Pregnancy: Current Evidence. Open Journal of Obstetrics and Gynecology. 2017;7,420-431.
20. Seligman PA, Moore GM, Schleicher RB. Clinical studies of HIP: An oral heme-iron product. Nutrition Research. 2000;20:1279-86.
21. Abdelazim I, Abu-Faza M, Elbiaa A, Othman H, Alsharif D, Elsawah W. Heme iron polypeptide (proferrin®-ES) versus iron saccharate complex (ferrosac) for treatment of iron deficiency anemia during pregnancy. Acta Medica International. 2017;4(1):56-61.
22. Nagaraju SP, Cohn A, Akbari A, Davis JL, Zimmerman DL. Heme iron polypeptide for the treatment of iron defi ciency anemia in non-dialysis chronic kidney disease patients: a randomized controlled trial. BMC nephrol. 2013;14:64.
23. Dull RB, Davis E. Heme iron polypeptide for the management of anaemia of chronic kidney disease. Journal of clinical pharmacy and therapeutics. 2015;40(4):386-90.
24. Soga O, van Nostrum CF, Hennink WE. Poly(N-(2-hydroxypropyl) methacrylamide mono/di Lactate): A new class of biodegradable polymers with tuneable thermosensitivity. Biomacromolecules. 2004; 5;818–821
25. Talelli M, Rijcken CJF, Lammers T, Seevinck PR, Storm G, van Nostrum CF, Hennink WE. Superparamagnetic iron oxide nanoparticles encapsulated in biodegradable thermosensitive polymeric micelles: toward a targeted nanomedicine suitable for image-guided drug delivery. Langmuir. 2009;25:2060-2067.
26. Naksuriya O, Shi Y, van Nostrum CF, Anuchapreeda S, Hennink WE, Okonogi S. HPMA-based polymeric micelles for curcumin solubilization and inhibition of cancer cell growth. European journal of pharmaceutics and biopharmaceutics. 2015; 94:501–512.
27. DeLoughery TG. Microcytic Anemia. New england journal of medicine. 2014;371(14):1324-31.
28. Rimon E, Kagansky N, Kagansky M, Mechnick L, Mashiah T, Namir M, Levy S. Are we giving too much iron? Low-dose iron therapy is effective in octogenarians. American journal of medicine. 2005;118:1142-1147.
29. Zhou SJ, Gibson RA, Crowther CA, Makrides M. Should we lower the dose of iron when treating anaemia in pregnancy? A randomized dose-response trial. Eur J Clin Nutr 2009;63:183-190
30. Shi Y, van Steenbergen MJ, Teunissen EA, Novo Ls, Gradmann S, Baldus M, van Nostrum CF, Hennink WE. Π–Π stacking increases the stability and loading capacity of thermosensitive polymeric micelles for chemotherapeutic drugs. Biomacromolecules. 2013;14(6):1826-37.
31. Crielaard BJ, Lammers T, Rivella S. Targeting iron metabolism in drug discovery and delivery. Nature reviews drug discovery. 2017;16:400-423.
32. Marx JJM, van Asbeck BS. Use of iron chelators in preventing hydroxyl radical damage: adult respiratory distress syndrome as an experimental model for the pathophysiology and treatment of oxygen-radical-mediated tissue damage. Acta Haematologica. 1996;95(1):49-62.
33. Borgna-Pignatti C, Rugolotto S, De Stefano P, Zhao H, Cappellini M, Del Vecchio G, Romeo MA, Forni GL, Gamberini MR, Ghilardi R, Piga A, Cnaan A. Survival and complications in patients with thalassemia major treated with transfusion and deferoxamine. Haematologica. 2004;89(10):1187-93.
34. Olivieri NF, Brittenham GM, Matsui D, Berkovitch M, Blendis LM, Cameron RG, McClelland RA, Liu PP, Templeton DM, Koren G. Iron-chelation therapy with oral deferiprone in patients with thalassemia major. New england journal of medicine. 1995;332(14):918-22.
35. Borgna-Pignatti C, Marsella M. Iron Chelation in Thalassemia Major. Clinical Therapeutics. 2015 37(12):2866-77.
36. Nyström AM, Fadeel B. Safety assessment of nanomaterials: Implications for nanomedicine. Journal of controlled release. 2012 161(2):403-8.
37. Schellekens U, Klinger E, Muhlebach S, Brin JF, Storm G, Crommelin DJ. The therapeutic equivalence of complex drugs. Regulatory toxicology and pharmacology. 2011;59:176-183.
38. EMA, 2015. Reflection Paper on the Data Requirements for Intravenous Iron-based Nano-colloidal Products Developed with Reference to an Innovator Medicinal Product. 2015; EMA/CHMP/SWP/620008/2012. http://www.ema.europa.eu/docs/en_GB/document_library/Scientific_guideline/2015/03/WC500184922.pdf
39. Geisser P. Iron Therapy: with Special Emphasis on Oxidaitive Stress. *Georg Thieme Verlag, Stuttgart.* 1996.
40. Lesnefsky EJ. Reduction of infarct size by cell-permeable oxygen metabolite scavengers. Free Radical Biology and Medicine. 1992;12(5):429-46.
41. Beshara S, Lundqvist H, Sundin J, Lubberink M, Tolmachev V, Valind S, Antoni G, Långström B, Danielson BG. Kinetic analysis of ^{52}Fe-labelled iron(III) hydroxide–sucrose complex following bolus administration using positron emission tomography. British Journal of Haematology. 1999;104(2):288-95.
42. Elford P, Bouchard J, Jaillet L, Pearson N, Rogue A, Sabadie C, Forster R. Biodistribution and predictive hepatic gene expression of intravenous iron sucrose. Journal of Pharmacological and Toxicological Methods. 2013;68(3):374-83.
43. Schümann K, Szegner B, Kohler B, Pfaffl MW, Ettle T. A method to assess ^{59}Fe in residual tissue blood content in mice and its use to correct ^{59}Fe-distribution kinetics accordingly. Toxicology. 2007;241(1-2):19-32.
44. Spicher K, Brendler-Schwaab S, Schlosser C, Catarinolo M, Futterer S, Langguth, P, Enzmann H. Differences in tissue distribution of iron from various clinically used intravenous iron complexes in fetal avian heart and liver. Regulatory Toxicology and Pharmacology. 2015;73:65-72.
45. Lê BVon, Khorsi-Cauet H, Villegier A-S, Bach V, Gay-Quéheillard J. New rat models of iron sucrose-induced iron overload. Experimental biology and medicine. 2011;236(7):790-9.

46. Toblli, JE, Cao, G, Oliveri, L, & Angerosa, M. Differences between original intravenous iron sucrose and iron sucrose similar preparations. Arzneimittelforschung. 2009;59:176-190.
47. Kudasheva DS, Lai J, Ulman A, Cowman MK. Structure of carbohydrate-bound polynuclear iron oxyhydroxide nanoparticles in parenteral formulations. Journal of Inorganic Biochemistry. 2004 Nov;98(11):1757-69.
48. Mac Kenzie WF, Garner FM. Comparison of Neoplasms in Six Sources of Rats. Journal of the National Cancer Institute. 1973;50:1243-1257.

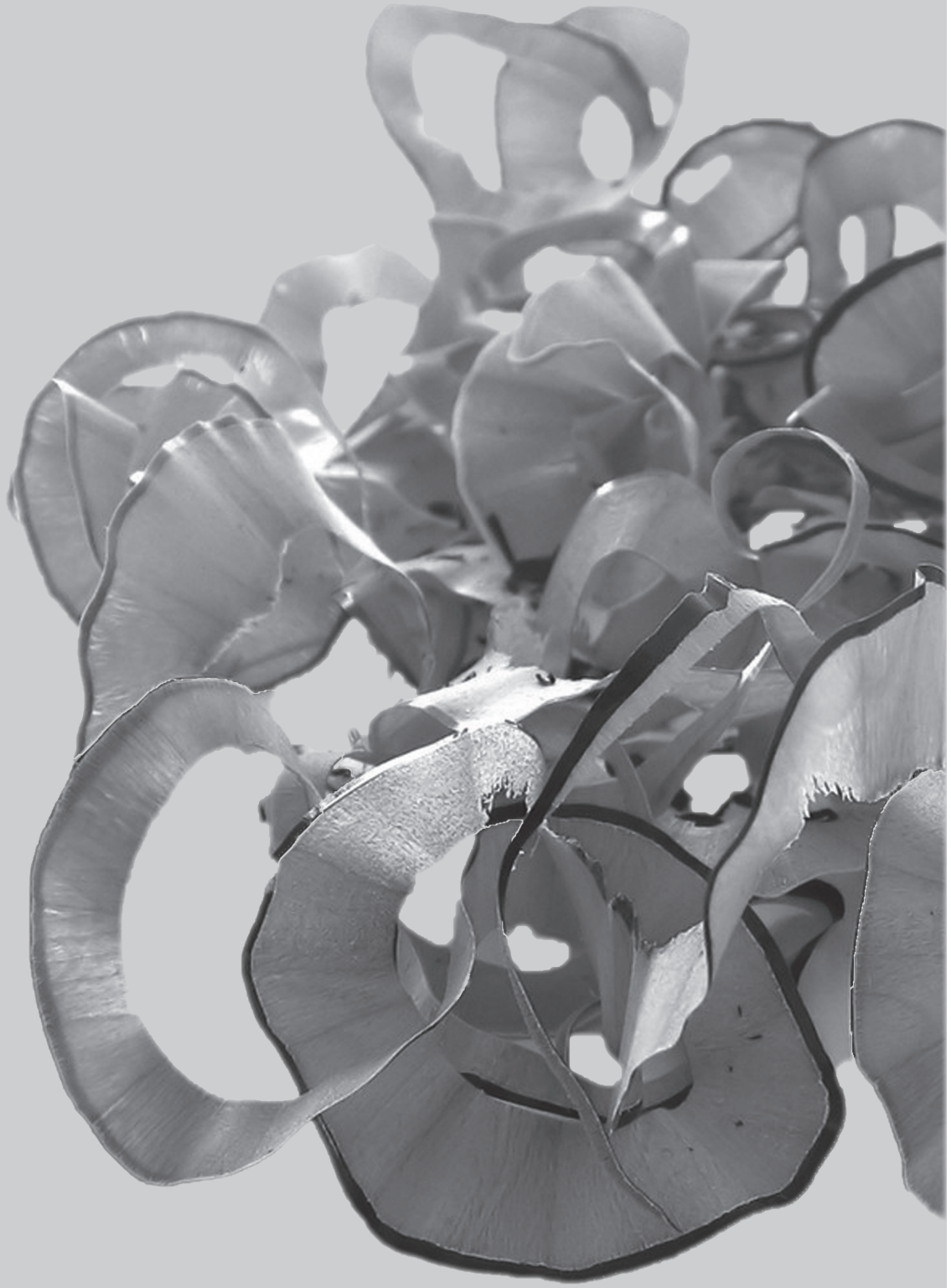

CHAPTER 7

Nederlandse samenvatting

IJzersuppletie wordt toegepast wanneer er sprake is van een ijzertekort dat veroorzaakt kan worden door verschillende klinische aandoeningen zoals bijvoorbeeld in geval van chronische ziekten. Een teveel aan ijzer kan een redox-onbalans veroorzaken die tot oxidatieve stress kan leiden en dus tot ernstige schade aan weefsel en organen. Daarom is het van belang om ijzertherapieën te ontwikkelen die effectief en daarnaast ook veilig zijn om geen ijzerstapeling te veroorzaken. Vooral in het geval van intraveneuze ijzercomplexen, die uit een polynucleaire ijzer (III) oxyhydroxide kern en een koolhydraat-omhulsel bestaan, hebben verschillende factoren zoals de fysisch-chemische eigenschappen en productieprocessen aangetoond hun efficiëntie en veiligheid *in-vivo* te kunnen beïnvloeden. Tot op heden is het een uitdaging om evaluatiemethoden te ontwikkelen en vast te stellen, voornamelijk *in-vivo* preklinische modellen, om goede vergelijkingen en diepgaande evaluatiestudies van ijzertherapieën uit te voeren.

In **Hoofdstuk 1** wordt een algemene inleiding gegeven over het belang van ijzer als voedingsstof en de betekenis van het behouden van een gezond ijzermetabolisme. Verder worden de verschillende ijzerbehandelingen, oraal en intraveneus, beschreven, evenals hun mogelijke invloed op ijzerstapeling. IJzer speelt een belangrijke rol in de Fenton-reactie, wat oxidatieve stress kan veroorzaken in organen en weefsels. Vandaar dat het essentieel is om de verschillende ijzerproducten te beoordelen op veiligheid en werkzaamheid, vooral bij het vaststellen van de gelijkenis tussen het origineel ijzerproduct en de generieke versie.

In **Hoofdstuk 2** werd een ijzercomplex voor orale ijzerbehandeling onderzocht, op basis van hemine-geladen polymeer micellen. Dit, met als doel een oraal ijzersupplement te ontwikkelen met een betere biologische beschikbaarheid en met mogelijk minder bijwerkingen dan de meest gebruikte ijzerpreparaat, namelijk ijzersulfaat. Aangezien heemijzer een superieure biologische beschikbaarheid heeft in vergelijking met non-heemijzer, werd de heem-analogon hemine geladen in het biologisch afbreekbare temperatuurgevoelige polymeer, methoxy-poly (ethyleenglycol) -b-poly [N-(2-hydroxypropyl) methacrylamidedilactaat], om vervolgens hemine-micellen te vormen. De hoogste beladingscapaciteit voor hemine in mPEG-b-p (HPMAm-Lac2) -micellen was 3.9% en de gemiddelde grootte van de hemine- micellen, afhankelijk van de hemine concentratie, was 75-140 nm. De hemine-micellen bleken stabiel te zijn bij pH 2 gedurende ongeveer 3 uur en tot 17 uur bij een neutrale pH van 7.4. Na incubatie van Caco-2-cellen met hemine- micellen, werden ferritine waarden van 2500 ng / mg eiwit waargenomen. Deze waarden zijn 10 keer hoger dan de ferritine waarden afkomstig van Caco-2 cellen die geïncubeerd werden met ijzersulfaat. De resultaten beschreven in hoofdstuk 2, laten zien dat hemine- geladen micellen een veelbelovend nieuw ijzercomplexformulering kan zijn voor orale toediening.

In **Hoofdstuk 3** werd de reproduceerbaarheid van niet-klinische studies, gerelateerd aan intraveneus ijzermedicijnen, onderzocht. Hier werd het originele ijzersucrose product Venofer® vergeleken met twee ijzer sucrose-similars (ISS) in een bijna vergelijkbare onderzoeksopzet als eerder in de literatuur is beschreven. Tijdens deze studie werd een vergelijkbare dosis van het originele ijzer product en de similars wekelijks toegediend aan mannelijke en vrouwelijke Sprague Dawley ratten gedurende 4 weken. Bloed en urine werden afgenomen om bloed-gerelateerde parameters te meten en biochemische analyses uit te voeren. Dit om inzicht te geven in mogelijke toxische effecten van de verschillende ijzerproducten, voornamelijk in de lever en nieren. Postmortem werd oxidatieve stress in lever en nieren gemeten en de hoeveelheid ijzer in de lever vastgesteld. De resultaten beschreven in hoofdstuk 3 tonen geen duidelijke verschillen tussen de originele ijzersucrose Venofer® en de twee ijzer sucrose-similars. Dit is in tegenstelling tot resultaten beschreven in literatuur waarin dezelfde ijzerproducten werden onderzocht. Bovendien werd er verschillen in resultaten tussen mannelijke en vrouwelijke ratten aangetoond, terwijl deze aan dezelfde behandelingen en experimentele omstandigheden waren onderworpen. Hoofdstuk 3 geeft aan dat het niet gemakkelijk is om resultaten te reproduceren en te standaardiseren van vergelijkbare preklinische studies die als doel hebben om de verschillen tussen de ijzerproducten aan te duiden. Omdat het interessant was om na te gaan of het diermodel dat gebruikt wordt tijdens deze studies, sensitief genoeg is om voldoende inzicht te geven in potentiële toxiciteitsverschillen van de ijzermedicijnen, hebben we in **Hoofdstuk 4** een dosis-respons experiment uitgevoerd. Hier werden hogere concentraties (> 40 mg ijzer / kg) van zowel Venofer® en Ferrlecit® dan de klinisch toegediende concentratie van maximaal 7 mg / kg, geïnjecteerd in mannelijke Sprague Dawley-ratten. De biomarkers de in dit hoofdstuk zijn gemeten waren vergelijkbaar met die in hoofdstuk 3. De bloed-gerelateerde ijzerparameters, namelijk serumijzer en transferrinesaturatie, toonden geen statistische verschillen tussen de ijzerbehandelingen, maar vertoonden wel hogere waarden voor deze parameters in dezelfde groep dieren na meerdere injecties in de loop van tijd. Bovendien vertoonden de buikorganen, in het bijzonder de lever, een dosis-effect gerelateerde bruinachtige kleur. Dit werd echter niet weerspiegeld in andere gemeten parameters zoals oxidatieve stressniveaus en 'Prussian blue' kleuring van de lever. Daarbij gaven de resultaten afkomstig van het lever enzym aspartaat –aminotransferase, geen significante verschillen tussen de verschillende behandelingen. Verder laat, in tegenstelling met wat werd verwacht, de evaluatie van de nierfunctie ook geen tekenen van renale toxiciteit na het injecteren van dergelijke hoge dosering van ijzer zien. De verschillende analyses in hoofdstuk 4 toonden noch een duidelijke behandeling noch een dosis-effect na meerdere injecties van de twee verschillende ijzerpreparaten aan. Daarom is het nog steeds de vraag of dit vaak toegepaste diermodel gevoelig genoeg is om een goed inzicht te verkrijgen in mogelijke toxische effecten van de twee onderzochte ijzerpreparaten. Karakterisering van de fysisch-chemische eigenschappen (bijvoorbeeld grootte, lading

en stabiliteit) van een intraveneus ijzerpreparaat is niet voorspellend voor het klinisch effect van geïnjecteerde ijzer producten. Om die reden moet er gedegen onderzoek uitgevoerd worden naar de *in-vivo* ijzerdistributie.

In **Hoofdstuk 5** onderzochten we de mogelijkheid om voor deze doeleinden magnetisch resonantie beeldvorming (MRI) te gebruiken. De resultaten toonden aan dat Venofer® (ijzersucrose) voldoende contrast genereerde om de distributie ervan in organen met behulp van MRI te evalueren. Sprague Dawley-ratten werden *in-vivo* tot 3 uur na injectie gemeten en 24 uur na injectie van zowel 10- als 40 mg / kg Venofer® postmortem gemeten. Als controle werd een zoutoplossing toegediend. Binnen 10 tot 20 minuten na injectie werd in de lever, milt en nieren (inclusief nier- medulla en cortex) een toename van ijzerdispositie waargenomen. Postmortem 24 uur na één injectie van het ijzerpreparaat werd, zoals verwacht, ijzeraccumulatie hoofdzakelijk in de lever en de milt waargenomen. De resultaten van dit hoofdstuk laten zien dat de MRI-techniek een krachtige niet-invasieve modaliteit is om ijzerdistributie na toediening van exogeen ijzer te kunnen onderzoeken.

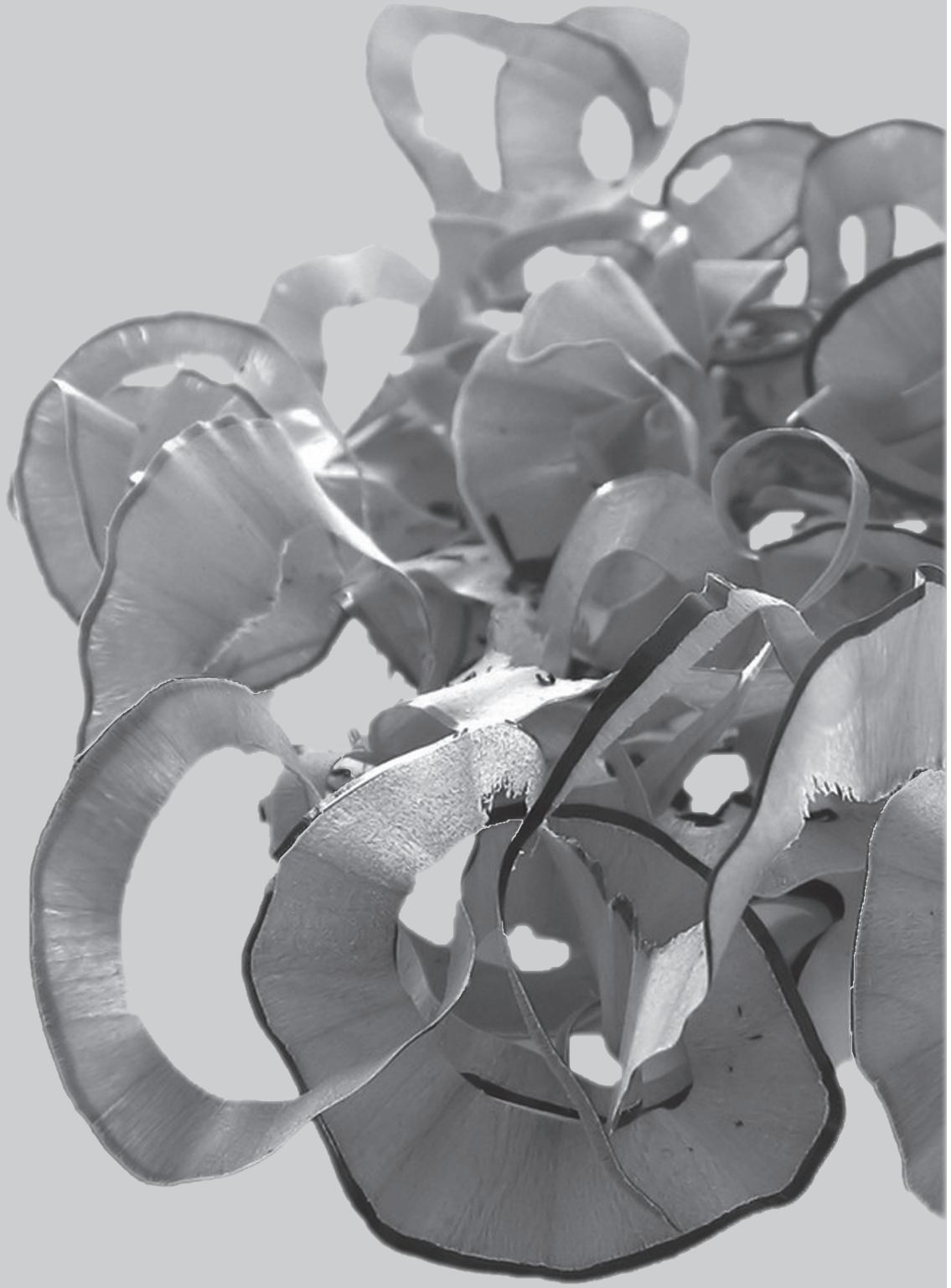

Appendix

LIST OF CO-AUTHORS

Vera Brinks
ProQR Therapeutics BV, Leiden, The Netherlands

Rick M. Dijkhuizen
Biomedical MR Imaging & Spectroscopy Group, Center for Image Sciences University Medical Center Utrecht, Utrecht University, The Netherlands

Wim E. Hennink
Utrecht Institute for Pharmaceutical Sciences, Department of Pharmaceutics, Utrecht University, The Netherlands

Hedi Hunt
Teligent Pharmaceuticals Inc. Estonia
University of Tartu, Lab of Cancer Biology, Estonia

Cornelus F. van Nostrum
Utrecht Institute for Pharmaceutical Sciences, Department of Pharmaceutics, Utrecht University, The Netherlands

Ebel H. E. Pieters
Utrecht Institute for Pharmaceutical Sciences, Department of Pharmaceutics, Utrecht University, The Netherlands

Huub Schellekens
Utrecht Institute for Pharmaceutical Sciences, Department of Pharmaceutics, Utrecht University, The Netherlands

Geralda A. F. van Tilborg
Biomedical MR Imaging & Spectroscopy Group, Center for Image Sciences University Medical Center Utrecht, Utrecht University, The Netherlands

Anette van der Toorn
Biomedical MR Imaging & Spectroscopy Group, Center for Image Sciences University Medical Center Utrecht, Utrecht University, The Netherlands

Johan J.F. Verhoef
Utrecht Institute for Pharmaceutical Sciences, Department of Pharmaceutics, Utrecht University, The Netherlands

ACKNOWLEDGMENT

It is not possible to complete a PhD without help. There are many people that were involved in my project in one way or another and therefore it is now time to express my gratitude to all those people.

First, I would like to thank my promotors for giving me the opportunity to do a PhD at the department of Pharmaceutics. I especially would like to thank Prof. Wim Hennink. Wim, you might not realize it but I have been a student, doing a traineeship at your department, since the year 2007. This means that you have been putting up with me for almost 11 years. When I applied for a PhD you did not have a PhD project available and therefore decided to offer me a job as a student assistant for a couple of months until a suitable project presented itself. My PhD project was not an easy one and the subject was also not within your usual expertise, but you have managed to help me and give me advice. I particularly would like to thank you for the patience and understanding of the last years when I fell ill and therefore needed to extend the time of the PhD project. You have always given me many opportunities, never gave up on me and partially because of you I made it!

I also want to thank my co-promotor Vera. You were a great daily supervisor during the first years of the PhD. Unfortunately, you had to leave before I could finish but you remained involved and helped me throughout the writing process and with the final preparations for my defense. Thank you!

This project would have not been possible at all if it wasn't for the help I received from Vifor Pharma. Besides financially supporting all intravenous iron related research, you also provided me with the chance to perform *in-vivo* experiments with the oral iron-complex at your facility in Switzerland. Unfortunately, the results were not what we expected, but nevertheless gave me valuable information regarding the developed hemin-micelles. I especially would like to thank Stefan, Susanna, Felix and Beat for all their support throughout the years and for providing me with their expertise during the writing of the articles.

Next, my paranymphs. Andhyk, thank you for accepting to be my paranymph at the last moment. You were a great colleague and bench- and desk partner. But more important also a friend. Even though we do not see each other often outside the university you have always been very attentive. Ebeltje, where to start? I seriously believe that without you none of the experiments would have been done. You were my "partner in crime" for almost all experiments described in this thesis. Whenever I was stressed during the *in-vivo* experiments you would help me focus, keep me on track and made me smile during

those long days. You are one of the few that know that my 'lidwoorden' are wrong most of the time and that when I am tired I involuntarily start speaking Papiamentu. Thank you for being such a good listener!

I also would like to express my gratitude to all the other people that assisted me during the experiments. The analysts Kim, Mies, Louis and of course Joep that helped me during the *in-vivo* studies. The MR Imaging group, especially Geralda, thank you for all the hard work, input and for supporting me until the article was accepted for publication. Prof. Rick Dijkhuizen, for giving me the opportunity to perform experiments and use the imaging facilities. Also a heartfelt thank you to Jan-Jaap and Hedi for all the work you did for the development of the oral iron formulation. I wish you both the best in your future endeavors. Finally, thank you Barbara for making sure everything runs smoothly. Your friendliness has helped make this experience more pleasurable.

During all those years, from being a student to finishing the PhD, I had the privilege to meet many people of which some I now consider my friends. You are too many to mention but I would like to thank you all for the great atmosphere, nice dinners and Friday drinks and for enriching me with new knowledge of countries I haven't yet had the opportunity to travel to.

I also want to give a big hug to my best-friends outside the university. Friends that I have known for many years and that in one way or another have always supported me. Love you my sisters!!!

Last but certainly not least, my dear family. This dissertation is as mine as it is yours. Maybe you were not able to help me with the content, but you helped me with so much more. You literally provided me with the warmth of a home when times were difficult. This journey was not only about the PhD, there were so many lessons more. The most valuable lesson I learned, is that you are always able to rise above all difficulties if you have people in your life who truly care. Thank you for always being there, for the patience and for over and over hearing my same stories and every time trying to give me encouraging words. Without you I would have never been able to finish this chapter of my life. You are simply the best!

"Gratitude is a vaccine, an antitoxin and an antiseptic"
- J. H. Jowett

Hora est!
Kimberley

ABOUT THE AUTHOR

Kimberley Span was born on the 25th of August, 1982 in Guayaquil Ecuador. She grew up on the island of Curaçao and moved to the Netherlands to pursue her studies. She obtained her Bachelor's degree in Organic Chemistry in the year 2005 and afterwards worked as Quality Manager at Pepsi Co. (Aruba). After moving back to the Netherlands to finish her Master's degree in Science & Business Management she landed a traineeship at the Netherlands consulate in San Francisco as a trend watcher within the Netherlands Office for Science and Technology department (Innovatie Attaché Netwerk). Here, she searched for technology developments and associated policies, related to Regenerative Medicine, for companies, knowledge institutions and government in order to establish possible collaborations between the Netherlands and the state of California.
Prior to starting her PhD, Kimberley then worked in research and development of biomaterials for controlled drug delivery and matrices for tissue engineering at the Department of Pharmaceutics at Utrecht University. During her PhD project, she studied methods to assess the safety profiles of intravenous iron medicinal products including the evaluation of all related regulations and policies and she developed a novel formulation for oral iron delivery. The results of this project are described in this thesis.